UNIVERSITAT POLITÈCNICA DE CATALUNYA
BARCELONATECH
Escola d'Enginyeria de Telecomunicació
i Aeroespacial de Castelldefels

FINAL DEGREE PROJECT

TFG TITLE: Dynamic scheduling of aircraft high-lift devices and landing gear deployment for optimized continuous descent operations with required times of arrival

DEGREE: Grau en Enginyeria d'Aeronavegació

AUTHOR: David Duran Pérez

ADVISOR: Ir. Ronald Verhoeven

SUPERVISOR: Dr. Xavier Prats i Menéndez

DATE: 22 de juliol de 2015

Títol: Assignació dinàmica del moment de desplegament de dispositius hipersustentadors de vol i del tren d'aterratge per operacions òptimes de descens continu amb temps d'arribada requerits

Autor: David Duran Pérez

Director: Ir. Ronald Verhoeven

Supervisor: Dr. Xavier Prats i Menéndez

Data: 22 de juliol de 2015

Resum

Aquest document presenta una implementació innovadora de Time and Energy Managed Operations (TEMO) en el qual l'assignació dinàmica del moment de desplegament de dispositius hipersustentadors (flaps/slats) i del tren d'aterratge s'usa per tal de reduir el consum de fuel i l'ús d'aerofrens (speed brakes) mentre s'assoleixen temps requerits d'arribada (Required Time of Arrivals (RTAs)) precisos al llindar de la pista d'aterratge.
Es proposen dues solucions: una resolent les desviacions de temps i energia amb re-planning estratègic del moment de desplegament de dispositius hipersustentadors i/o del tren d'aterratge; i una altra solucionant les desviacions d'energia estratègicament, però anul·lant els errors en temps de manera contínua amb un controlador tàctic de la configuració de vol. L'actuació d'ambdues implementacions ha estat avaluada en aquest projecte. S'han considerat tres escenaris meteorològics: Atmosfera Estàndard Internacional (ISA), atmosfera real sense errors en la predicció de vent i atmosfera real incloent errors de vent. 6 RTAs diferents han estat testejades pel cas ISA mentre que 5 pels altres dos escenaris meteorològics. Tots aquests escenaris han estat provats per ambdues solucions i el cas de referència. A més, tres diferents "temps a la següent configuració"(0, 30 i 60 segons) s'han simulat tant en la solució tàctica com estratègica. En total, s'han executat 112 simulacions diferents.
Els resultats demostren que el consum de fuel i l'ús d'aerofrens ha estat reduït en tots els escenaris meteorològics quan l'assignació dinàmica de flaps/slats i tren d'aterratge s'ha usat. La solució tàctica mostra millor control sobre el temps durant tot el descens de l'aeronau. A més, s'ha observat que es produeixen menys re-plans i s'obté un marge més ampli de possibles RTAs amb les noves implementacions.
Per altra banda, s'ha demostrat que per tal d'assolir RTAs més precises a la pista d'aterratge i incrementar l'altitud d'estabilització, s'ha de modelar millor l'actuació dels motors de l'aeronau per tal de tenir en compte la seva dinàmica.

Title : Dynamic scheduling of aircraft high-lift devices and landing gear deployment for optimized continuous descent operations with required times of arrival

Author: David Duran Pérez

Advisor: Ir. Ronald Verhoeven

Supervisor: Dr. Xavier Prats i Menéndez

Date: July 22, 2015

Overview

This report presents a novel implementation of Time and Energy Managed Operations (TEMO) in which the dynamic scheduling of high-lift devices (flaps/slats) and landing gear deployment is used in order to reduce fuel consumption and speed brakes usage while achieving accurate Required Time of Arrivals (RTAs) at the landing runway threshold.
Two solutions are proposed: one resolving time and energy deviations with strategic re-planning of the high-lift devices and/or gear deployment; and another one solving energy deviations strategically but nullifying time errors continuously with a tactical aircraft configuration controller. The performance of both implementations has been assessed during this project.
Three meteorological scenarios have been considered: International Standard Atmosphere (ISA), real atmosphere without wind prediction errors and real atmosphere including wind errors. 6 different RTAs have been tested for the ISA case while 5 for the other two weather scenarios. All these scenarios have been tested for both mentioned solutions and the baseline case. Moreover, three different "time to next configuration" (0, 30 and 60 seconds) have been simulated both in the tactical and strategic solution leading to a total of 112 different simulations.
Results demonstrate that fuel consumption and speed brakes usage are reduced in all the studied weather scenarios when using dynamic scheduling of flaps/slats and landing gear. The tactical solution also shows better time metering during the entire flight descent. Moreover, it has been observed that less unable re-plans are produced and a wider margin of feasible RTAs is obtained with the new implementations.
On the other hand, it has been shown that to achieve more accurate RTAs at the runway and increase the stabilization altitude, the performance of the aircraft engines should be better modeled to take into account their dynamics.

To my dear family

CONTENTS

LIST OF FIGURES

LIST OF TABLES

GLOSSARY

This list presents the most important specific terms used during this report. Some of the definitions have been obtained with the aid of the Cambridge Aerospace Dictionary written by Bill Gunston [3].

Approach mode Mode of the autopilot activated when intercepting the Instrumental Landing System (ILS) in order to capture and follow the glideslope and localizer, which is preceded by the selected descent mode. 15

Autopilot Airborne electronic system, which automatically stabilizes aircraft about its three axes (sometimes, in light aircraft, only two, rudder not being served), and, in modern aircraft, pressed by pilot or remote radio control to cause aircraft to follow any desired trajectory or speed. 6, 26

Autothrottle Power control system for main propulsion engines linked electromechanically to the aircraft flight control system and automatic-landing system so that thrust is varied automatically to keep aircraft on a specific target of indicated airspeed or thrust level. 26

B-spline It is a spline that has minimal support (set of points where the function is not zero-valued) with respect to a given degree, smoothness and domain partition. Any spline function of a given degree can be expressed as a linear combination of B-splines of that degree. 19

Drag Retarding force acting upon body in relative motion through fluid, parallel and opposite to direction of motion. 5, 7

Elevator Movable control surface, usually at the rear of an aircraft, which control the angle of attack and the lift of the wing. 3, 5, 62, 71

Flap Movable surface forming part of leading or trailing edge of aerofoil, able to hinge downwards, swing down and forwards, translate aft on tracks or in some other way alter wing camber, cross-section and area in order to exert powerful effect on low-speed lift and drag. iii, v, 1, 4, 5, 47, 71, 81

G/s on elevator Autopilot mode in which the glideslope is followed by changes on the aircraft elevator. 26

Gear Any portions of aircraft or spacecraft whose function is to enable a landing to be made; this includes wheels/skis/floats and attachments, and hook, but not flaps or lift-dumpers. v, 1, 4, 5, 25, 47, 57, 71, 81

Glideslope Radio beam in ILS providing vertical guidance. i, v, 1, 3, 13, 19, 25, 29, 62, 71

GRIB file Type of binary files used to store meteorological data of a given region of the Earth. It includes, for instance, magnitudes such as pressure, temperature and winds. 8, 19, 20, 21

Lift Upwards force acting upon body in relative motion through fluid, perpendicular to direction of motion. 7

Path on elevator Autopilot mode in which the vertical path is followed by changes on the aircraft elevator. 3, 62

Pitot tube Open-ended tube facing forwards into fluid flow, thus generating internal pressure equal to stagnation pressure (in case of supersonic flow, that downstream of normal shock). 79

Slat Movable portion of leading edge of aerofoil, which in cruising flight is recessed against main surface and forms part of profile; at high angle of attack either lifts away under its own aerodynamic load or is driven under power to move forward and down and leave intervening slot. iii, v, 1, 71

Speed on thrust Autothrottle mode in which the calibrated airspeed is controlled by changes on the thrust coming from the engines. 63, 71

Speed brake Passive device extended from aircraft to increase drag. Most common form is hinged flap(s) or plate(s), mounted in locations where operation causes no significant deterioration in stability and control at any attainable airspeed. iii, v, 1, 3, 5, 19, 25, 71, 81

Speed on elevator Autopilot mode in which the calibrated airspeed is controlled by changes on the aircraft elevator. 3, 15, 26, 53, 63, 71

Spline A spline is a numeric function that is defined as piecewise by polynomial functions and which has enough smoothness at the connections between polynomials. It is used to have a function connecting all the input data points. i, 19

Throttle Input control, usually hand lever rotating through arc, for aircraft propulsion/thrust. v, 1

Thrust Force imparting propulsion to the aircraft in a given direction. 1, 3, 5, 7, 25

ACRONYMS

ATC Air Traffic Control 1, 25, 80
BADA Base Of Aircraft Data 19, 81
BOT Begin Of Turn 48
CAS Calibrated Airspeed 3, 5, 26, 71, 79
CDO Continuous Descent Operation 1, 4, 48
DNLP Nonlinear Programming With Discontinuous Derivatives 12, 85
EOT End Of Turn 48
ETA Estimated Time Of Arrival 33, 54
FAS Final Approach Speed 66
F-LND Flaps Landing 25, 26, 59, 81, 85
F-APP Flaps Approach 25, 26, 57, 81, 85
FAP Final Approach Point 13, 49
FASTOP FAST OPtimizer 4, 15, 18, 25, 31, 57
FMS Flight Management System 1, 3, 15
G/S Glideslope 62
GPS Global Positioning System 80
GSA Green Sustainable Airports 48
IAF Initial Approach Fix 4, 31, 47, 49
IAS Indicated Airspeed 27, 79
IF Intermediate Fix 49
ILS Instrumental Landing System i, v, 1, 30
ISA International Standard Atmosphere v, 8, 19, 35, 54, 80
LP Linear Programming 12
MCDU Management Control Display Unit 15
MCP Mode Control Panel 17
MINLP Mixed Integer Nonlinear Programming 26, 86
ND Navigation Display 17, 31, 36, 87
NLP Non-Linear Programming 9, 11, 12, 20, 26, 85, 86
NLR Nationaal Lucht- En Ruimtevaartlaboratorium 2, 4, 15, 48
PFD Primary Flight Display 5, 17
QCP Quadratic Constrained Programs 12
RFMS Research Flight Management System 15, 18, 25, 31, 57
RTA Required Time Of Arrival iii, v, 1, 3, 4, 15, 18, 25, 26, 49, 54, 58, 71
RWY Runway 4, 25
SGO System For Green Operations 2
SVN Subversion 15
T/D Top Of Descent 3, 10, 25
TA Transition Altitude 80
TAS True Airspeed 7, 79
TEMO Time And Energy Managed Operations iii, v, 1, 3, 49
TL Transition Level 80
TMA Terminal Manoeuvring Area 1
TUD Technical University Of Delft 4
UPC Polytechnical University Of Catalonia 4
WGS84 World Geodetic System 84 9

NOMENCLATURE

The following nomenclature defines the most important variables used throughout the report.

C_D	Aerodynamic drag coefficient
C_L	Aerodynamic lift coefficient
D	Aerodynamic drag
E_s	Specific energy of the aircraft
E_T	Total energy of the aircraft
f	Flaps configuration
FF	Aircraft fuel flow
g	Gravity acceleration
GS	Ground speed
h_G	Geometric altitude
h_p	Pressure (barometric) altitude
J	Cost functional
K_β	Slope of *arctan* function for gear deployment
L	Aerodynamic lift
m	Aircraft mass
M	Mach
$N1$	Percentage of rotational speed of the low-pressure spool
$N2$	Percentage of rotational speed of the high-pressure spool
p	Atmospheric pressure
p_{SSL}	Pressure at sea level
R	Gas constant of dry air
R_E	Radius of the Earth
s	Along path distance
S	Aircraft surface
t	Time
T	Aircraft thrust
v	True airspeed
w_e	East wind component
w_n	North wind component
w_s	Along track wind component
w_v	Airspeed wind component
w_x	Cross track wind component
x	Along path distance (nodes)
x_{sw}	Switching distance of gear deployment
β	Speed brake setting
β_{gear}	Gear setting
γ	Aerodynamic flight path angle
γ_a	Specific heat ratio
γ_{ILS}	ILS glideslope angle
γ_g	Ground flight path angle
δ	Pressure ratio
θ	Temperature ratio
π	Throttle setting
ρ	Atmospheric density
τ	Atmospheric temperature
τ_{SSL}	Temperature at sea level
ϕ	Aircraft bank angle
φ	Geometric latitude
χ_a	Heading angle
χ_g	Track angle

INTRODUCTION

Reducing the environmental impact of air transportation is one of the most important public concerns in the aviation community. At the same time, the current air traffic system has to deal with the expected growth in air traffic, which will probably lead to increased delays. The United States with the NextGen project [4] and Europe with SESAR [5] and Clean Sky [6] are pioneer in research projects that aim to address capacity, environmental impact, safety and economic issues of aviation.

Nowadays, Flight Management Systems (FMSs) of aircraft compute the descent profile in cruise by using backwards numerical integration. This calculation takes into account all the necessary constraints and aircraft dynamics, but the descent is only performed with idle thrust until the first constrained waypoint. Moreover, most current FMSs cannot include a time constraint such as a Required Time of Arrival (RTA) in one or several waypoints along the descent route.

In addition to the aforementioned restrictions, today's descents are also limited by Air Traffic Control (ATC), which uses altitude, heading and speed instructions to maintain spacing between aircraft. By commanding these instructions, the efficiency of the trajectory, in terms of fuel and time consumption, but also environmental impact, is far from being optimal (e.g. some extra segments with thrust are added, longer distances are flown, non-optimal speeds are followed...).

In contrast, Continuous Descent Operations (CDOs) [7] consist of descents with nearly idle thrust, from the cruise to the interception of the ILS glideslope. CDOs are arrival procedures that aim at reducing level flight segments at low altitudes. In this manner, they reduce fuel consumption (and gaseous emissions) and noise levels in Terminal Manoeuvring Areas (TMAs) [8].

The main disadvantage of such type of descents is that they often limit airport capacity due to uncertainties in predicting the arrival time and spacing between aircraft caused by errors in estimating the wind forecast and aircraft performance. Variations of pilot response also affect the prediction of these descents. Thus, existing CDO implementations require ATC to introduce additional sequencing buffers to ensure enough separation among aircraft, consequently reducing airport capacity.

To solve this issue, time constraints along the route can be set. With these RTAs, ATC can efficiently handle separation tasks without needing to increase separation intervals or commanding path changes. Nevertheless, the aircraft FMS must be able to guide the aircraft efficiently through these RTAs with enough accuracy.

Reference [9] describes the Time and Energy Managed Operations (TEMO) concept for guidance and planning (see chapter 1), which is used in this project. In TEMO, the energy of the aircraft, which is a combination of speed and altitude, is managed such that RTAs are always fulfilled. Hence, if the aircraft needs to fly faster in order to meet an early RTA, the flight path will be adjusted to loss altitude quickly (gain speed) and vice-versa. If throttle or speed brakes are needed to meet an RTA, an optimization process determines the best trajectory minimizing these contributions.

Usually, flaps/slats and gear are deployed at a given speed and/or altitude. However, these devices are useful to subtract energy from the system. In fact, most pilots deploy these

devices later/earlier as a function of the actual path of the aircraft. This practice, however, is done manually and at the pilot's best judgment, without any kind of automated support. In TEMO, an intelligent planning of flaps/slats and/or gear could give more flexibility to manage energy producing a more efficient aircraft trajectory while meeting a specific RTA. So far, the only way to do so was using thrust, when energy was needed, or speed brakes to subtract energy from the system.

This report explains a novel implementation of TEMO in which the dynamic scheduling of high-lift devices (flaps/slats) and landing gear deployment are used in order to reduce fuel consumption, speed brakes usage and noise emissions while achieving accurate RTAs at the landing runway threshold. The dynamic scheduling of these devices has never been tested in TEMO and it is thought that it will aid to achieve a reduction of the environmental impact of the operations.

The specific objectives for this study are to:

- Demonstrate the ability of the algorithm to **reduce fuel and speed brakes** usage.
- Demonstrate the ability of the dynamic aircraft algorithm to **meet absolute time requirements** at the runway threshold.
- Demonstrate the ability of the dynamic flaps/gear algorithm to **provide accurate and safe aircraft guidance** toward the Stabilization Point (1000 ft AGL).
- Evaluate the **performance of the system** under test.

The report starts with a chapter devoted to explain the TEMO concept besides the optimal control problem and mathematical modeling. Then, the software packages involved in this project are briefly explained. The two proposed types of implementations (strategic and tactical) to schedule high-lift devices are presented in chapter 3 and chapter 4 respectively. In order to test these implementations and compare them to the current situation, the experiment plan is defined in chapter 5. Finally, the results are discussed and the main conclusions of the project are given.

This research has been done at the Nationaal Lucht- en Ruimtevaartlaboratorium (NLR). The TEMO optimizer, which was a result of the System for Green Operations (SGO) project of Clean Sky [6], a public-private initiative between the European Commission and the aviation industry, has served as base for this research.

CHAPTER 1. TIME AND ENERGY MANAGED OPERATIONS

1.1. Planning and guidance

Before entering the Top of Descent (T/D) of a flight, Flight Management System (FMS) plan an initial descent trajectory, which may comply with one or more constraints such as altitude, speed and/or time constraints. The generation of this initial plan is not an optimization process: idle thrust is assumed during the descent, speed brakes are not used at all and some standard procedures fix the remaining degrees of freedom.

As said in [1], nowadays the FMS will calculate and freeze the initial idle descent path before T/D and the aircraft will be guided along the path with idle thrust and path on elevator. Thus, the elevator is used to follow the aircraft's path in the vertical guidance function. Model inaccuracies, however, will lead to speed deviations and therefore time deviations when trying to fulfill a Required Time of Arrival (RTA).

In Time Management Operations (TEMO), the trajectory is optimized with respect to predefined objectives, such as fuel, noise, usage of speed brakes, etc. Then, the planned descent trajectory is executed following speed on elevator (until glideslope interception), meaning that the aircraft elevator is used not to control the aircraft's path but its calibrated airspeed (CAS) [10]. By following speed on elevator, adherence to RTA is better at the expense to have altitude (path) deviations in presence to modeling errors.

In TEMO, if the energy or time deviation is bigger than given maximum allowable thresholds (defined along the descent), a **re-plan** is triggered. This means that the current planned descent trajectory is updated with a new optimized descent trajectory, taking into account the current state, applicable constraints and optimality objectives (see Figure 1.1). This optimized trajectory is computed by a solver minimizing fuel flow and speed brakes usage, at the same time the RTAs (if applicable) are fulfilled.

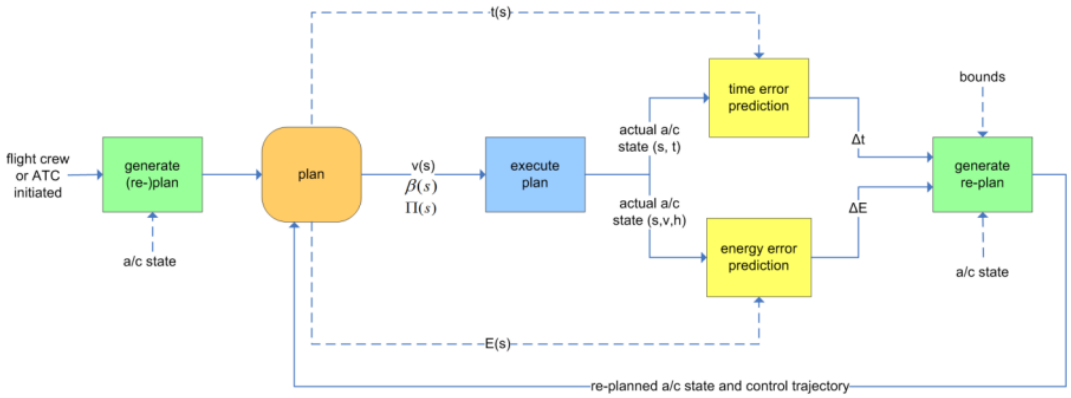

Figure 1.1: Trajectory optimizer block diagram (Source: [1])

Hence, a re-plan can be triggered due to two situations:

- ATC may request the aircraft to comply with a specific RTA at the Initial Approach

Fix (IAF) and/or the Runway (RWY) threshold[1].

- Due to model inaccuracies, meteorological uncertainties or flight guidance errors, the aircraft deviates from the planned trajectory. The boundaries used in this project are:
  - Maximum time deviation of $\pm$ 15 s at T/D, $\pm$ 10 s at IAF and $\pm$ 5 s at the runway threshold .
  - Maximum energy deviation of $\pm$ 500 ft at T/D, $\pm$ 200 ft at IAF and $\pm$ 100 ft at the runway threshold.

Alternatively, any sustained time and/or energy error could be resolved using **tactical control**, which takes immediate action to resolve the time and or/energy error. Usually, these errors are nullified by commanding calibrated airspeed (or thrust) changes. TEMO uses **strategic re-planning** for both energy and time deviation as explained above. However, in this project, a tactical controller scheduling flaps and gear has been developed to nullify time deviations over the aforementioned strategic algorithm. Thus, when using this error-nullifying mechanism, re-plans can still occur if the energy goes out of bounds.

1.2. TEMO concept

The aim of this research is to dynamically schedule high-lift devices in order to obtain more precise RTAs while using the TEMO concept for the descent and approach of a flight.

The TEMO concept has been developed by Nationaal Lucht- en Ruimtevaartlaboratorium (NLR) in cooperation with Technical University of Delft (TUD) within the Clean Sky initiative [6]. Version 2 of TEMO has been developed by NLR while the FAST OPtimizer (FASTOP) consortium (GTD, Polytechnical University of Catalonia (UPC), ASCAMM) has developed the last version of the concept (see [8]). TEMO consists on using energy principles in Continuous Descent Operations (CDOs) that contain a time constraint. The aim is to reduce the noise footprint and fuel consumption while complying with time constraints.

It is well-known that energy can be expressed as:

$$E_T = mgh + \frac{1}{2}mv^2 \tag{1.1}$$

where m is the mass of the aircraft, g the gravity at the Earth's surface (9.8067), h the altitude of the airplane and v is the speed. See Appendix A for altitude and speed definitions used thorough this document.

Hence, an aircraft has basically two ways of adding/removing energy from the system. When flying higher than planned, the aircraft has more energy due to the potential contribution whereas when flying faster than planned, it also has more energy due to the kinetic energy.

In order to know how the aircraft can change its energy, Equation 1.1 can be differentiated obtaining:

[1] In this project, RTAs are only requested for the runway threshold

$$\dot{E}_T = mg\dot{h} + mv\dot{v} \tag{1.2}$$

Before proceeding further, the acceleration of the aircraft needs to be defined. It can be obtained with the equations of flight mechanics, assuming a point mass (3 degrees of freedom) model [11], which taking into account wind derivatives becomes:

$$\dot{v} = \frac{T - D}{m} - gsin\gamma - \dot{w}_v \tag{1.3}$$

Where T is the thrust, D is the drag, γ is the flight path angle (negative in descents) and $\dot{w}_v$ is the contribution of wind derivatives in the airspeed dynamics.

By substituting Equation 1.3 in the acceleration term of Equation 1.2 and using that $\dot{h} = v\sin\gamma$, the energy rate expression can be obtained:

$$\dot{E}_T = v \cdot (T - D - m\dot{w}_v) \tag{1.4}$$

To sum up, the total energy of an aircraft can be increased either by increasing thrust or decreasing the derivative of wind speed and drag. As commented in [12], this process is called **energy state change** while the exchange of potential energy for kinetic energy and vice versa is called **energy modulation**.

In a continuous descent, thrust is set to idle. Moreover, wind cannot be controlled. Thus, the only means to change the energy are speed brakes and aircraft configuration (gear and flaps) while the elevator is used to modulate the energy. Since it is desired to reduce speed brakes usage, the focus of this project is set on the usage of high-lift devices and the elevator. This means that if the aircraft needs to arrive later to a given point of the route, thus less speed, it will have to maintain a higher altitude or use flaps/gear earlier than planned.

The main difference with respect to the TEMO concept implemented so far is that, in this study, there is also the option to use high-lift devices in order to change the energy, which can lead to less fuel consumption and speed brake usage.

Finally, in order to correctly compute energy, the correct type of speed and altitude have to be chosen for its computation. In the current project, calibrated airspeed (CAS) and barometric altitude are used, because they are the variables used operationally (see Appendix A for their definition). A pilot tries to achieve the target value of speed and altitude displayed in the Primary Flight Display (PFD) and the issue is that these values are expressed in terms of calibrated airspeed and barometric altitude. Hence, the pilot, or autopilot, expects that if the target value of CAS and barometric altitude are achieved, the energy display (see section 2.3.) shows no deviation of energy. This is the main reason for choosing calibrated airspeed and barometric altitude for the computation of the energy.

Thus, the equation of specific energy, normalized with the weight of the aircraft, that will be used through this study is:

$$\boxed{E_S = h_p + \frac{CAS^2}{2g}} \tag{1.5}$$

It is worth mentioning that this magnitude is expressed in **feets**.

1.3. Phases and profile

The profile and phases used for the experiments and discussion of this report are displayed in Table 1.1. In this table (valid for the Cessna Citation aircraft, which is used in the current study) we can see the different trajectory phases and the phase exit criteria applied in the backwards integration process used to compute the nominal trajectory.

Phase	Name	Flaps/S-lats conf.	Phase exit condition	Trajectory constraints
1	GS_STAB	LND	$h_p = h_{STAB} + h_{THR} = 1000ft$	$\dot{\gamma}_g = 0; \gamma_g = \gamma_{ILS}; \dot{CAS} = 0; CAS = v_{FAS}$
2	GS_LND	LND	$CAS = v_{LND}$	$\dot{\gamma}_g = 0; \gamma_g = \gamma_{ILS}; \ddot{CAS} = 0$
3	GS_THR	APP	$h_p = 2000ft$	$\dot{\gamma}_g = 0; \gamma_g = \gamma_{ILS}; T = T_{req}$
4	FPA	APP	$s = s_{GS} - 2NM$	$\ddot{CAS} = 0; \dot{CAS} = \dot{CAS}_{LOC}$
5	APP_DCL_2	CLEAN	$s = s_{EH740}$	$\ddot{CAS} = 0; \dot{CAS} = 0$
6	APP_DCL_1	CLEAN	$CAS = v_{APP}$	$\ddot{CAS} = 0; \dot{CAS} = \dot{CAS}_{APP}$
7	APP_SPD	CLEAN	$s = s_{TOLKO}$	$\dot{CAS} = 0; CAS = v_{APP}$
8	DES_DCL	CLEAN	$CAS = CAS_{CRZ}$; $h_p = h_{CRZ}$	$\ddot{CAS} = 0; \dot{CAS} = \dot{CAS}_{DES}$
9	CRUISE	CLEAN	-	$\dot{CAS} = 0; \dot{h_p} = 0; h_p = h_{CRZ}$

Table 1.1: Profile for the Cessna Citation

1.4. Mathematical modelling

In this section, the mathematical modeling used throughout this project is explained.

1.4.1. Aircraft model

A three-degree of freedom model is adopted, typically called point mass model. This means that only translational dynamics are considered, assuming rotational dynamics much faster and effectively controlled by the autopilot system of the aircraft. Moreover the aircraft is assumed as a rigid-body moving over a flat non-rotating earth with constant gravity acceleration (g) and where angle of attack and side-slip angles are neglected. The effect of wind and wind shear are only considered in the horizontal plane and it is assumed that they can change only as a function of the along path distance and altitude. Thus, vertical wind components and temporal wind variations are neglected.

In this project the state (x) and controls (u) vectors are defined as:

$$\begin{aligned} \vec{x} &= [v, s, h, m] \\ \vec{u} &= [\gamma, \pi, \beta] \end{aligned} \tag{1.6}$$

v is the true airspeed (TAS), s the along track distance, h is the altitude, m the mass of the aircraft, γ is the aerodynamic flight path angle, π the throttle setting and β represents the usage of speed brakes (ranging from 0 to 1).

Bearing in mind the above state vector and mentioned assumptions, the aircraft dynamics expressed in the air reference frame are given by [13]:

$$\begin{aligned} \dot{v} &= \frac{T-D}{m} - g\sin\gamma - \dot{w}_v \\ \dot{s} &= v \cdot \left(\sqrt{\cos^2\gamma - \bar{w}_x^2} - \bar{w}_s \right) \\ \dot{h} &= v \cdot \sin\gamma \\ \dot{m} &= -FF \end{aligned} \tag{1.7}$$

where FF is the fuel flow and T, L and D are the thrust, lift and drag respectively. On the other hand, the wind components that appear in the previous equations are by order of appearance: wind derivative contribution to the true airspeed, normalized cross track wind (perpendicular to the path) and normalized along track wind (parallel to the path). By previously knowing the component of wind in the north and east direction and their derivatives, the aforementioned wind contributions can be obtained as:

$$\begin{aligned} \dot{w}_v &= \cos\gamma \cdot (\dot{w}_n \cos\chi_a + \dot{w}_e \sin\chi_a) \\ \bar{w}_s &= \frac{w_s}{v} \\ \bar{w}_x &= \frac{w_x}{v} \end{aligned} \tag{1.8}$$

where χ_a is the heading angle and the along and cross track wind components can be obtained by projecting the track angle:

$$\begin{aligned} w_s &= w_n \cos\chi_g + w_e \sin\chi_g \\ w_x &= -w_n \sin\chi_g + w_e \cos\chi_g \end{aligned} \tag{1.9}$$

On the other hand, the aerodynamic forces acting on the aircraft can be expressed as:

$$\begin{aligned} D &= \frac{1}{2}\rho S v^2 C_D \\ L &= \frac{1}{2}\rho S v^2 C_L \end{aligned} \tag{1.10}$$

where ρ is the density, S is the wing surface, C_D the drag coefficient and C_L the lift coefficient.

The drag and thrust model for the aircraft used in this study, which is the Cessna Citation C550, can be found in Appendix B.

1.4.2. Atmosphere model

In this project, some scenarios are within ISA whereas others consider real atmosphere. Even significant wind prediction errors (offsets) are taken into account in some cases.

For the current study, the aircraft descent is always below the tropopause, located at 11 km if ISA atmosphere is considered. Then, from the hydrostatic equation:

$$dp = -\rho \cdot g \cdot dh_p \tag{1.11}$$

where dh_p is the differential of barometric altitude (see section A.2. for a complete definition of the barometric and geometric altitude). Applying the law of the gases, assuming a linear decrement of the temperature, the following equation arises:

$$dp = \frac{-pgdh_p}{R(\tau_{SSL} - \lambda h_p)} \tag{1.12}$$

Where R=287.05287 m^2/(s^{2}K), λ=0.065 K/m and τ_{SSL} is the temperature at sea level (15 $^\circ$C).

After integrating from sea level to a given altitude, it can be obtained that:

$$\ln \frac{p}{p_{SSL}} = \frac{g}{R\lambda} \cdot \ln \frac{\tau_{SSL} - \lambda h_p}{\tau_{SSL}} \tag{1.13}$$

where p_{SSL} is the pressure at sea level (101,325 Pa).

By powering to the e number the entire equation, the barometric altitude for **ISA atmosphere** can be obtained:

$$h_p = \frac{\tau_{SSL}}{\lambda} \cdot \left(1 - \left(\frac{p}{p_{SSL}}\right)^{\frac{R\lambda}{g}}\right) \tag{1.14}$$

On the other hand, in **real atmosphere**, barometric altitude and temperature are function of the pressure and position (latitude and longitude or along track distance if the trajectory is correctly projected). This data comes from binary GRIB files (GRIB files) of the geographical region of interest.

For both ISA and real atmosphere, CAS and Mach are obtained with equations involving the atmosphere model, so it is essential to correctly model it:

$$CAS = \sqrt{\frac{2p_{SSL}}{\mu\rho_{SSL}} \cdot \left[\left(\delta\left(\left(\frac{\mu v^2}{2R\tau} + 1\right)^{\frac{1}{\mu}} - 1\right) + 1\right)^{\mu} - 1\right]} \tag{1.15}$$

$$M = \frac{v}{\sqrt{\gamma_a \cdot R \cdot \tau}}$$

where μ can be expressed according to the specific heat ratio of the air ($\gamma_a = 1.4$) as:

$$\mu = \frac{\gamma_a - 1}{\gamma_a} \tag{1.16}$$

1.4.3. Wind model

When considering real atmosphere, wind has to be taken into account. The recorded data gives us the north and east components of the wind and by using Equation 1.9, the along and cross track wind components can be obtained.

As mentioned before, derivatives of north and east wind during this project do not consider variations in time; only in distance and altitude:

$$\begin{aligned} \dot{w}_n &= \frac{\partial w_n}{\partial s}\dot{s} + \frac{\partial w_n}{\partial h}\dot{h} \\ \dot{w}_e &= \frac{\partial w_e}{\partial s}\dot{s} + \frac{\partial w_e}{\partial h}\dot{h} \end{aligned} \tag{1.17}$$

1.4.4. Earth model

In this project, the gravity depends only on the latitude (φ). It is computed supposing the World Geodetic System 84 (WGS84) ellipsoid:

$$g(\varphi) = 9.7803267714 \cdot \frac{1 + 0.00193185138639 \sin^2\varphi}{\sqrt{1 - 0.00669437999013 \sin^2\varphi}} \tag{1.18}$$

On the other hand, it is interesting to highlight that the curvature of the Earth is considered even though the flown distance is relatively short. Hence, as demonstrated in [13], the angle during the glideslope is not strictly three negative degrees, but it follows the next equation:

$$\gamma_g(s) = \gamma_{ILS} + \frac{s}{2R_E} \tag{1.19}$$

where $\gamma_{ILS} = -3$ deg and R_E is the radius of the Earth (6,371 km).

1.5. Non-linear optimization problem

The optimization of an aircraft trajectory, as a 4 dimensional continuum, is a multi-phase (N phases) constrained optimal control problem (see [14]). These problems are not easy to solve since, in this case, non-linear functions appear in the definition of the objective and/or the constraints. Real-life optimal control problems cannot be solved analytically and numerical methods must be applied, such as transforming the original infinite and continuous problem into a finite and discrete problem that can be solved with Non-Linear Programming (NLP). This process is typically known as ”collocation” and has been widely used in the recent decades to solve this type of problems [15]. This section gives some basic background on optimal control problems and collocation methods to solve them numerically.

1.5.1. Optimal control problem formulation

The aim of the optimal control is to minimize a given cost function J involving the state $\vec{x}^{(j)}(t)$, control $\vec{u}^{(j)}(t)$ and non-time dependent parameter $\vec{p}^{(j)}$ vectors of each phase *j*, as defined in Equation 1.6, over all the flight phases:

$$J\left(\vec{x}^{(1)}(t),\vec{u}^{(1)}(t),\vec{p}^{(1)},\vec{x}^{(2)}(t),\vec{u}^{(2)}(t),\vec{p}^{(2)},\vec{x}^{(N)}(t),\vec{u}^{(N)}(t),\vec{p}^{(N)}\right) \tag{1.20}$$

For the computation of the optimal trajectory when requesting an RTA or triggering a re-plan due to a time or energy deviation, the objective function is given by the combination of fuel flow (FF) and speed brakes (β) contributions as follows:

$$J=\int_{t_{TOD}}^{t_f}\left(c_1 FF(t)+c_2\beta(t)\right)dt+\int_{t_0}^{t_{TOD}}c_2\beta(t)dt \tag{1.21}$$

where t_0, t_{TOD} and t_f are respectively the initial time, the time at Top of Descent (T/D) and the final time at the runway. As it can be seen, during the cruise phase the fuel flow is not taken into account in the objective function.

In order to guarantee a feasible and acceptable trajectory, several constraints have to be set. First of all, the dynamics of the system modelled with a typical non-linear point-mass of the model as defined in Equation 1.7:

$$\frac{dx^{(j)}}{dt}=f^{(j)}\left(x^{(j)}(t),u^{(j)}(t),p^{(j)}\right) \tag{1.22}$$

On the other hand, initial and final conditions (e) at the different phases (j) plus some algebraic path constraints (h) have to be verified:

$$\begin{gathered}\vec{e}_L^{(j)}\leq\vec{e}^{(j)}\left(\vec{x}^{(j)}\left(t_0^{(j)}\right),\vec{x}^{(j)}\left(t_f^{(j)}\right),\vec{u}^{(j)}\left(t_0^{(j)}\right),\vec{x}^{(j)}\left(t_f^{(j)}\right),\vec{p}^{(j)}\right)\leq\vec{e}_U^{(j)}\\ \vec{h}_L^{(j)}\leq\vec{h}^{(j)}\left(\vec{x}^{(j)}(t),\vec{u}^{(j)}(t),\vec{p}^{(j)}\right)\leq\vec{h}_U^{(j)}\end{gathered} \tag{1.23}$$

where $t_0^{(j)}$ and $t_f^{(j)}$ are respectively the initial and final time at each specific phase.

In addition, there are also simple bounds on state, control, parameter and time variables in each different phase:

$$\begin{gathered}\vec{x}_L^{(j)}(t)\leq\vec{x}^{(j)}(t)\leq\vec{x}_U^{(j)}(t)\\ \vec{u}_L^{(j)}(t)\leq\vec{u}^{(j)}(t)\leq\vec{u}_U^{(j)}(t)\\ \vec{p}_L^{(j)}\leq\vec{p}^{(j)}\leq\vec{p}_U^{(j)}\\ t_{0_L}^{(j)}\leq t_0^{(j)}\leq t_{0_U}^{(j)}\\ t_{f_L}^{(j)}\leq t_f^{(j)}\leq t_{f_U}^{(j)}\end{gathered} \tag{1.24}$$

Finally, it is important to ensure that state variables across two consecutive phases are equal. This is called the link condition and means that the final node of the previous phase has to be equal to the initial node of the next phase:

$$\vec{x}^{(j)}(t_f^{(j)}) = \vec{x}^{(j+1)}(t_0^{(j+1)}) \tag{1.25}$$

1.5.2. Collocation methods

In order to solve the presented problem, different collocation methods can be used. By applying these collocations methods, the original infinite and continuous problem is discretized and transformed to an NLP problem with a finite set of variables. The current software implementation does have the possibility to use both Euler and Trapezoidal methods.

Given the following system:

$$\begin{aligned} \dot{\vec{x}} &= f(t, \vec{x}) \\ \vec{x}(t_0) &= \vec{x}_0 \end{aligned} \tag{1.26}$$

the **Euler method** is an explicit first-order numerical procedure for solving ordinary differential equation in which the step is maintained constant. The global error produced by this method is proportional to the step size. The formula for the Euler method in order to obtain the next discretization point $(k+1)$ is:

$$\vec{x}_{k+1} = \vec{x}_k + h \cdot f(t_k, \vec{x}_k) \tag{1.27}$$

where $h = t_{k+1} - t_k$.

On the other hand, the **Trapezoidal method** is an implicit second-order numerical procedure. Thus, the global error is proportional to the squared step size. The trapezoidal method follows the following equation:

$$\vec{x}_{k+1} = \vec{x}_k + \frac{h}{2} \cdot (f(t_k, \vec{x}_k) + f(t_{k+1}, \vec{x}_{k+1})) \tag{1.28}$$

Although the two methods can be used, to obtain the results of this study, the trapezoidal collocation scheme has been used, since it has shown a good compromise between the achieved trajectory accuracy and algorithm execution time.

Thus, the original infinite and continuous problem is discretized and transformed to an NLP problem with a finite set of variables. Each phase contains several nodes separated by $\Delta t^{(j)}$ being $M_0^{(j)}$ the initial node of the phase j and $M_f^{(j)}$ the final node of the phase j. This leads to a total of K nodes.

Hence the discretized cost function for the Trapezoidal method is:

$$J = \left[\sum_{\substack{j=1 \\ j \neq crz}}^{N} \Delta t^{(j)} \sum_{i=M_0^j}^{M_f^j} \left(c_1 \cdot \frac{FF^{(i)} + FF^{(i+1)}}{2} + c_2 \cdot \frac{\beta^{(i)} + \beta^{(i+1)}}{2} \right) \right] + \left[\sum_{\substack{j=1 \\ j = crz}}^{N} \Delta t^{(j)} \sum_{i=M_0^j}^{M_f^j} \left(c_2 \cdot \frac{\beta^{(i)} + \beta^{(i+1)}}{2} \right) \right] \quad (1.29)$$

1.5.3. Non-linear programming (NLP)

An NLP problem, as mentioned in [16], can be mathematically expressed as:

$$\text{Minimize } J(x) \quad (1.30)$$

$$\text{Subject to } g(x) \leq 0$$
$$L \leq x \leq U$$

Hence, an NLP problem requires finding a finite number of variables *x* (in this case, the state and control vectors at each collocation node plus the parameter vector), which are bounded within certain values *L* and *U*, in order to optimize an objective function *J(x)* without violating a set of constraints *g(x)*, which are the constraints explained in subsection 1.5.1., at each collocation node, plus the algebraic constraints that are obtained when applying the collocation process explained in subsection 1.5.2. in the set of differential equations (see Equation 1.22).

Unlike Linear Programming (LP), the function to optimize and the set of constraints do not need to be linear; they can be squared constraints, logarithmic, quadratic... A special case of the NLP is the Quadratic Constrained Programs (QCP), in which all the non-linearities are quadratic.

Consequently, in aircraft optimization, NLP model is used since a lot of flight mechanics equations are nonlinear. In fact, NLP is extremely useful since all the implied functions are smooth. Hence, non-smooth functions such as abs, min, max cannot be used in such a model. The problem is that sometimes it is necessary to use them and, then, two options are available:

1. To use the Nonlinear Programming with Discontinuous Derivatives (DNLP) type. This model type can be solved by most of NLP solvers but they attempt to solve the DNLP model as if it was an NLP model. The fact that some of the derivatives may change discontinuously is ignored [17]. This leads to the second option in most cases.

2. To solve a DNLP model is necessary to reformulate the model as an equivalent smooth NLP model. Smooth approximations can also be used. An example that occurs in our model is left in section 3.6..

To sum up, the used model type is NLP since nonlinear equations with real variables are involved and it is desired have a smooth behavior. A good reading for the nonlinear programming problems is the book from Betts [15], where most methods are explained accompanied with some optimal control examples.

1.6. Addition of two new phases in the descent profile

In this section, the addition of two useful phases respect to the CONCORDE experiments [13] is explained. They are not strictly part of the strategic or tactical implementation, but they have considerably changed, and improved, the vertical and speed profile (and FASTOP algorithm in general). These new phases are:

- **FPA phase**: It is a phase in which a flight path angle is maintained with constant casdot. In the current case, it is added just before the interception of glideslope. Hence, there is a FPA from 2NM earlier up to the glideslope. The aim of this phase is to ensure the interception of the glideslope. This purpose is achieved by setting a FPA of around -1 deg (less steepness than the -3 deg of the glideslope).

- **GS_THR**: This is a phase during glideslope in which thrust is inserted in order to maintain the derivative of speed within reasonable values. This is done with a simple loop that tries different values of throttle starting with a logical one (22 %). Thus, the thrust is changed during this phase according to this principle. It begins at Final Approach Point (FAP) and ends when achieving the speed of F-LND deployment. This phase is implemented so it is done without constant CAS. By doing so, two basic aspects are achieved:

  – Give more freedom to the optimizer.

  – Make the change of flaps when reaching a given CAS and not wait until the end of phase with the same speed as it was previously implemented.

  It is interesting to see the equation used in this phase to compute the thrust in subsection 1.4.1..

CHAPTER 2. SOFTWARE PACKAGES

This project has used different software modules, which are displayed in Figure 2.1.

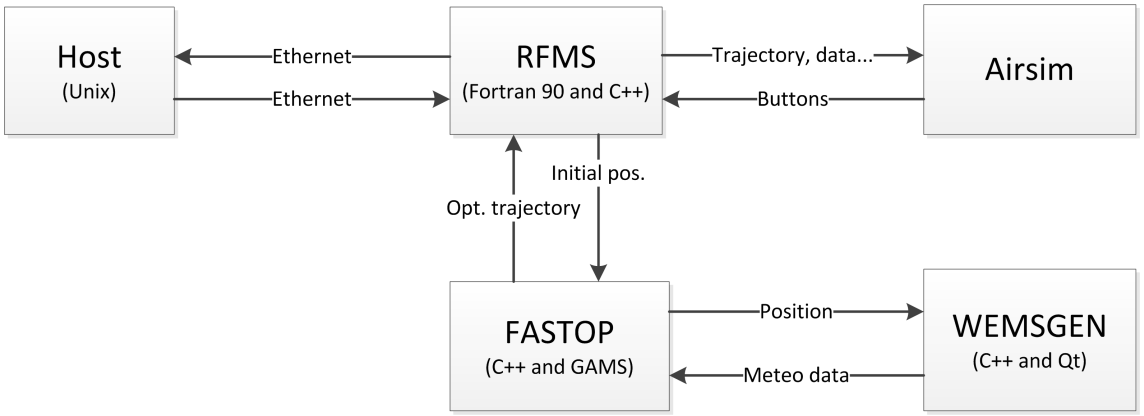

Figure 2.1: Diagram of all the involved modules

In this chapter each module is explained in detail. However, it is important to bear in mind that the packages that have been modified in order to obtain the results of this project have been the Research Flight Management System (RFMS) and FASTOP.

Some other tools have been also used such as: Subversion (SVN), Unix, Gnuplot, Ethernet network of the NLR, .bat files, Visual Basic scripts, Excel macros... They are not explained here because they are beyond the scope of this document, but some of the used documentation can be found in reference [18], [19], [20] and [21] respectively.

2.1. RFMS

The RFMS is an application from NLR (see its manual [22]) which tries to simulate as close as possible the behavior of a real FMS and that is used for research purposes.

The RFMS is used with other NLR applications (some of them explained in the following sections) via Ethernet [21]. Thanks to the RFMS, it is possible to plan flight routes, comply with RTAs, select a specific mode such as the approach mode, set a guidance mode such as speed on elevator and so on. Hence, it is necessary to study its code to develop an algorithm for the guidance of time deviations.

In order to have a better understanding of all the features of a real FMS, the FMS Pilot's Guide of the A320 [23] has been used. Although its functions are not going to be explained because it is out of the scope of this report, this guide has been useful to deeply understand the capabilities of a real FMS. In Figure 2.2, it can be seen the interface of the RFMS and the Management Control Display Unit (MCDU), in which the user can navigate through the typical MCDU pages such as "F-PLN", "PERF", "INIT"... Going component by component in the aforementioned figure, the following elements can be found:

1. **Console outputs**: The pressed keys and results from FASTOP.
2. **Error messages**: Messages that usually indicate to stop the program.

3. **Warning messages**: The user is warned about some issues but there should be no problem to continue with the simulation.

4. **MCDU**

5. **Footer**: It includes the configuration file, the number of host that the user is using, the ICFPNO, which is the reference number to the used scenario, and the ”keystack” file, which contains the keys which need to be pressed before initializing the RFMS in order to free the user from this hard and tedious work.

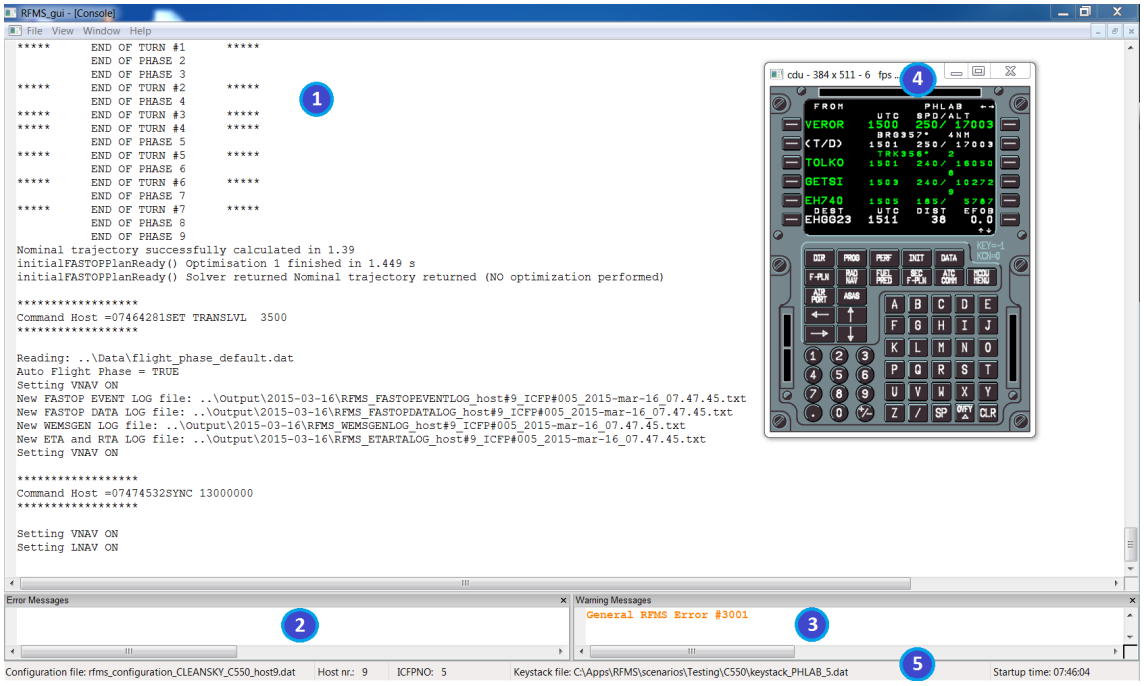

Figure 2.2: RFMS GUI and the MCDU

The RFMS is mainly coded in Fortran 90 (see book from Merchant [24]), except from some recent files written in C++ (see [25] and [26]), especially files needed for the communication with FASTOP. This means that the RFMS uses a mixed language programming.

2.2. Host

The Host simulates the aircraft dynamics and also the autopilot functionality. It is run in a Unix system and can be accessed through Ethernet.

It is basically the module that makes possible to fly in a nearly real world so it is important that FASTOP matches the model used for the Host. Otherwise, the optimal trajectory is not going to be correctly followed during the simulations.

For the host aircraft model, a tool called “Eurosim” is used. It can be seen in Figure 2.3.

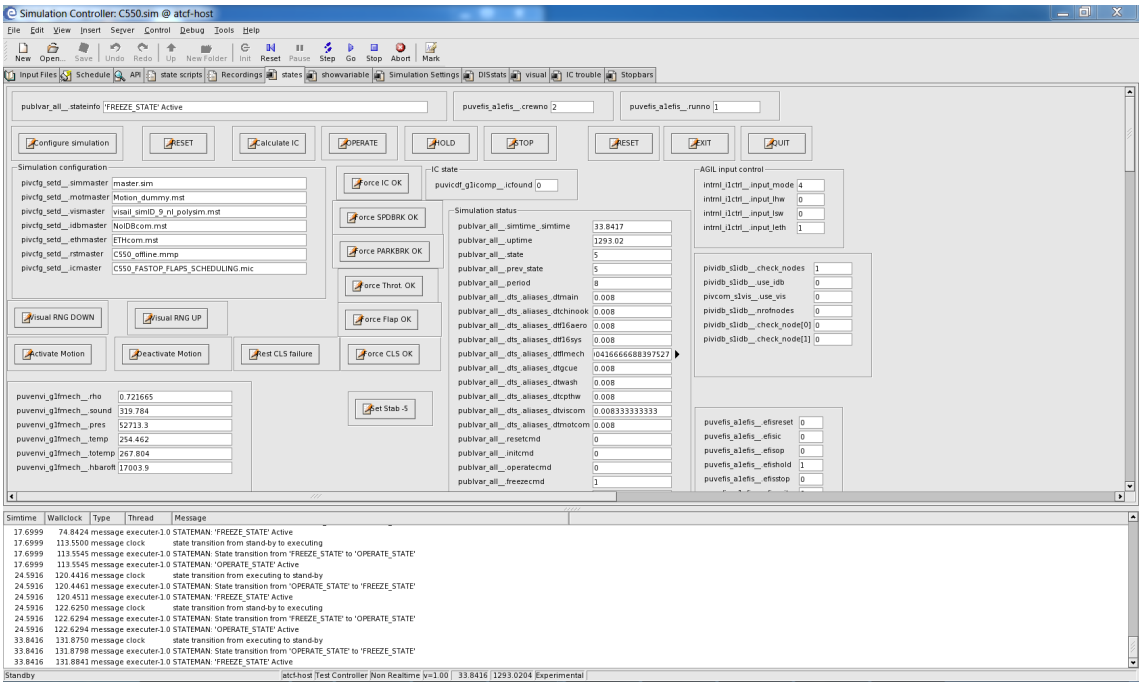

Figure 2.3: Eurosim aircraft model interface to control Host

2.3. Airsim

Airsim is an NLR application that can simulate the cockpit displays of a wide variety of aircraft. Through a connection with Ethernet, the RFMS and the Host can send data to the Airsim application, which then displays this information.

Hence, Airsim displays the information from both the RFMS and Host. At the same time, when pressing Airsim panel buttons, some kind of information is passed to the RFMS, which processes the received information and sends data back.

The displays of the Airsim that are used in this project are left in Figure 2.4.

1. Chronometer
2. PFD
3. Mode Control Panel (MCP)
4. Navigation Display (ND)
5. Display of the engine performance and, if the user switches the screen (with ”L” button of the keyboard), the speed brakes and flaps
6. Energy display: The x-axis is the time deviation (s) and the y-axis the energy deviation (ft)
7. Throttle quadrant

Figure 2.4: Airsim displays

2.4. FASTOP

FASTOP is the third implementation of the TEMO concept; the first two have been GPOPS and PSOPT respectively. It is a dynamic library, written in C++ and GAMS by the FASTOP consortium (GTD, UPC, ASCAMM), which is used by the RFMS to compute the nominal and optimized descent trajectories of a flight (see [8] and [27]).

First of all, FASTOP computes a nominal trajectory from an initial position and speed given by the RFMS. Then, when an RTA is demanded or the energy goes out of bounds, an optimized trajectory is computed by FASTOP using the CONOPT solver.

Since FASTOP is of relevant importance in this project and, in fact, it has been improved during the course of this project, the main characteristics of this dynamic library are going to be briefly described.

To start with, FASTOP includes a project called **fastop**. This module is responsible for the calculation of the nominal trajectory and serves as glue between the RFMS and the optimizer.

The nominal trajectory is a first guess to the optimal solution. Despite not being optimal, it is computed in the most precise possible manner since, in NLP problems it is of considerable importance to give the optimizer a good guess to start the process [15]. Giving a good guess to the optimizer can dramatically reduce the time of optimization. However, since NLP solvers cannot guarantee a global solution, different initial guesses can lead to different suboptimal solutions. This nominal trajectory is also needed for the first display of the trajectory in the RFMS, when not having optimized yet. After having obtained one optimized trajectory, the guess passed to the NLP solver is the current plan flown by the aircraft.

The aforementioned first nominal trajectory is computed with backwards integration from the threshold of the runway. The following features/assumptions are included in the **fastop**

project:

- Two types of aircraft can be simulated: A320 and C550 with their particular characteristics and performance coefficients. This project makes use of the C550.
- The atmosphere can be selected to be ISA or real. If real atmosphere is the user choice, then WEMSGEN (see section 2.5.) is called in order to read and process the GRIB files. In this manner, FASTOP can deal with a real atmosphere. To use WEMSGEN, it is necessary to link the **fastop** project to a static library called **einspline**, which is able to deal with splines and, in particular, B-splines.
- The Earth can be modeled as flat or spherical. The last option is the default one. It appears unimportant to consider spherical Earth in descents, where the traveled distance is not so much, but it makes difference, for instance, in the interception of the glideslope.
- A trajectory with turns can be modeled with the correct value of bank angle and aerodynamic heading.
- All the computed data in the nominal trajectory is passed to GAMS through writing in a GDX file by virtue of the static library called **gamsapi**.

For the manipulation of data in matrices and vectors, a static library called **DMatrix** is used, which helps providing some functions to manage vectors with a similar nomenclature to *Matlab*.

Then, in order to call the solver, the aircraft is modelled with GAMS; this is the **gams** project of FASTOP. Some of the equations are really similar to the equations involved in the **fastop** project, but the aim of the **gams** project is to minimize the fuel consumption and the usage of speed brakes.

It is also necessary to manage inputs and outputs. The input data is:

- CSV data for the performance of the aircraft. A spreadsheet is available for both the A320 and the C550. These coefficients are more exact than the ones given by the Base of Aircraft Data (BADA) model of EUROCONTROL.
- GDX input file: Data sent to GAMS.
- Environment data file: To know the path of GAMS and FASTOP.
- Knobs data file: A file with all the options the user can activate.
- Profile data file: The phases of the descent with constraints of speed, altitude, time...
- Route data file: File with the waypoints of the route.

The output from the FASTOP library is:

- A file with the values of the variables of the nominal trajectory (distance, altitude, CAS, flight path angle, wind, thrust, drag...) at all the collocation points. This includes state, controls and extended variables.

- A file with the value of the variables after the optimization with GAMS, which will be the actual flown plan.
- The routes of, respectively, the nominal and optimal trajectory in *KML* format. They can be opened with *Google Earth*. These .kml representations have been improved during the current project. Instead of using headings and its subsequent precision errors to compute the turns, now turns are computed converting first the latitude/longitude to UTM and then applying circle formulas, which gives much better results.

With the data files, several graphs can be plotted with the aid of *Gnuplot* (see the manual at [20]). Scripts ".plt" or ".gp" files have been developed so that the researcher does not have to issue the *Gnuplot* commands manually every time. In fact a batch file can be made to take the correct input file and run all these ".plt" files every time it is desired.

Figure 2.5 displays the different modules involved in FASTOP library.

As it can be seen in the mentioned figure, GAMS language is used for the optimization part of FASTOP.

GAMS is a high-level language for the compact representation of large and complex mathematical models. In other words, by using the programming language GAMS, a model (with equations, variables, sets...) of some field of the reality can be represented and optimized with the aid of all the available solvers that GAMS dispose of. There are other optimization languages in the market, not used herein but of considerable relevance such as AIMMS; see [28] for a complete list of mathematical modeling tools with their pros and cons.

In this project, GAMS is used by FASTOP to model all the aerodynamic, atmosphere, earth... equations for the descent of an aircraft. Moreover, the used solver is the commercial "CONOPT" (see its home page [29]) since it has proven to be really fast in our NLP model. All the information to consider about this solver when writing down a given model can be found in "The Solver Manuals" [30].

CONOPT is a solver specialized in NLP models (see [17] for a complete list of all the model types that this and other optimizers can solve). On average, in FASTOP, there are around 4000 variables to optimize, such as x, v, h, γ, $\dot{v}$, $\dot{x}$, $\dot{h}$, FF, C_D..., with constraints given by equations and physical bounds such as limiting operations.

In order to dynamically schedule the high-lift devices in the strategic mode, it is essential to understand the aforementioned language and how to correctly add the contribution of flaps and gear inside the model. All the details of this language can be found in the manual of GAMS: GAMS User's Guide [31].

For further understanding of the FASTOP library, documentation of FASTOP can be found in reference [13], [27] and [32].

2.5. WEMSGEN

WEMSGEN is an application that is able to read input GRIB files of a given region of the Earth. After reading the files that the user has selected, the "wemspline" library is called. This library contains the necessary functions that FASTOP needs to call in order to include

the real atmosphere in its model. Hence, FASTOP can obtain from WEMSGEN variables such as:

- w_n: Value of the north component of wind speed for a given geographical position.
- w_e: Idem for the east component of the wind.
- χ_a: Direction of the wind for a given position
- $|w|$: Absolute value of the wind speed magnitude for a given position.
- $\frac{\partial w_n}{\partial s}$: Derivative of the north wind component with the distance.
- $\frac{\partial w_e}{\partial s}$: Idem for the east component of the wind.
- $\frac{\partial w_n}{\partial h}$: Derivative of the north wind component with the altitude.
- $\frac{\partial w_e}{\partial h}$: Idem for the east component.
- τ: Temperature of a given geographical position.
- $\frac{\partial \tau}{\partial h}$: Derivative of the temperature with the altitude.
- p: Pressure of a given geographical position.
- $\frac{\partial p}{\partial h}$: Derivative of the pressure with the altitude.

Besides reading the GRIB files, WEMSGEN is also able to introduce wind prediction errors (offsets) in the direction and magnitude of wind and in the pressure and temperature variables. This is useful to test applications in real scenarios, where we never have the same value of winds as obtained from the GRIB files.

In Figure 2.6, a screenshot of the WEMSGEN interface can be seen.

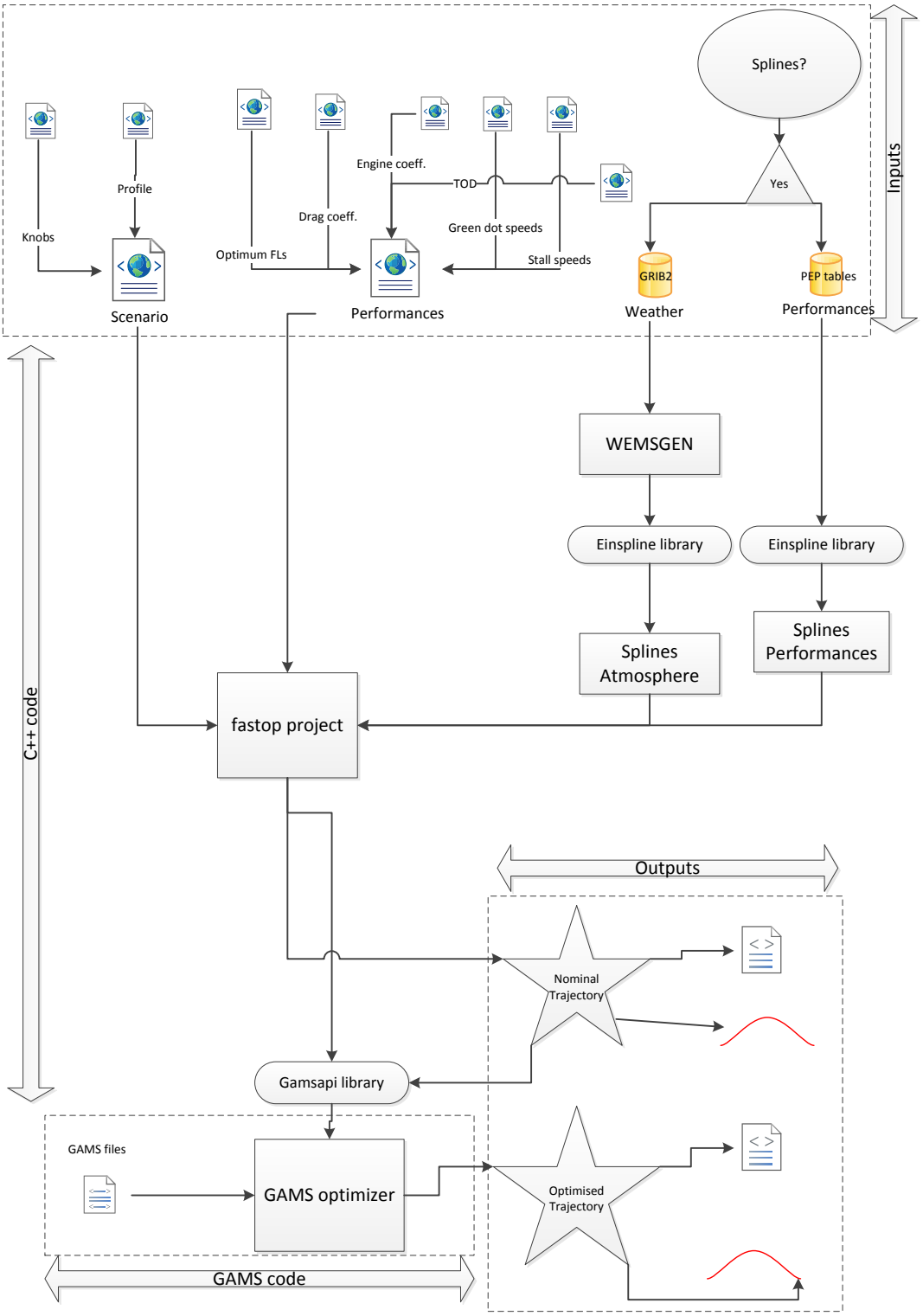

Figure 2.5: Involved modules in the FASTOP library

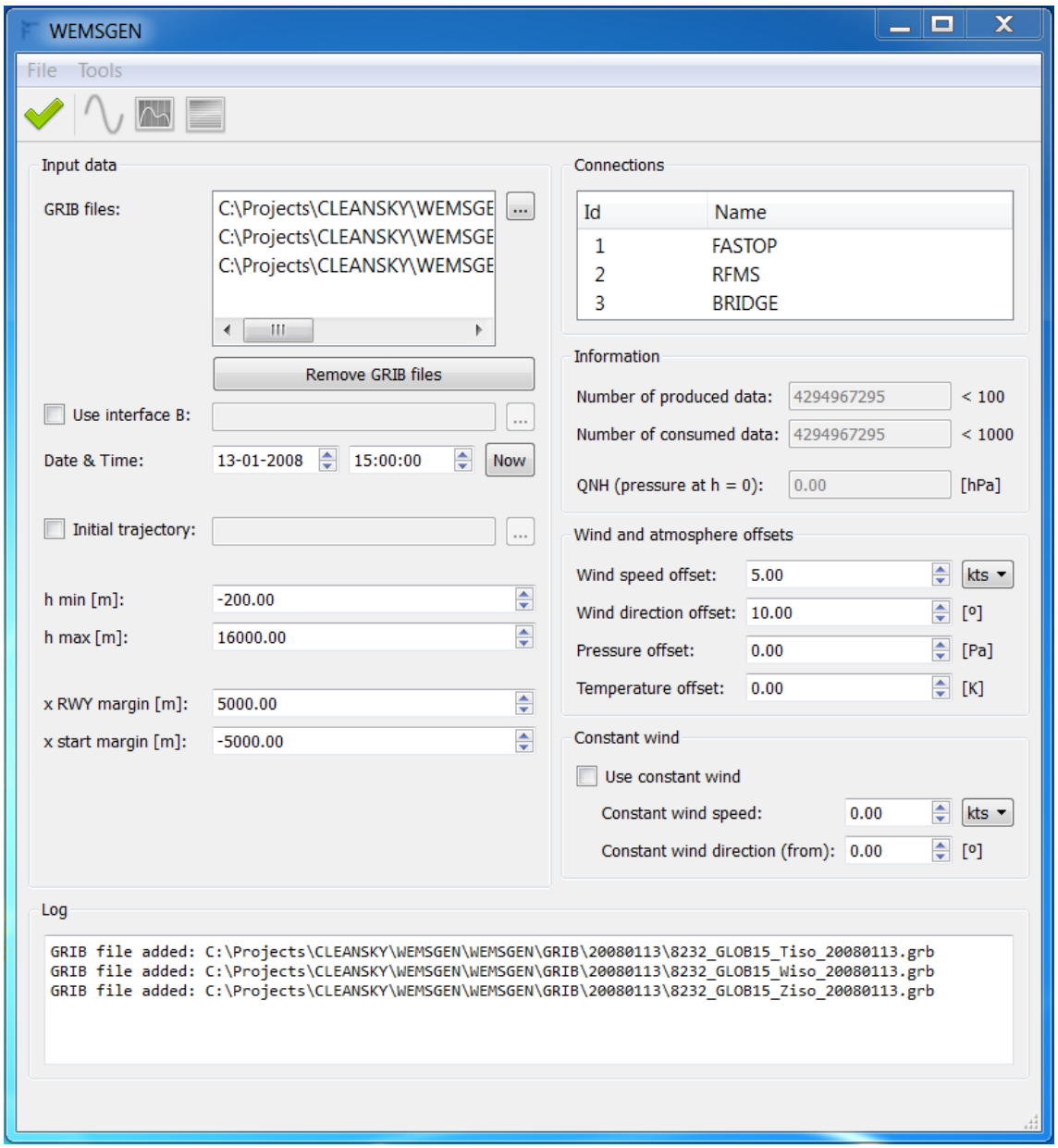

Figure 2.6: WEMSGEN interface

CHAPTER 3. IMPLEMENTATION OF A STRATEGIC SOLUTION TO SCHEDULE HIGH-LIFT DEVICES

As explained before, a trajectory re-plan occurs when the aircraft needs to update its optimal descent trajectory due to one of the following causes:

- An RTA is required by the ATC.
- The energy (see section 1.1. for its complete definition) of the aircraft goes outside the energy bounds, which dynamically change during the descent. This margin starts with $\pm$ 500 ft at T/D and it is reduced linearly down to $\pm$ 200 ft at IAF and $\pm$ 100 ft at the runway threshold.
- The time deviation exceeds $\pm$ 15 s at T/D, $\pm$ 10 s at IAF and $\pm$ 5 s at the RWY. These margins are also reduced linearly.

Thus, in a re-plan, the RFMS calls FASTOP in order to compute a new (optimal) trajectory. Hence, this is considered a strategic control since the time and energy are not continuously nullified by acting on the controls.

So far, in order to comply with the given RTA or the required energy/time, the aircraft could change thrust, speed brakes and/or Flaps Approach (F-APP)[1] deployment moment. This was because in the previous implementation of TEMO only the phases until flaps approach could be optimized. Phase 4 (for C550) was assigned to F-APP, phase 3 to gear and phase 2 to Flaps Landing (F-LND). Thus, in the previous implementation, phase 4 was the last optimized phase and the gear and F-LND remained always in the same position. See Table 1.1 for a complete overview of the phases used in this project.

The new strategic implementation considers the glideslope segment up to the stabilization point, makes the optimization of the gear flexible through the whole flight, implements a "time to next configuration" and improves, in general terms, the speed/convergence of the optimization algorithm.

The stabilization point is defined as the point at 1000 ft when the aircraft has to be already correctly configured to land. Hence, not only changes of thrust and speed brakes are considered but also changes on the moment/time of the deployment of the F-APP, gear and F-LND[2].

The typical sequence of deployment of the aircraft devices in a C-550 is F-APP, gear and F-LND. However, in this project, to let having more freedom, the gear will be free (according to the optimization) between two constraints. These constraints are:

- First possible point: When CAS below 250 kt
- Last possible point: When 1500 ft are achieved

[1] In C550, F-APP means a deployment of flaps of 15 degrees.
[2] In C550, F-LND means a deployment of flaps of 40 degrees.

In this manner, the gear, which is an important control parameter to influence the energy state of the aircraft, can contribute to change the aircraft energy and/or achieve a specific RTA along the entire route.

It is worthwhile noting that before intercepting the glideslope, the autopilot uses speed on elevator to control CAS changing the altitude as necessary; hence, energy deviations occur basically due to the contribution of potential energy. After intercepting the glideslope, the autopilot actives g/s on elevator in order not to have deviations in altitude and the autothrottle can command thrust to maintain the required speed. Then, deviations of the RTA can easily occur in this last phase of the flight since the engines are not as fast as the elevator in following the commanded speed.

In the following subsections, it is explained the necessary changes undertaken both in FASTOP and RFMS programs in order to include the effect of all the flaps/slats and the gear. Bear in mind that other generic improvements have been applied during the course of this project such as the one explained in section 1.6..

In the strategic implementation, FASTOP is the most affected project because it is in charge of the re-plans. See section 2.4. for a complete understanding of this library.

3.1. Added knobs (user options)

In order to implement the strategic solution, three new knobs have been added.

The user has the option to set the ”time to next configuration”, which is defined as:

> **(Time to next configuration)** *It is the minimum time between the initial position of the new plan and the most immediate configuration change (flaps or gear).*
>
> *If the aircraft is within this minimum time, then no aircraft configuration can come earlier than the aforementioned most immediate configuration change. However, any configuration can go further this point.*

For instance, if the aforementioned time is 1, it means that within a minute from the next configuration change, the aircraft will not be able to have any configuration change before the most immediate configuration change after optimizing. This time is implemented so that the pilot is not surprised with the new position of deployment of the high-lift devices.

On the other hand, the user has the option to make dynamic or not the moment the gear is deployed. In the dynamic case, the gear down action does not depend on any phase while if it is fixed, it is associated to a given phase (the phase between F-APP and F-LND in the case of the C550). For the dynamic scheduling of high-lift devices, gear deployment does not depend on the phase.

Finally, the optimization process can be solved as an NLP or Mixed Integer Nonlinear Programming (MINLP) (see section 3.6. for the reason of this knob).

3.2. Location of flaps and gear

The baseline strategic implementation had two main drawbacks:

- If phases (see Table 1.1) of the input profile file were added or removed, it could occur that the program computed the aircraft configuration erroneously. If, for instance, an extra phase was added between F-APP and Gear, then F-APP did not correspond to phase 4 anymore. Then, it should have been phase 5.
- It did not enable to have a flexible gear which was independent of the phase.

In order to fix these two problems, the following changes have been undertaken:

- First the input profile file is read and by looking into the attribute ”phase.config” and ”phase.gear”, it is possible to know which phase corresponds to which configuration. Thus, it is independent of the input file.
- The previous action is fine for flaps, but for gear it is desired not to depend on the phase. Then, if flexible gear is activated, gear is assigned to the first phase in which indicated airspeed (IAS) is less than 250 kt and it can be deployed at any point from this phase until 1500 ft of altitude. It does not necessarily have to be activated at the beginning of a phase, but it can be deployed at any collocation node (inside the aforementioned limits) of the descent trajectory (see section 3.4. to know how this is achieved).

3.3. Algorithm for minimum time to next configuration change to re-schedule the aircraft configuration

As said in subsection 5.2.4., the experiment will also include a time to next configuration. For instance, if this time is 1 minute, there are two options:

- If the initial position of the new plan is further than 1 minute from the most immediate aircraft configuration (before re-planning), all the flaps/gear can be optimized.
- If the initial position of the new plan is less than 1 minute from the most immediate aircraft configuration (before re-planning), no configuration can come before the aforementioned most immediate aircraft configuration.

Then, the flowchart of the algorithm is displayed in Figure 3.1.

Hence, if all the cases are validated, the earliest possible distances of flaps and gear, and the index of next flaps configuration are obtained. When referring to the gear distance, it is the switching distance (see section 3.4.). This variable is computed after an interpolation. The corresponding *if* statement is valid for any value of gear higher than 0.5, but the gear should be deployed exactly when 0.5, which usually does not correspond to any collocation point.

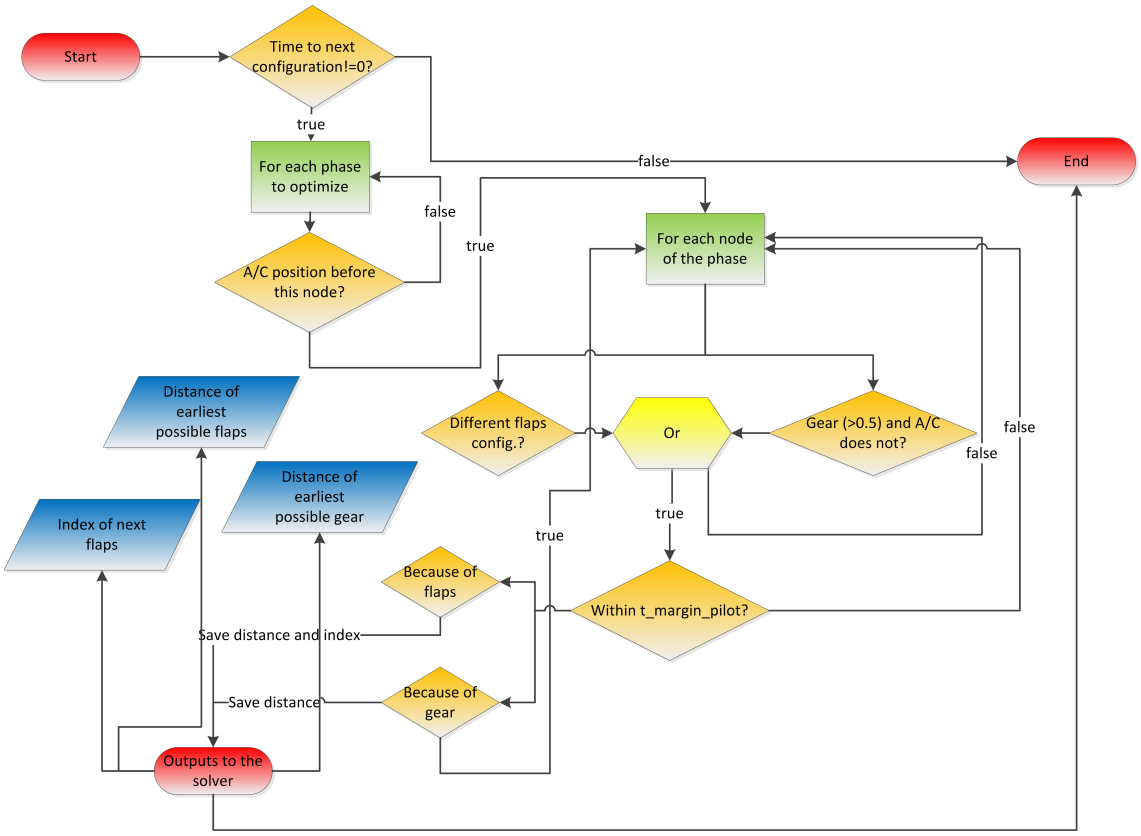

Figure 3.1: Algorithm of time to next configuration

In order to refine the algorithm, an interpolation is undertaken with the following formula for the collocation node where gear is higher than 0.5:

$$x_{configsc} = \frac{(x_{plan_i} - x_{plan_{i+1}}) \cdot (0.5 - \beta_{gear_i})}{\beta_{gear_i} - \beta_{gear_{i+1}}} + x_{plan_i} \tag{3.1}$$

Where i is the corresponding collocation node, β_{gear} takes values from 0 to 1 and represents the deployment of gear and x_{plan} is the distance, negative, of the planned node.

Then, these aforementioned variables are passed to GAMS in order to fix the distance of the correct collocation node. This results in an exact value for flaps and nearly exact result for gear since interpolation is obviously not perfect.

3.4. Switching gear function

In the previous TEMO implementation, the moment the gear was deployed was known because this action was performed at the end of a phase. In the new implementation a switching function has been implemented to model the gear contribution. Thus, two new variables have been defined: $\beta_{gear}(t)$ and x_{sw}.

$\beta_{gear}(t)$ ranges from 0 to 1 and represents the gear status in a similar way as $\beta(t)$ does it for speed brakes (0 gear up and 1 gear down). On the other hand, x_{sw} represents the

switching distance, where the gear is deployed.

For numerical reasons, the switching function must be continuously and differentiable at least two times. Thus, step functions cannot be used to model gear contributions. In this project the *arctan* function has been implemented since it presents a good numerical behavior:

$$\beta_{gear}(t) = \frac{1}{2} + \frac{1}{\pi} \cdot \arctan\left(K_\beta \cdot (x(t) - x_{sw})\right) \tag{3.2}$$

Where K_β is the slope that can be adjusted to model, somehow, the time that the gear takes to be deployed. In this project we have chosen K_β=0.003 because it has been proven to behave well, after some tests, in our model. It is the correct value in order to have some collocation nodes in the step and reaching the value of 1 within a reasonable distance.

The switching distance must lie between 1500 meters before reaching 1500 ft of altitude and 1500 meters after reaching 250 kt of CAS. Moreover, when the aircraft is not in the gear set, beta must be 0. The margin of 1500 m is left in order to leave the *arctan* enough space to reach 1 and 0 values. This is done because it can occur that the *arctan* function does not exactly take 1 at this distance (maybe 0.98 or so).

The gear function $\beta_{gear}(t)$ can be plotted with a GDX viewer file coming from GAMS with a result similar to the one displayed in Figure 3.2.

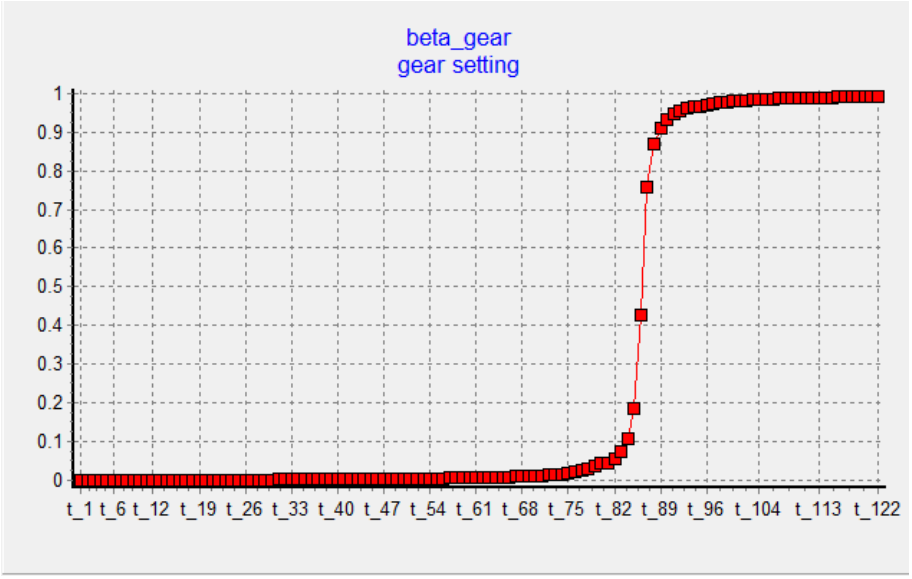

Figure 3.2: Example of the arctan function in a given scenario

3.5. ILS flight path angle constraint

It is necessary to include a constraint related to the flight path angle, which was not necessary so far since the glideslope was not optimized. However, now a part of the glideslope is optimized and it is not desired to have any possible value of flight path angle in this

region. This angle has to be adjusted to -3 degrees allowing some deviation to avoid possible numerical inaccuracies during the optimization. Instead of using γ, the altitude of the glideslope has been constrained in the following manner:

$$h_i = h_{i-1} + \tan\left((-3 \pm \Delta_{ILS}) \cdot \frac{\pi}{180} + \frac{x_i}{2R_{earth}}\right) \cdot (x_i - x_{i-1}) \tag{3.3}$$

As it can be seen, the curvature of the Earth is taken into account as shown in subsection 1.4.4.. Moreover, the margin (Δ_{ILS}) left when having wind is larger than in ISA atmosphere since when wind is present, the flight path angle respect to the air does not have to be necessarily -3 deg. This phenomenon is correctly explained by De Prins [33]. The addition of wind generates a small difference between ground flight path angle γ_g and the aerodynamic flight path angle γ_a. Assuming no vertical wind component, there is the following relationship between the aerodynamic and ground angle [13], which corresponds to the exact -3 degrees of the ILS glide path if the Earth's curvature is not taken into account:

$$\gamma_a = \arcsin\left(\left(\sqrt{1 - \bar{w}_x^2 - \bar{w}_s^2 \sin^2\gamma_g} + \bar{w}_s \cos\gamma_g\right) \sin\gamma_g\right) \tag{3.4}$$

Where $\bar{w}_x$ and $\bar{w}_s$ are, respectively, the cross and along track component of the wind normalized with the true airspeed.

In the case of the Cessna Citation, due to the low speed compared to other aircraft, there can be a difference of around 0.5 degrees when facing 20 kt of headwind, as it happens in our real atmosphere scenarios. This can be seen in Figure 3.3, where the value of the aerodynamic flight path angle is around -2.5 degrees.

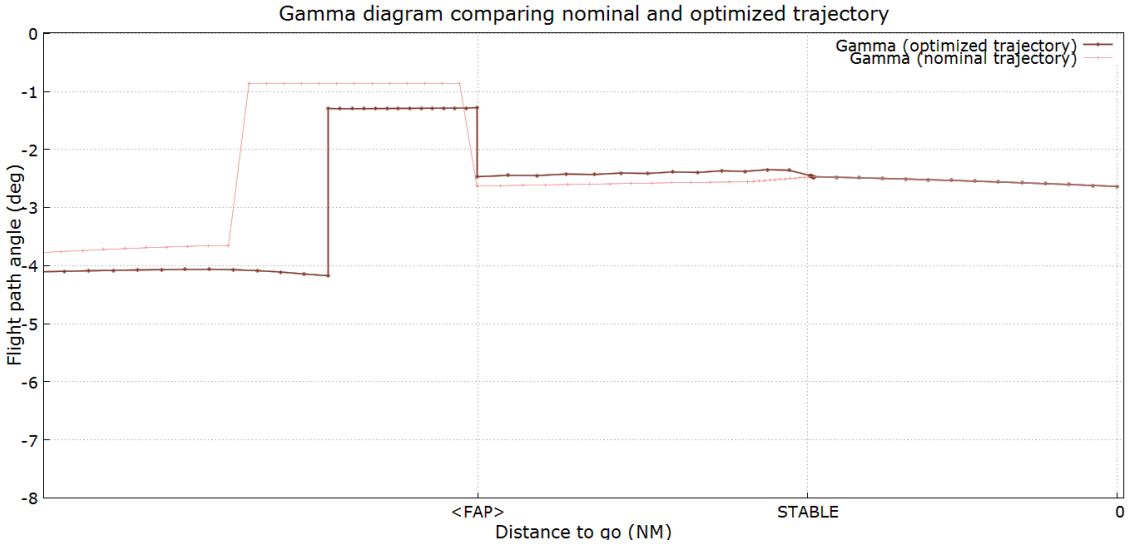

Figure 3.3: Flight path angle profile for a real weather scenario with wind prediction errors

3.6. Constraint of time between configurations

As previously said, in the current implementation of TEMO, gear can be activated anywhere from IAS 250 kt to an altitude of 1500 ft. Thus, the optimizer could lead to a solution where F-APP and gear are too close to each other. To avoid such kind of situation, a constraint has to be inserted in order to leave 15 s between gear and any flap configuration (F-APP or F-LND). The reasons behind this are:

- The pilot needs some time between aircraft configurations to correctly answer.
- The cue indicating Gear or Flaps last 10 seconds

This constraint is not easy to implement in GAMS; see Appendix C for the workaround used in order to include the aforementioned constraint.

3.7. Correct display of TCPs and cues

RFMS changes, for the strategic case, are basically related to the display into the navigation display of the improvements done in the FASTOP project. TCPs are the points displayed in the ND representing the different nodes of the route, which indicate for instance when flaps or gear have to be activated. On the other side, 10 seconds before reaching these TCPs, a timer cue is activated. This cue is a timer that when reaching the TCP starts to flash.

Until now the gear was related to the initial node of a phase. Now, it can be in any collocation node. Hence, it is needed to implement a search algorithm in order to find the node where gear is activated and save this. It is also important to highlight that in order to have the gear at any node, an unused extended state has been filled (similar to the extended state of speed brakes), which was devoted to the gear but was not used since the gear was known by its phase.

The algorithm to obtain the aforementioned node ID (called ”ipntgear_”) is displayed in Figure 3.4.

Note that the possibility of having two consecutive special name nodes has not been considered. By “special” we are referring to nodes with a name, such as the IAF ”TOLKO”, and not with simply the number of node on it. In fact this possibility is really rare since waypoints are not usually one next to the other one in terms of TCP.

Finally, the algorithm of triggering the cue has been modified since so far the sequence of aircraft configuration was fixed, meaning that the software always expected to occur first F-APP, then the Gear and finally F-LND.

The flowchart displayed in Figure 3.5 shows this algorithm, in which the next TCP is continuously monitored when flying. In order to understand the aforementioned diagram, some variables needed to be described first:

- ipnt+”X”: It is the node (for instance, 75) of the ”X” configuration (gear, flap1 or flap2). A higher number means earlier in the descending trajectory.

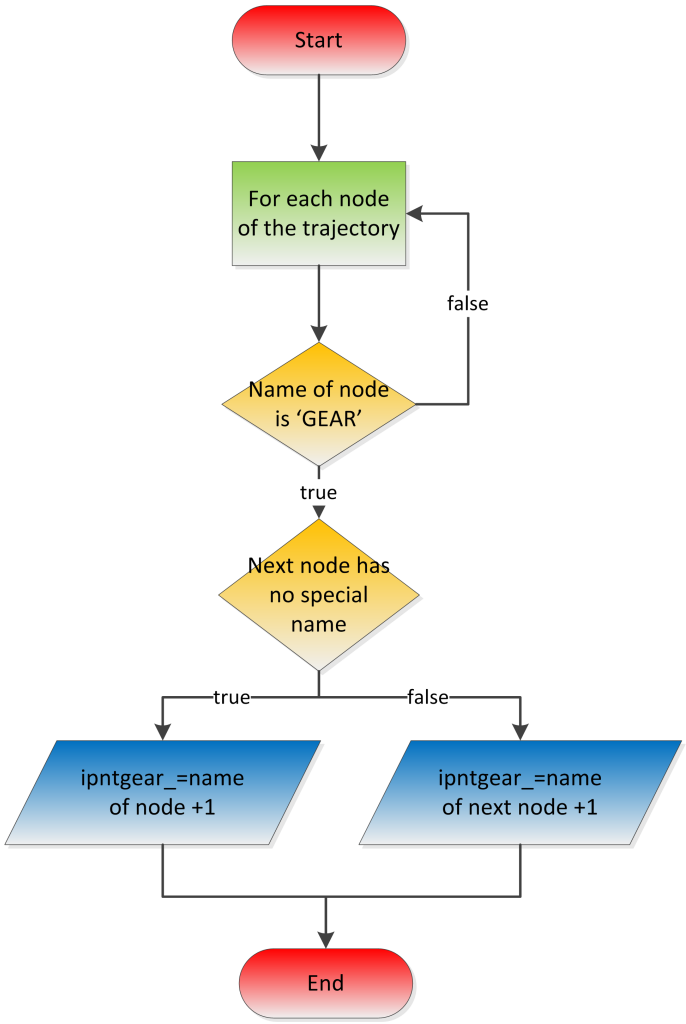

Figure 3.4: Flowchart for the algorithm to obtain the ID of gear node

- ”SFCC1FSCONF” takes value 0 if F-APP has not been passed, 4 if F-APP has been passed and 7 if F-LND has been deployed.

The validity of this algorithm has been tested and it has succeeded in displaying correctly all the following sequences in the ND of the aircraft:

- **F-APP, GEAR and F-LND**
- **GEAR, F-APP and F-LND**
- **F-APP, F-LND and GEAR**

With this algorithm, the RFMS code has been maintained as close as possible to the original one.

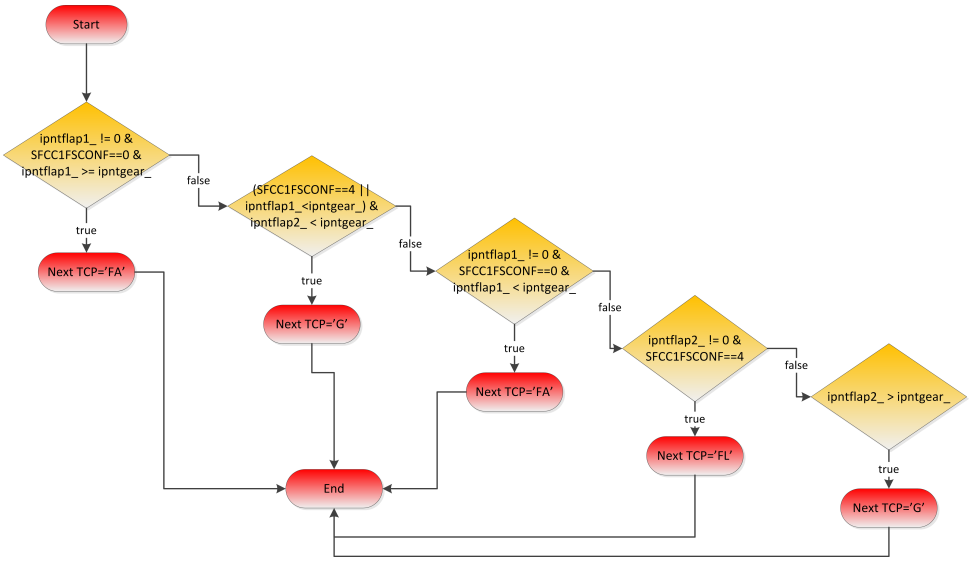

Figure 3.5: Flowchart for the algorithm to monitor next TCP

3.8. Plotting a given strategic re-plan

To better understand how the strategic solution works, an example is given herein. In order to see that the gear can come earlier than F-APP, an RTA of +60 seconds respect the nominal Estimated Time of Arrival (ETA) is given. The scenario is simulated in ISA atmosphere. In Figure 3.6, it can be seen the trajectory before and after the strategic re-plan. The optimizer has set the gear before F-APP and the T/D is closer to the aircraft.

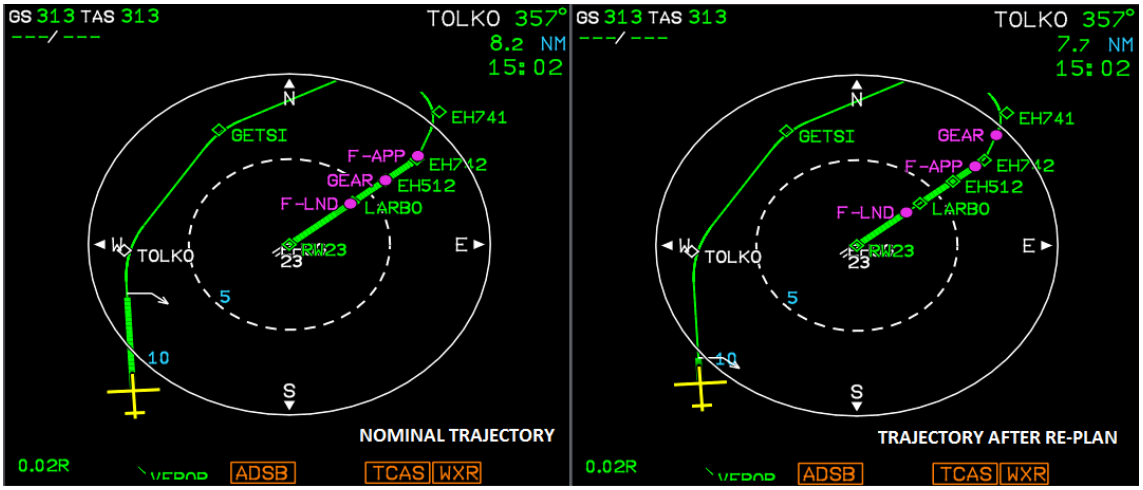

Figure 3.6: Comparison between nominal (left) and optimized trajectory (right)

In Figure 3.7, the vertical and CAS profile is given. As it can be seen, the speed of the optimized trajectory (bold one) is reduced in the entire trajectory in order to arrive 60 seconds later to the runway.

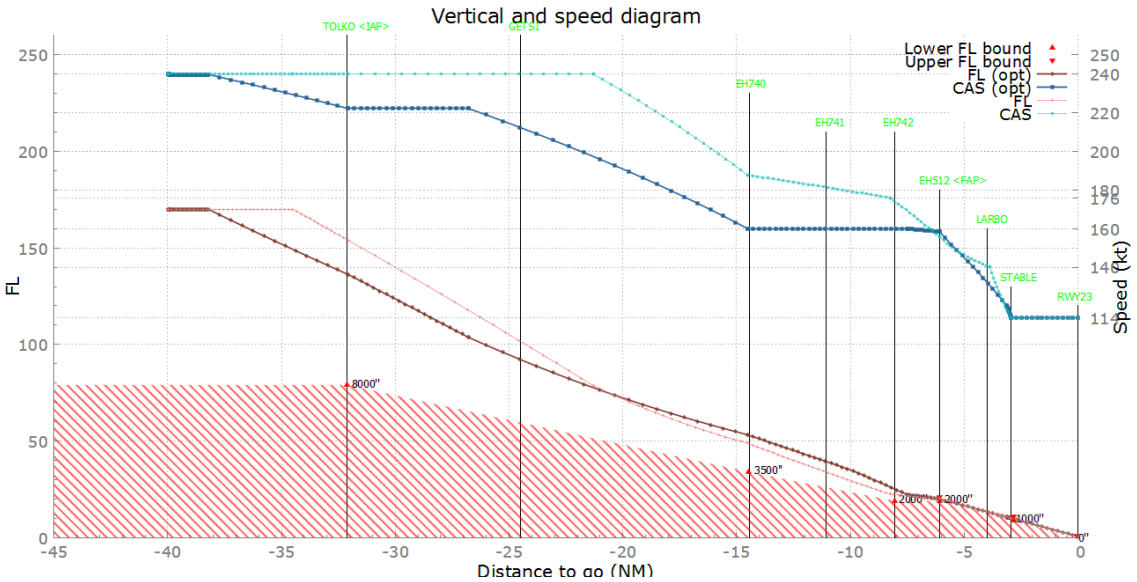

Figure 3.7: Vertical and speed profile comparing nominal and optimized trajectory

CHAPTER 4. IMPLEMENTATION OF A TACTICAL SOLUTION TO SCHEDULE HIGH-LIFT DEVICES

Contrary to the strategic control, which has been developed from a previous base, the tactical control algorithm has been built from scratch.

The first option when implementing the tactical controller was to use a typical PID and try to figure out which were the most correct coefficients for the C550. However, this case is not feasible for several reasons. First of all, the parameters to change are located in the future; changes in the location of flaps or gear have no effect in the present situation. Thus, it is not possible to make a feedback circuit. It is not like tactical speed controllers that change the current speed and can modify it according to the obtained output. On the other hand, it is not as easy as changing one parameter such as the speed; F-APP, F-LND and gear have to be changed and these changes have an effect on the speed, drag, thrust, flight path angle...

These reasons added to the fact that, indeed, the model of our aircraft is approximately known, have led to the decision of developing a more complex controller. However, the main principle when developing this controller has been to keep it as simple as possible.

4.1. Architecture

The architecture of the tactical controller with its main blocks can be seen in Figure 4.1.

As it can be seen, the tactical controller is a thread that is called by the RFMS. In this manner, the RFMS is not frozen during the time that the tactical controller is running. In ISA there would not be any problem, but in real atmosphere the tactical controller computations could last 2-3 seconds, time that the RFMS would not do anything if the tactical controller is not defined as a thread. This thread is called every time that the time deviation of the aircraft exceeds 0.5 s.

Hence, we are dealing with a multithread program. In this kind of programming, it is really important to be sure that the secondary thread, the tactical controller in this case, is being called and killed correctly. In order to do so, some functions, described in Appendix D, are used.

In general terms, what the tactical controller does is:

1. Choose the aircraft configuration to change.
2. Once the aircraft configuration is known, the nodes to change are found.
3. The variables associated to these nodes are changed so that the aircraft configuration is changed in such a way that the time deviation can be compensated.
4. Step 3 is done both with flight mechanics' equations and some interpolations in variables such as winds, pressure or temperature.
5. To accept the changes done in the aforementioned variables, all the constraints (hdot, casdot, distance...) have to be verified. Otherwise, step 3 is tried with other time intervals between nodes.

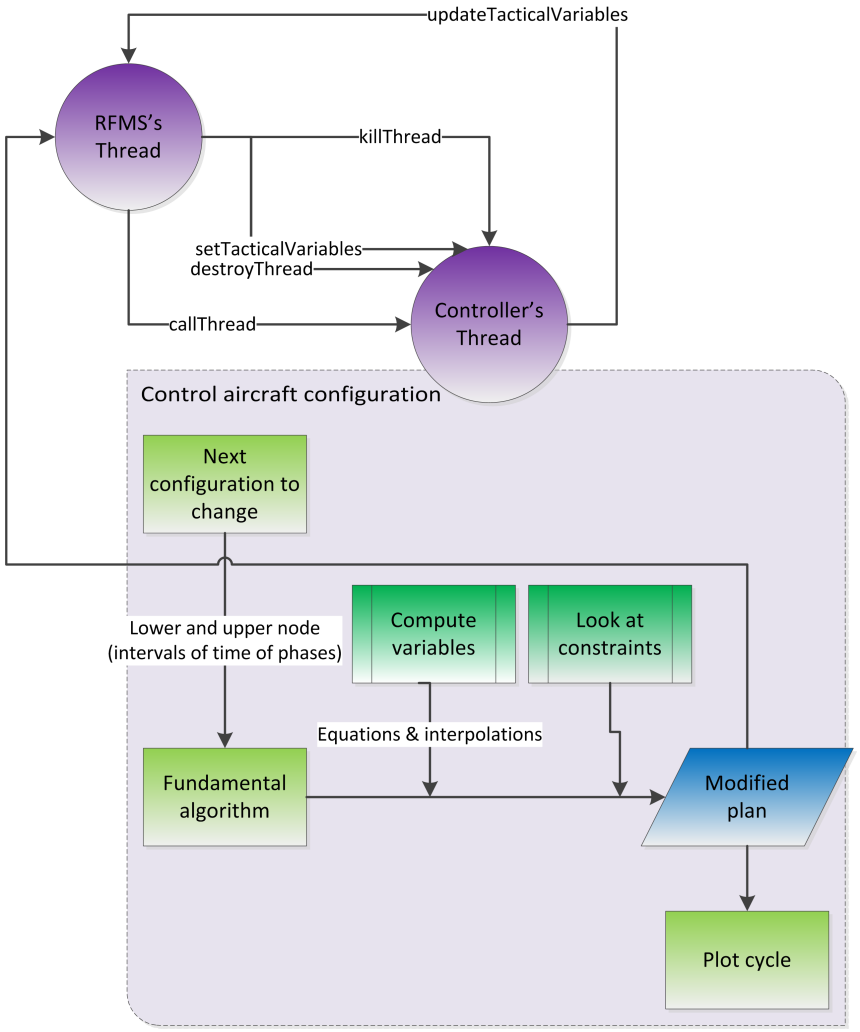

Figure 4.1: General architecture of the tactical controller

6. Once the constraints are verified, the plan can be definitely modified.

7. This modified plan is sent back to the RFMS and the result is saved in a file. Moreover, the RFMS will redraw this new plan in the ND.

The exit code of the controller can take the following values:

- -1: The controller cannot compensate more time if the deviation of time respect to the plan is negative since the trajectory would violate one or more constraints. This means that the aircraft will arrive earlier than planned. If, later on in the descent, there are positive time deviations, the RFMS will call again the tactical controller.

- 0: Everything is alright. The controller can continue compensating time in its next call.

- 1: The controller cannot compensate delays with respect to the planned trajectory. The RFMS could call again the tactical controller if the aircraft has negative deviations.

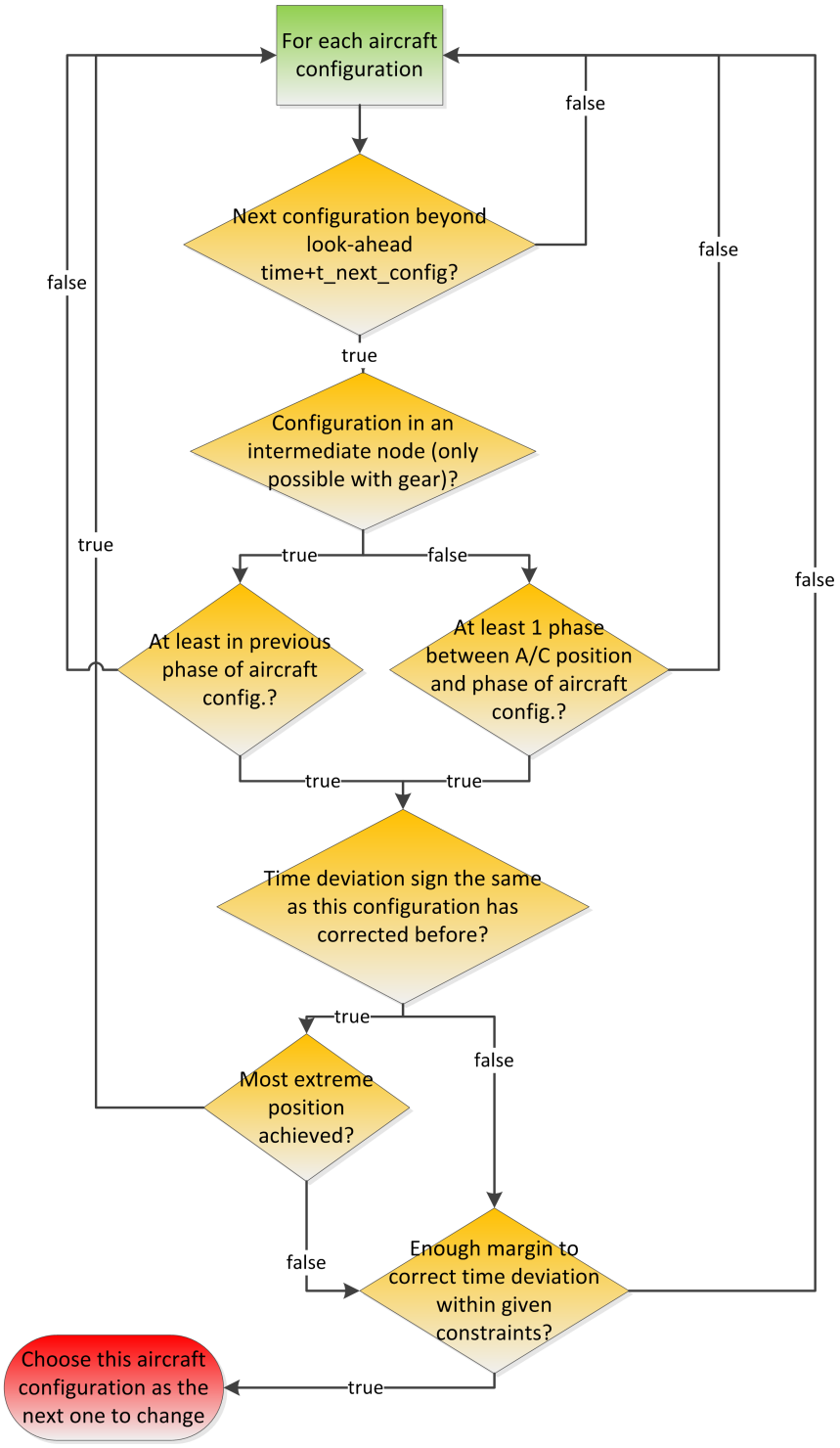

Figure 4.2: Logic to choose the next aircraft configuration to change

- 2: The controller cannot move more aircraft configurations, since the aircraft is really close to the last possible configuration to change it or it has passed all of them.

When being in the three first cases, every time a strategic re-plan occurs, the exit code is reset to 0 because, with a new plan, the tactical controller will probably be able to change again aircraft configurations.

4.2. Next aircraft configuration to change

One of the most challenging issues of the current tactical controller has been to develop the algorithm to choose which aircraft configuration needs to be changed at any precise moment. The reason of the difficulty lies in the great amount of possibilities. The choice made on this project is one of the easiest ones to implement and one of the choices that enable to correct more time deviations.

First of all, it is important to note that the tactical control changes the variables of the phases that come before and after the configuration change that is currently updated with the tactical algorithm (see section 4.3. for a complete description of this code). Hence it is not possible to choose to change an aircraft configuration if the aircraft is just in the earlier phase of this configuration since the current aircraft position would be affected (in variables such as altitude, thrust...).

The main principle behind the tactical controller is that in each tactical cycle (every time that the tactical controller is called), only one aircraft configuration is changed. Hence, if for some reason (a too large time deviation, a lot of small deviations have been corrected with a precise aircraft configuration...), the controller cannot correct the entire time deviation with the chosen aircraft configuration, it will correct the remaining time deviation in the next call using another high-lift device configuration.

The algorithm tries first to change the most immediate aircraft configuration, which can be done as long as the following conditions are met:

- The aircraft is before deploying the aircraft configuration, including the look-ahead time and time to next aircraft configuration, which can be 0, 30 or 60 seconds depending on the type of scenario.
- The aircraft is before the previous phase of the aircraft configuration deployment or just in the previous phase of the aircraft configuration if the configuration is in a middle node of a phase (this can only occurs with the gear, which is flexible and it is not associated to the first node of a phase).
- This aircraft configuration is not restricted by a constraint, such as hdot, casdot, time interval between nodes, phase constraints of FPA, altitude, distance... It is important to note that if in the previous cycle a later aircraft configuration than the most immediate has been modified, the controller will look again if it can compensate some time with this immediate configuration in some cases because the restrictions could be loose due to the change of the other aircraft configuration.

The diagram displayed in Figure 4.2 shows the logic mentioned above.

In Figure 4.2, there is a block which is quite interesting to comment: the block of whether the aircraft has achieved the most extreme position or not. In order to understand how it works, suppose that the initial sequence of aircraft configuration is F-APP, Gear and F-LND. This block works like this:

1. First of all, the controller tries to change the moment F-APP are deployed. As it continues changing F-APP, each time there is less margin (if the deviation in time is always of the same sign) respect to constraints of vertical speed, CAS rate change, distance...

2. When the tactical controller achieves the maximum position of F-APP, it starts changing the location of Gear deployment.

3. The issue is that if the aircraft changes the gear further away from F-APP, the constraints of F-APP will probably relax. This only occurs with delays. When the aircraft is faster than planned, Gear will come closer to F-APP and the constraints will not relax. Anyway, in the first case, the tactical controller comes back to F-APP to correct some amount of delay (maybe not all) with it.

4. The same procedure is followed until the controller cannot change any other aircraft configuration.

As it can be seen, with this iterative process, the tactical controller tries to correct the maximum time deviation. It does not change several aircraft configurations at the same time, but only one at a time. If all the time deviation is not corrected with one aircraft configuration, the controller tries with the next one if it is possible. This has several advantages:

- Only adjacent phases to only one aircraft configuration are modified.
- The controller tries to correct the time deviation with the most immediate aircraft configuration. If the controller would try to correct the time deviation with the latest aircraft configuration, it could come up with the situation of having passed the other aircraft configurations without having used them and then it probably needs them. In this way, the most advantage of all aircraft configurations is being taken.

4.3. Fundamental algorithm of the controller

As said in the previous section, if the aircraft configuration is located on the first node of a phase (always the case for flaps), the tactical controller changes the variables of the previous and current phase of the aircraft configuration. If the gear is not located at the beginning of a phase, then the phase of the gear is split into two phases, with different time intervals length, and these two ”new” phases will be modified.

Besides changing the main variables in the aforementioned phases, the controller will change the time nodes from the initial point of the phase of the changed aircraft configuration up to the current position of the aircraft.

The main idea behind the controller is that variables, such as altitude and distance, will remain untouched outside the two mentioned phases (except for the time, which will be modified from the aircraft current position up to the phase of the changed aircraft configuration). In order to obtain the involved equations, suppose a practical example.

Imagine that the configuration to change is F-APP. In our current scenarios F-APP is located at the beginning of phase 4; this is between phase 4 and 5. A representation of the nodes of this trajectory can be something like Figure 4.3.

As it can be seen, along a phase, the difference in time between the nodes is constant. Imagine there is a delay in time of 1 second. This means that the current position should have been flown one second before according to the plan. In order to compensate this delay with the F-APP, flaps should be deployed nearer the runway since when flaps are

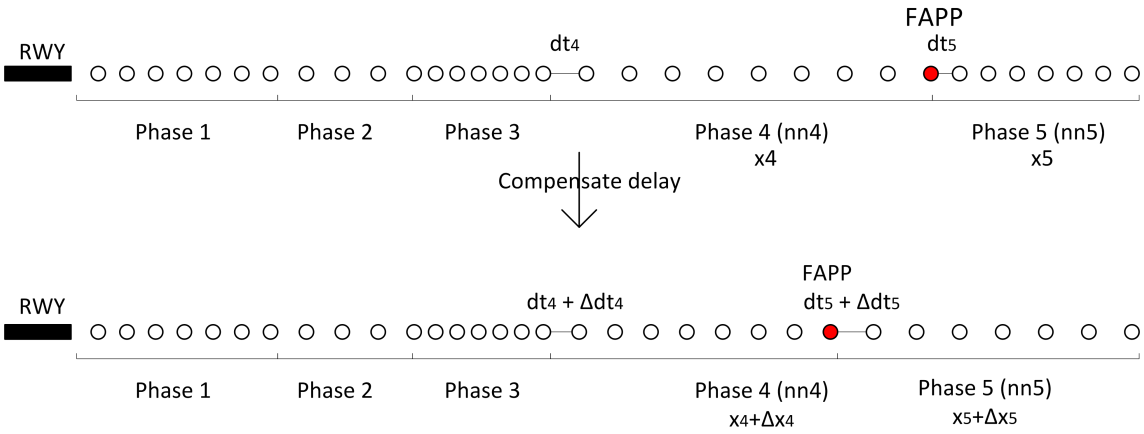

Figure 4.3: Example of correction of time with the nodes of the trajectory

deployed, drag increases and the speed decreases. Thus, it is interesting to fly more distance without deploying F-APP in order to go faster and compensate this delay of 1 second.

The idea, in this case, is to reduce the time interval of the phase of the aircraft configuration so that the initial node is closer to the RWY and, hence, F-APP are deployed closer to the RWY. To do so, and in order to respect the premise of keeping untouched the distance of the first node of phase 5 and last node of phase 4, the time between nodes of phase 5 has to be increased by some amount. Thus, each interval of time of phase 4 (dt_4) is decreased a certain amount (Δdt_4) and each interval of time between nodes of phase 5 (dt_5) is increased another certain amount (Δdt_5). Hence, by knowing the number of nodes of phase 4 (nn_4) and phase 5 (nn_5), an equation to compensate the current time deviation (Δt) is obtained:

$$\Delta dt_4 \cdot (nn_4 - 1) + \Delta dt_5 \cdot (nn_5 - 1) = -\Delta t \tag{4.1}$$

The sign is implicit in all Δ quantities, being positive for delays and negative for anticipations.

On the other hand, these increments/decrements of time in each time interval will inevitably cause an increment/decrement of the distance of both phase 4 (Δx_4) and phase 5 (Δx_5) respect to the original distance of both phases (x_4, x_5). However, as it has been said, the sum of the distances of both phases must remain untouched:

$$x_4 + x_5 = (x_4 + \Delta x_4) + (x_5 + \Delta x_5) \tag{4.2}$$

This leads to:

$$\Delta x_4 = -\Delta x_5 \tag{4.3}$$

These increments can be approximated by the sum of the product of ground speed (GS) times the increment of time interval in each node. By knowing that the increment of time interval is always the same in a given phase, the following equation results:

$$\Delta dt_4 \cdot \sum_{i=i_0^{(4)}}^{i_f^{(4)}} GS_i = -\Delta dt_5 \cdot \sum_{i=i_0^{(5)}}^{i_f^{(5)}} GS_i \tag{4.4}$$

Where i represents each particular node, $i_0^{(N)}$ the initial node of the Nth phase and $i_f^{(N)}$ the final node of the Nth phase.

By combining Equation 4.1 and Equation 4.4, the controller can know how much it has to increase the time interval between nodes of each phase:

$$\Delta dt_5 = \frac{-\Delta t}{\left(\frac{-\sum_{i=i_0^{(5)}}^{i_f^{(5)}} GS_i}{\sum_{i=i_0^{(4)}}^{i_f^{(4)}} GS_i} \right) \cdot (nn_4 - 1) + (nn_5 - 1)} \tag{4.5}$$

$$\Delta dt_4 = -\Delta dt_5 \cdot \frac{\sum_{i=i_0^{(5)}}^{i_f^{(5)}} GS_i}{\sum_{i=i_0^{(4)}}^{i_f^{(4)}} GS_i} \tag{4.6}$$

If the previous equations are generalized for a specific phase *N* and the next phase *N+1*, it can be obtained that:

$$\Delta dt_{N+1} = \frac{-\Delta t}{\left(\frac{-\sum_{i=i_0^{(N+1)}}^{i_f^{(N+1)}} GS_i}{\sum_{i=i_0^{(N)}}^{i_f^{(N)}} GS_i} \right) \cdot (nn_N - 1) + (nn_{N+1} - 1)} \tag{4.7}$$

$$\Delta dt_N = -\Delta dt_{N+1} \cdot \frac{\sum_{i=i_0^{(N+1)}}^{i_f^{(N+1)}} GS_i}{\sum_{i=i_0^{(N)}}^{i_f^{(N)}} GS_i} \tag{4.8}$$

Note that the time deviation and the number of nodes of each phase are known. However, the sums of speeds depend on the time interval that is obtained because by changing the time interval, nearly all the variables associated to each node are changed. The conclusion is that an iterative algorithm has to be implemented so that some specific values are given to the increment of time intervals and see the difference between what the sum of ground speed should be according to the previous equations and computing the new ground speed from flight mechanics equations with the aforementioned new time intervals. When these ground speeds are the same (in fact, less than a given tolerance), it will mean that the correct intervals of time have been chosen.

In Figure 4.4, the aforementioned iterative algorithm can be seen. When referring to use flight mechanics' equations, we mean the equations displayed in Appendix E.

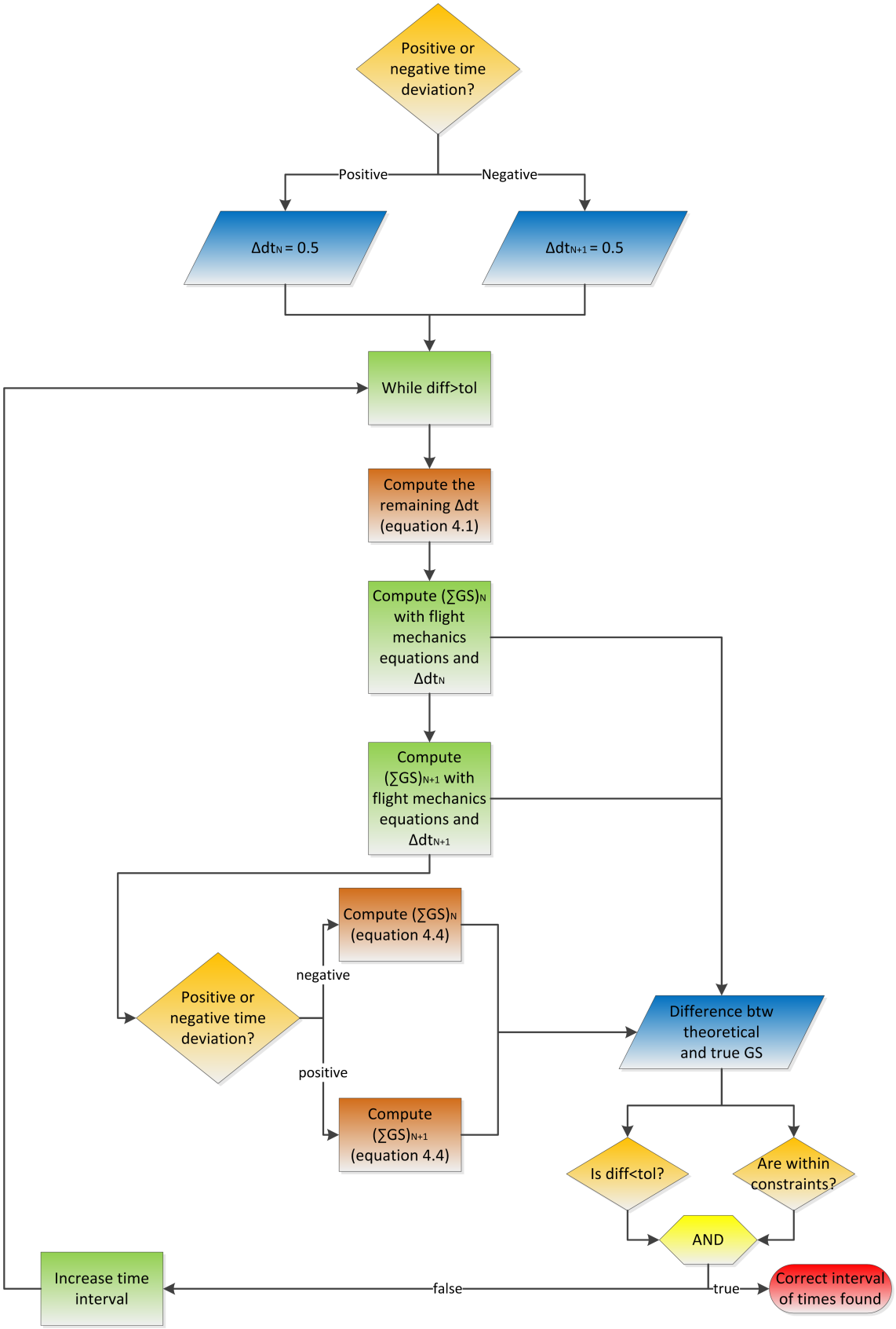

Figure 4.4: Iterative algorithm to obtain the correct time intervals between nodes

4.4. Trajectory update

In this section, the assumptions taken into account by the tactical controller when computing the variables of the affected phases are explained. As previously said, these affected phases are the phases in whose change of phase a specific aircraft configuration (flaps/gear) is deployed. This section corresponds to the block "compute variables" of Figure 4.1.

Besides being useful to have correct and real values of the variables according to the new time intervals of the affected phases, the computation of variables is also necessary to compare the sum of ground speeds with the value computed with the theoretical equations of the previous section since this computation is called every time inside the aforementioned iterative algorithm.

This computation is done in a given phase. Once the new time interval of the phase (positive *dt*) is known, which may not be the true value since we are inside the iterative algorithm, the variables are computed. When the correct interval of time is found after several iterations (according to section 4.3.), the trajectory plan is updated (only the affected phases) with the computed variables of the last iteration.

In order to calculate the variables of the affected phases, some assumptions have been made. The specific equations and type of interpolations used to compute these variables can be found in Appendix E.

First of all, it is worth noticing that the Euler collocation method has been applied through all the nodes of the trajectory. Then, it is assumed that the calibrated airspeed is maintained at each node as in the original trajectory, which is a reasonable hypothesis since the same aircraft configuration is used at each node. This is because only the location of nodes is changed, but each node of the trajectory has the same associated aircraft configuration and speed brakes.

On the other hand, now no meteorological data is available. Hence, to obtain pressure and temperature, the tactical controller interpolates these values according to the current altitude. In a similar way to the pressure and temperature, the winds can also be interpolated and their derivatives obtained.

Another assumption is that mass, bank angle and track angle are maintained at each node as in the original trajectory, which is a good approximation considering that the tactical controller does not make extreme changes, only slight modifications.

After this, an important assumption comes depending on the type of phase the aircraft is:

- **GS phases**: γ is maintained in each node since the glideslope has to be followed. Thrust is changed according to the new drag. N_{1_i} and π_i are then computed according to this thrust.
- **FPA phase**: This is just the phase before the glideslope where a fixed flight path angle is maintained during the entire phase. γ is computed with Equation 3.4, where the flight path angle respect to ground is the necessary one to have the change of the aircraft configuration at an altitude corresponding to the descent of the original plan.
- **Other phases**: Thrust is maintained at each node (it will be idle so that the TEMO

philosophy is verified) and flight path angle will change (following an iterative process; not using the complex equations of computation of flight path angle) to maintain this thrust. The used equations, as previously said, are left in Appendix E.

4.5. Constraints

In order to see if the obtained position of the aircraft configuration is acceptable, the following constraints have to be verified:

- The GS and FPA phases have to verify that the rate of climb/descent is within $\pm$ 1500 ft/min at each node. The other phases have a limitation of $\pm$ 3500 ft/min.
- CAS derivative must be less than $\pm$ 3 kts/s.
- Thrust must be greater than idle thrust at each node.
- The constraint of distance of the last node of a phase, if it exists in the original plan, has to be verified.
- The constraint of altitude of the last node of a phase, if it exists, has to be verified.
- The constraint of flight path angle of the last node of a phase, if it exists, has to be verified.

If one of these constraints is violated, it means that not all the time deviation can be compensated with the current aircraft configuration change.

4.6. Plotting tactical changes

Every time that a tactical cycle is finished with success, meaning that, at least, some part of the time deviation has been corrected, all the variables are saved in a file with the same columns as the ”results.dat” file returned after a strategic re-plan. In this manner, the differences before and after the tactical control can be compared and the affected phases can be easily observed.

In Figure 4.5 and Figure 4.6, it can be respectively seen a comparison of the speed and vertical profile before and after applying the tactical controller. Only the modified zone is displayed in these figures (it is a zoom from a vertical and speed profile). In this case, there was a delay of around one second. From the figures, it can be seen that the two affected phases (F-APP is deployed between these phases) are modified such that the change of F-APP is done a little bit nearer the runway to try to go faster (with the speed of before changing F-APP). This can be easily seen in 4.7(a). As an indirect consequence, the altitude profile, besides other variables, is also changed.

When a lot of tactical cycles have been undertaken, it is more difficult to relate time deviations and changes in aircraft configurations. In 4.7(b), the flaps and gear diagram after making 15 tactical cycles without a strategic re-plan can be seen. This scenario had a

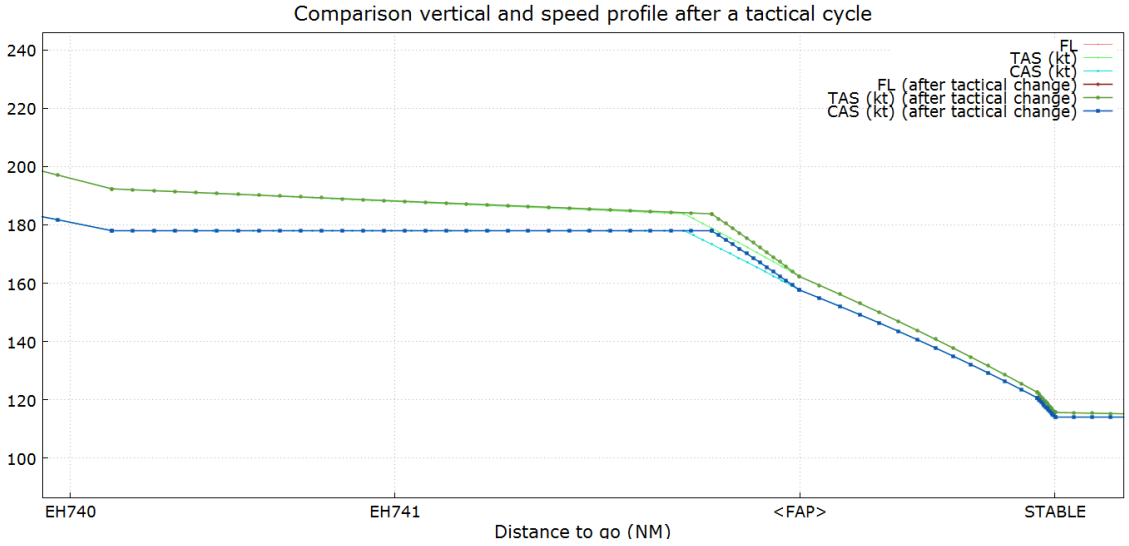

Figure 4.5: Speed profile of affected phases after a tactical cycle compensating a delay

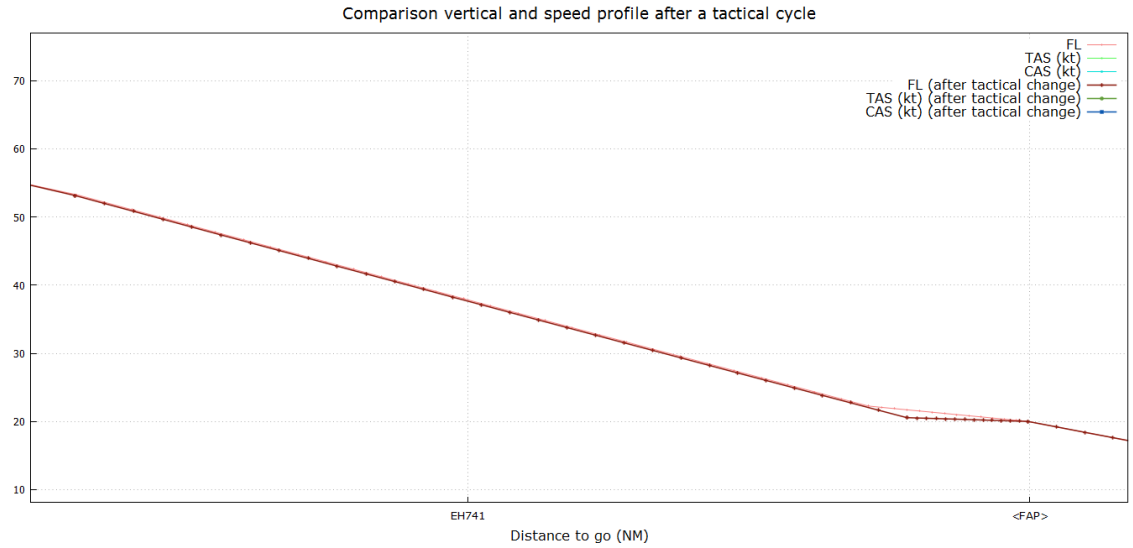

Figure 4.6: Vertical profile of affected phases after a tactical cycle compensating a delay

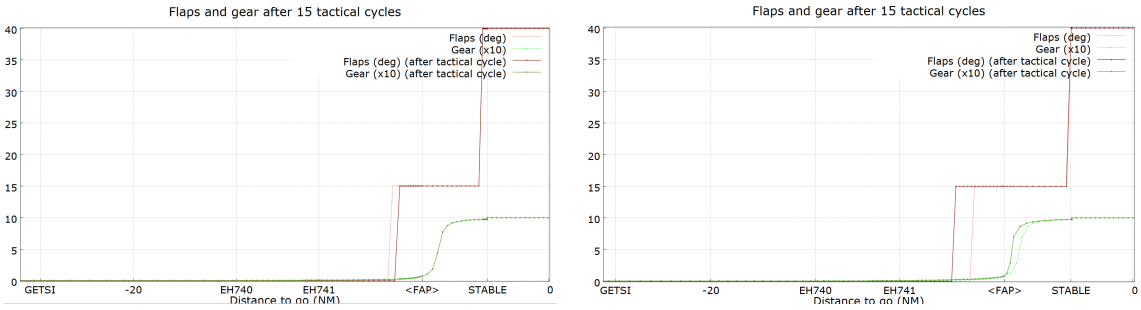

(a) One tactical cycle

(b) 15 tactical cycles

Figure 4.7: Flaps and gear diagram after tactical cycles

strong tailwind with wind prediction errors. Hence, the aircraft was going faster than expected, so aircraft configurations had to come earlier in order to decrease speed. Observe now how all the aircraft configurations are changed. F-LND is usually the aircraft configuration that is less changed since it is more restricted.

Most of the tactical cycles of 4.7(b) can be seen chronologically in Figure 4.8. The tactical controller is activated below 10,000 ft. In this case, there was a small delay due to collocation methods, which was corrected in the first tactical cycle. After this, all the corrections are corrections of negative time deviation due to the tailwind.

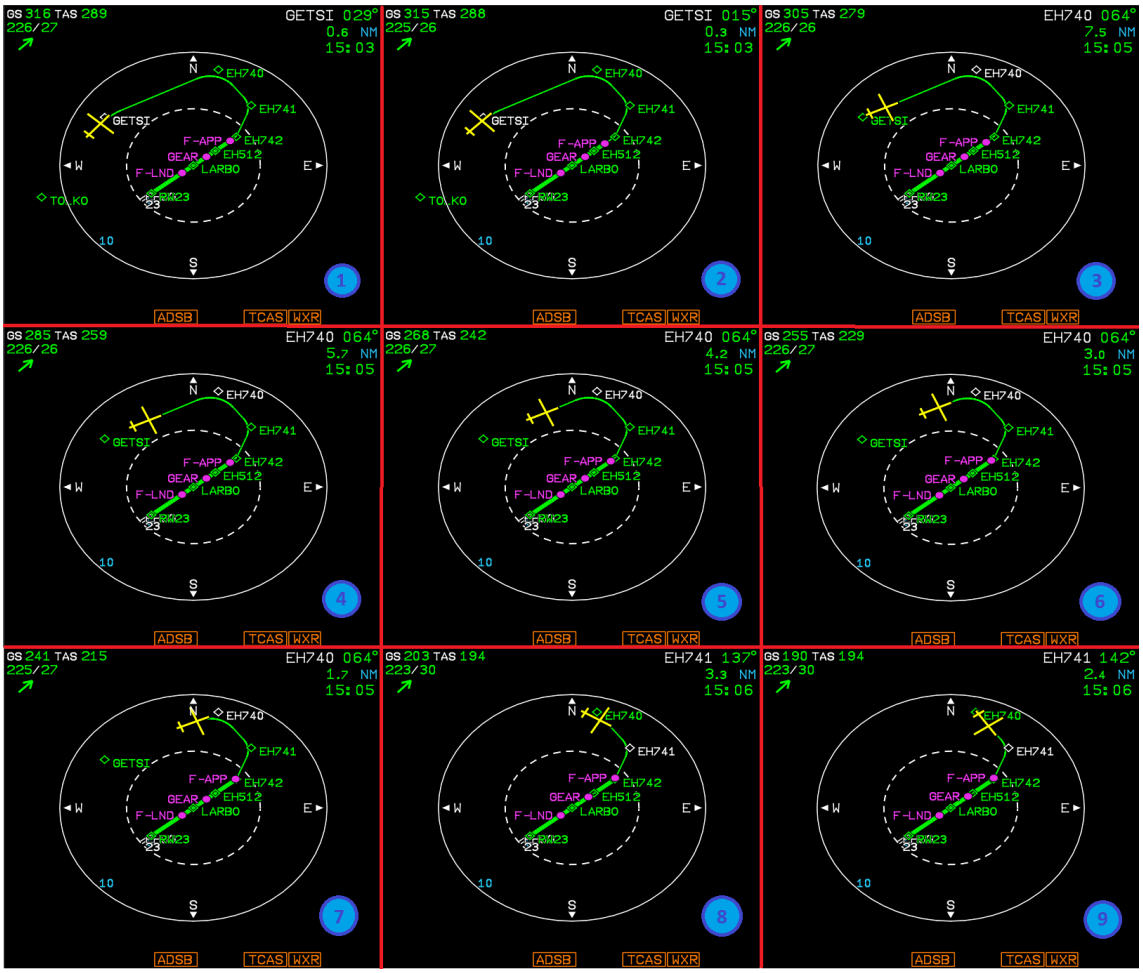

Figure 4.8: Tactical controller during a part of the descent

CHAPTER 5. EXPERIMENT PLAN

5.1. Scenario

The chosen scenarios are similar to the ones used in the CONCORDE simulation experiments in NLR's GRACE simulator on July 2014 [13]. However, since the part of interest is the one using flaps/gear, they have been adapted to start from the IAF.

The simulations will be done on an NLR laptop connected via Ethernet to the Host software (described in section 2.2.). Hence, any flight can be simulated with the same veracity as in the NLR simulators.

In this project, a Cessna Citation II will be used to carry out the scenarios. The main physical characteristics and performance data of the C550 are summarized in Table 5.1 (obtained from [34]):

Dimensions of the aircraft		**Relevant weights**	
Length	13.39 m	**Empty weight**	3,655 kg
Width	15.90 m	**Max take-off weight**	6,395 kg (14,100 lbs)
Height	4.57 m	**Max landing weight**	6,123 kg (13,500 lbs)
Wing surface area	31.83 m^2	**Max Payload**	1,406 kg (3,100 lbs)
Max number of cabin seats	8		
Performance			
Max Endurance	5 hours	**Max Mach (MMO)**	0.705
Engines	P&W JT15D-4 jet	**Max Speed (VMO)**	262 kt
Max thrust	2 x 11.12 kN	**Max speed flaps 15**	202 kt
Cruise MCT	N2 = 96, N1 = 104	**Max speed flaps 40**	176 kt
Cruise idle	N2 = 49, N1 = TBC	**Min controllable airspeed**	77 kt
Cruise alt	10,670 m (35,000 ft)	**Cruise speed**	746 km/h
Max Altitude	13,106 m (43,000 ft)	**Max vertical speed**	-2,500 ft/min TBC

Table 5.1: Characteristics of the Cessna Citation II

5.1.1. Aerodrome

The aerodrome used for the simulations is the Groningen Airport, also known as airport Eelde. This airport is a civil aviation airport, located near the town of Eelde, south of

the province capital of Groningen. The airport is mainly used by tourists and business travelers. Some low fare airlines, such as Transavia, Ryanair and Corendon, operate from this airport. In summer, these operators fly to fourteen destinations while only five in the winter. Aircraft landing there consist of private aircraft, military aircraft, medical flights, and training aircraft flights. The largest number of movements is accounted for lessons and fun flights. Currently, the airport handles around 50,000 passengers each year but would like to grow to 300,000 passengers annually.

Groningen Airport Eelde is part of the Green Sustainable Airports (GSA) initiative. In co-operation with various regional airports in Europe, Groningen Airport Eelde develops sustainable initiatives of which CDO operations is one example. Groningen Airport assumes responsibility to test and develop a blueprint and CDO application model for regional airports, supported by the GSA partnership and the NLR.

The main information of this aerodrome is left in Table 5.2, though most of this information can be also seen in section F.1., obtained from the Dutch AIS [35].

Name		Eelde	**IATA/ICAO code**	GRQ/EHGG
ARP coordinates		N53°07'30" E006°35'00"	**ARP elevation**	+18 ft
Runways	RWY 01	Coord.: N53°07'02.59" E006°34'36.69" THR Elev: 17 ft TODA: 1500 m ASDA: 1500 m		
	RWY 19	Coord.: N53°07'50.54" E006°34'48.97" THR Elev: 12 ft TODA: 1560 m ASDA: 1500 m		
	RWY 05	Coord.: N53°06'39.90" E006°33'39.23" THR Elev: 13.3 ft TODA: 2560 m ASDA: 2500 m		
	RWY 23	Coord.: N53°07'29.84" E006°35'24.96" THR Elev: 12.5 ft TODA: 2560 m ASDA: 2500 m		
Geoid undulation		135 ft	**Reference temperature**	20.9 °C (Jul)
Magnetic variation		VAR 1°E (2010)	**VAR annual change**	9'E

Table 5.2: Airport information

5.1.2. Route

The route to be followed is an instrument approach to the Groningen Airport. It is specifically the so-called TOLKO1G approach procedure, a P-RNAV ILS CAT-I approach for runway 23 at Eelde. The approach chart can be seen in Figure 5.1, where all the restrictions of altitude and speed at each waypoint are included. Table 5.3 also depicts the information of each waypoint of the route. If the specific waypoint is part of a turn, some orientative Begin Of Turn (BOT) and End Of Turn (EOT) are given (these points are correctly computed at each nominal trajectory). All the turns are fixed radius turns and, from RW23 to EH512, the waypoints are of type fly-by.

The constraints of altitude and speed of each waypoint can be seen in Figure 5.2 too.

Name	Latitude	Longitude	BOT lat.	BOT lon.	EOT lat.	EOT lon.
RW23	53.124954	6.590267	-	-	-	-
STABLE	53.155239	6.654494	-	-	-	-
LARBO	53.166023	6.677397	-	-	-	-
EH512 (FAP)	53.187500	6.723055	-	-	-	-
EH742 (IF)	53.208057	6.766667	53.21832	6.773595	53.20121	6.752139
EH741	53.254166	6.797778	53.26929	6.778069	53.23638	6.785769
EH740	53.506667	6.729445	53.29155	6.678541	53.27986	6.764359
GETSI	53.236740	6.492892	53.22181	6.476395	53.24470	6.519685
TOLKO (IAF)	53.118935	6.362581	-	-	-	-
INIT	53.013381	6.372222	-	-	-	-

Table 5.3: Waypoints of the approach route

5.1.3. Vertical and speed profile

Figure 5.2 shows a graphical representation of the phases plus all the constraints that the solver has to take into account during the optimization process.

5.2. Experiment design

In this section, the experiment design is explained. This experiment will serve to validate the dynamic high-lift devices and gear deployment implementation of this project.

5.2.1. Scope

The scope of the tests is limited to evaluate the performance of the TEMO implementation with dynamic configurations in various scenarios, while using two different implementations of the concept: absolute RTAs using strategic re-plans and absolute RTAs using strategic re-plans on energy + tactical controller on time. Inside each implementation, three cases will be tested, giving a different value of minimum time between the position of the aircraft after each re-plan and the most immediate aircraft configuration.

Moreover, some scope inherent objectives are:

- To obtain data for the analysis of the implementation performance.
- To compare the two aforementioned implementations with the reference implementation used in CONCORDE experiments.

To better restrict the scope of the validation, the following list presents a sort of main conditions and assumptions that will be followed during the experiment design:

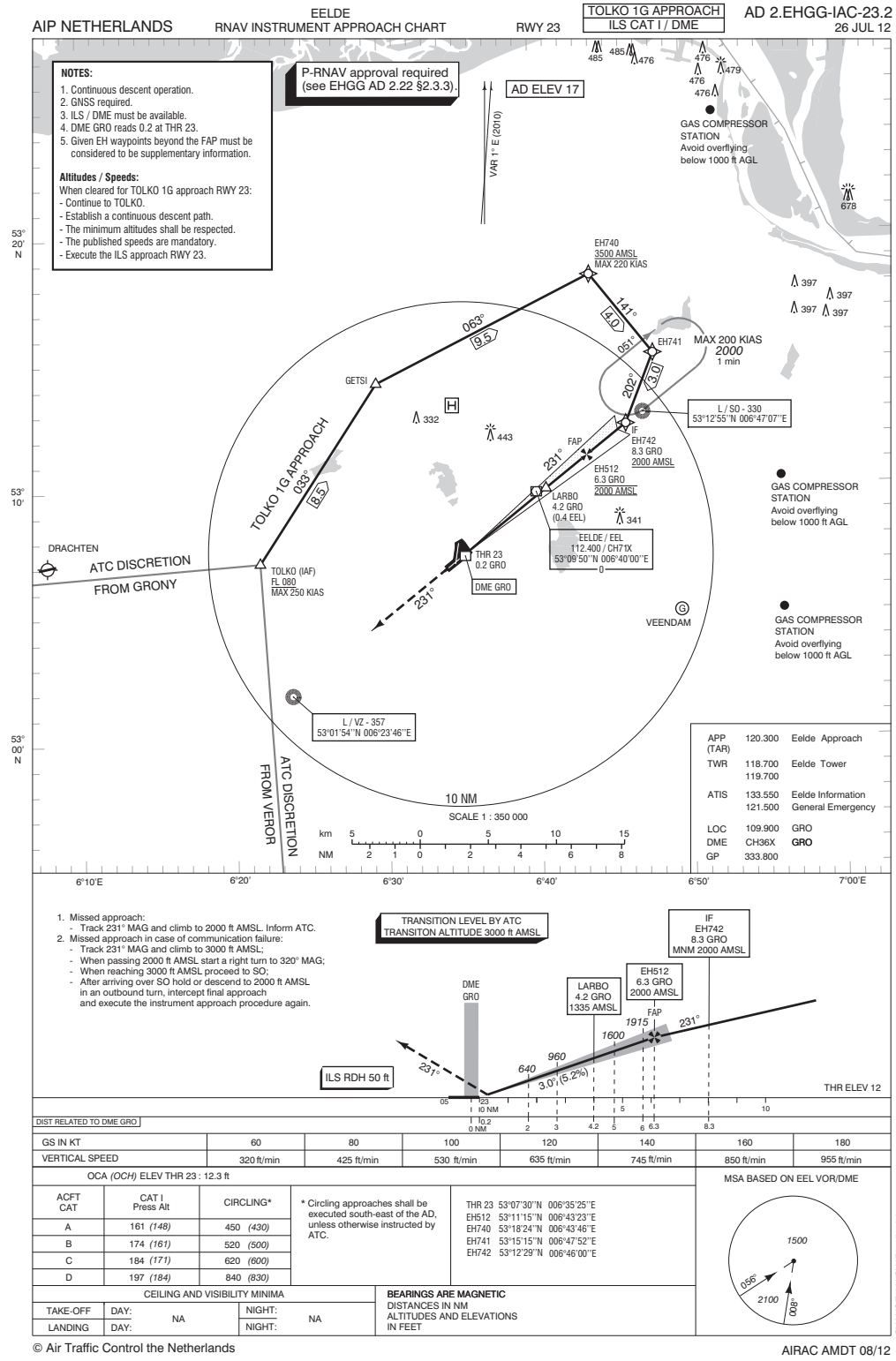

Figure 5.1: EHGG RNAV instrument approach chart RWY 23 TOLKO (IAC)

- The experiment is designed to follow the RNAV route and constraints for the Eelde airport. Only the TMA part (starting at the IAF TOLKO) is to be tested.

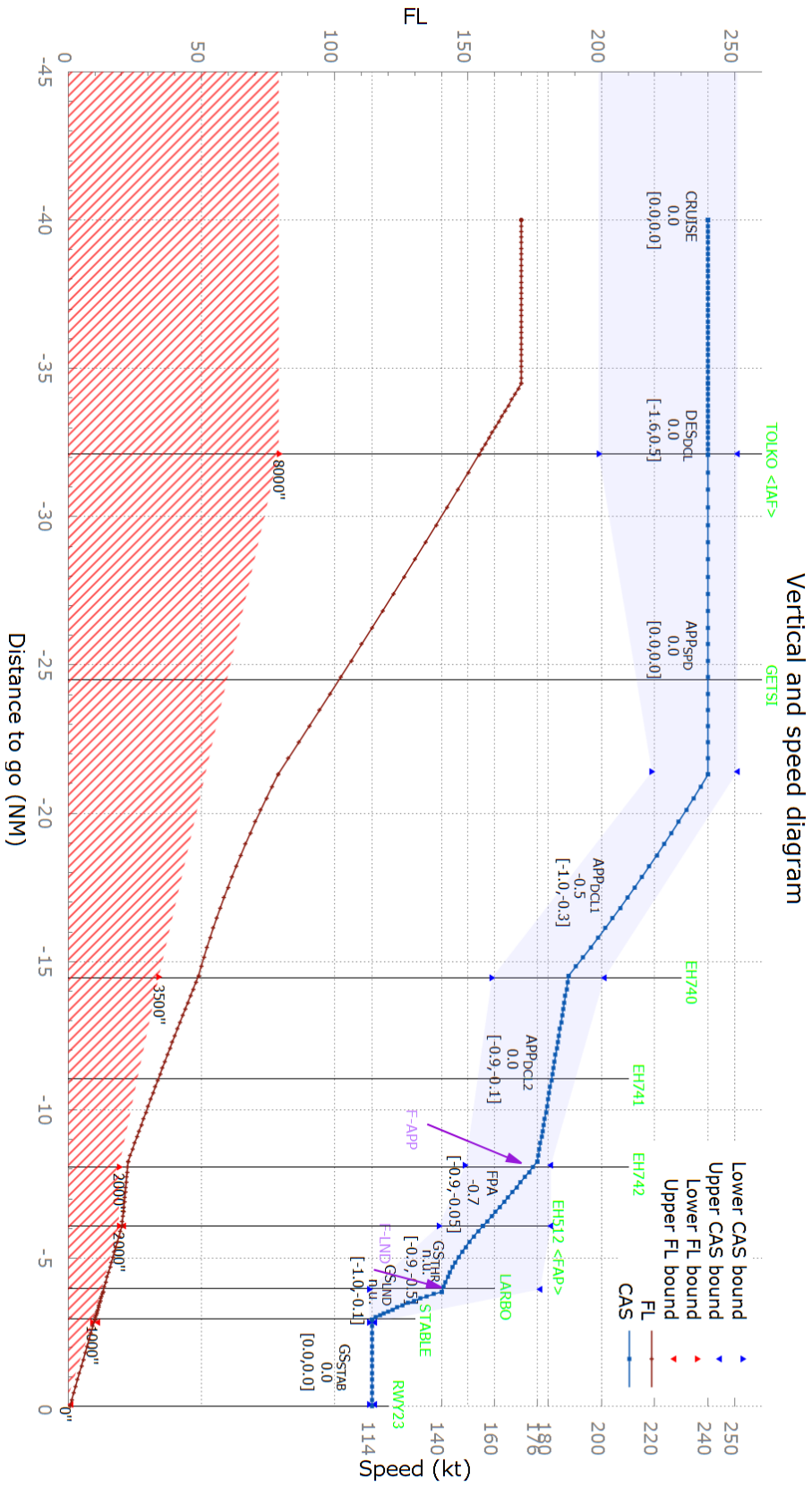

Figure 5.2: Nominal speed and vertical profile

- RTAs will be inserted into the RFMS between TOLKO and GETSI waypoints.
- It will be in line with the design of the CONCORDE experiment.
- No HMI validation will be done (out of scope).
- RTAs will be manually inserted into the RFMS without the aid of the pilot.
- No noise model (such as INM) will be used.
- Auto Throttle and Auto Speed Brakes automation systems will be available during the study.
- When using real atmosphere, data from 13 of January of 2008 will be used.

5.2.2. Research Questions & Hypotheses

The research questions and their corresponding hypothesis are formulated as follows:

RQ1: Does the dynamic aircraft configuration implementation improve the time metering at the runway threshold with respect to current static aircraft configuration implementation?

(H1.a) *The time metering at the runway threshold improves with both types of dynamic aircraft configuration methods compared to static aircraft configuration.*

(H1.b) *The tactical configuration controller shows better time performance than the strategic re-planning.*

RQ2: Is the aircraft stabilized at 1000 ft AGL in all three implementations?

(H2) *All the necessary operational requirements are met at the stabilization point for all three implementations.*

RQ3: Do both dynamic aircraft configuration methods reduce the fuel consumption and/or usage of speed brakes compared to the reference?

(H3.a) *The usage of speed brakes will be reduced with the dynamic aircraft configuration.*

(H3.b) *The fuel consumption will be reduced with the dynamic aircraft configuration.*

(H3.c) *The strategic variant shows a greater reduction on speed brakes usage than the tactical variant.*

(H3.d) *The strategic variant shows a greater reduction on fuel consumption than the tactical variant.*

5.2.3. Validation Questions

In order to aid the objective of the experiment, the following validations questions related to each research question have been formulated:

VQ1.1: Can the aircraft meet the time requirements in most scenarios (85%) in all three implementation variants?

VQ1.2: Is the mean time deviation and time variance of both the Tactical and Strategic Configuration Controller at the threshold less than in the reference scenarios?

VQ1.3: Is the mean time deviation and time variance at the threshold smaller for the Tactical Configuration Controller compared to the Strategic Configuration Controller?

VQ2.1: Are all the stabilization requirements met at the stabilization point?

VQ3.1: Is the usage of speed brakes less with both the dynamic flaps algorithm than the static method?

VQ3.2: Is the fuel consumption reduced on average with both the dynamic aircraft configuration methods than the static method?

VQ3.3: Is the usage of speed brakes greater in the tactical aircraft configuration method than the strategic method?

VQ3.4: Is the fuel consumption greater on average with the tactical aircraft configuration method than the strategic one?

5.2.4. Independent variables

The independent variables, which are set by the user in order to isolate causality within the model, are presented in this section and discussed in the subsequent sections.

1. Guidance Mode changing deployment time of aircraft configurations Variants (two levels)
   (a) Follow CAS speed plan (speed on elevator) with strategic re-plan to nullify time and energy deviations.
   (b) Follow CAS speed plan (speed on elevator) with strategic re-plan to nullify energy deviations and with tactical configuration controller to nullify time deviations during approach mode.
2. Time to next configuration[1] change Variants (three levels)

[1] Defined in section 3.1..

(a) Time to next configuration equal 60 seconds.

(b) Time to next configuration equal 30 seconds.

(c) Automatic: The aircraft configuration can come as close as possible to the current position.

5.2.5. Experiment Matrix

The experiment matrix follows from the selected independent variables and is shown in Table 5.4.

Guidance mode \ Time to next conf. change	**60 seconds**	**30 seconds**	**0 seconds**
Strategic re-plan	Scenarios A (W0, W1, W2)	Scenarios B (W0, W1, W2)	Scnearios C (W0, W1, W2)
Tactical configuration controller in time	Scenarios D (W0, W1, W2)	Scenarios E (W0, W1, W2)	Scenarios F (W0, W1, W2)
Baseline/Reference			Scenarios R (W0, W1, W2)

Table 5.4: Experiment Matrix

The reference scenarios are the ones where high-lift devices are fixed and only strategic re-plans can be done.

As it can be seen, in each cell, three different weather scenarios will be tested: ISA atmosphere (W0), real atmosphere without offsets in wind direction and speed (W1) and real atmosphere with typical offsets (5 kt more in wind speed and 10 degrees clockwise in wind direction) (W2). Then, each weather scenario will be repeated 5 times with different RTAs (+30, +15, +0, -15 and -30 respect to the nominal ETA), except for ISA case where a +60 RTA is also simulated.

Hence, there are 96 experiment runs of the dynamic aircraft configuration implementation and 16 for the reference case. Thus, there will be a total of 112 experiment runs.

Each scenario will start on the leg from VEROR to TOLKO. The experiment leader will initialize the FMS with a route to Eelde runway 23. This will trigger the TEMO algorithm to plan an initial descent profile. Then, the experiment leader will enter manually an RTA at the runway threshold. This will again trigger the TEMO algorithm, which will provide a new profile to the runway. At appropriate location along the route, the aircraft will be configured. Furthermore, Auto Speed-brakes should also be activated and set the lever on the correct position when necessary. In the case of scenarios D, E and F, the tactical controller will be activated when the altitude is less than 10,000 ft.

5.2.6. Dependent measures

The dependent measures that will be analyzed in order to find an answer to the research questions and to be able to reject or accept the hypotheses are given in Table 5.6. This table gives an overview of how these dependent measures relate to the validation questions and hypotheses during the experiment. Besides the displayed dependent measures in the mentioned table, the location of the deployment of each aircraft configuration has also been logged to validate the overall implementation.

5.3. Metrics for hypothesis acceptance

Table 5.5 provides the metrics and boundary conditions based on which the hypotheses will be accepted or rejected.

Hypothesis	Criteria
H1.a	RTA_{THR} - 5 sec $<$ Actual time at THR $<$ RTA_{THR} + 5 sec σRTA_{THR} dynamic config. $<$ σRTA_{THR} static config.
H1.b	σRTA_{THR} tactical config. method $<$ σRTA_{THR} strategic config. method
H2	At 1000 ft: $V_{REF} \leq V_{IAS} < V_{REF}$ + 5 kts Flap setting is LAND Gear is Down The aircraft is on G/S Thrust is at a value that maintains FAS
H3.a	Speed brakes usage dynamic conf. $\leq$ speed brakes usage static conf.
H3.b	Fuel consumption dynamic conf. $<$ fuel consumption static conf.
H3.c	Speed brakes usage strategic variant $\leq$ speed brakes usage tactical variant
H3.d	Fuel consumption strategic variant $<$ fuel consumption tactical variant

Table 5.5: Metrics for hypothesis acceptance

	Dependent Measure	VQ 1.1	VQ 1.2	VQ 1.3	VQ 2.1	VQ 3.1	VQ 3.2	VQ 3.3	VQ 3.4	H 1.a	H 1.b	H 2	H 3.a	H 3.b	H 3.c	H 3.d
1	Actual time at THR	X	X	X						X	X					
2	RTA at THR	X	X	X						X	X					
3	Flaps setting at 1,000 ft				X							X				
4	Altitude @ FLND				X							X				
5	Gear setting at 1,000 ft				X							X				
6	Altitude @ G				X							X				
7	IAS at 1,000 ft				X							X				
8	Altitude IAS=VREF+5 kt				X							X				
9	On GS at 1,000 ft				X							X				
10	Altitude interception of GS				X							X				
11	Thrust setting at 1,000 ft				X							X				
12	Altitude T to maintain FAS				X							X				
13	Fuel consumption during the whole flight						X		X					X		X
14	Duration of the usage of speed-brakes					X		X					X		X	

Table 5.6: List of dependent measures and their related validation questions (VQ) and Hypotheses (H)

CHAPTER 6. RESULTS AND DISCUSSION

In this chapter, the results from all the undertaken simulations are discussed and the proposed hypothesis will be validated or refuted according to them.

For the sake of clarity, some nomenclature has been used in several graphs. ”Ref”, ”Strat” and ”Tact” means, respectively, reference (baseline), strategic in both time and energy and tactical in time. They correspond to the three rows of the experiment matrix of Table 5.4. Moreover, the scenarios (A, B, C, D, E, F, R) and weather (W0: ISA atmosphere, W1: Real atmosphere, W2: Real atmosphere with wind prediction errors) nomenclature of that table is also used.

The results obtained in this chapter are basically obtained to compare the baseline with the two new implementations made in this project (strategic and tactical) in the three different weather scenarios since the research questions are devoted to this comparison. However, in the experiment matrix, the ”time to next configuration” is also included. The graphs comparing each scenario cell of the experiment matrix (not only the three rows) are left in Appendix G and will be mentioned in the current chapter if a significant difference in the results of different ”time to next configuration” is observed. Usually the difference is not significant enough and it is better to stick to the comparison of the three different implementations. Though these slight differences, it is worth noticing that the ”time to next configuration” helps in order prevent unexpected situations to aircraft crew by a sudden change of a high-lift device or gear deployment, which could occur when the ”time to next configuration” is 0.

All the simulations have been done in real-time (each one taking around 12 minutes) using Airsim, NLR Host, RFMS, FASTOP and WEMSGEN as shown in Figure 2.1 and the flown data has been logged from the RFMS at 5 seconds intervals. The resulting data of all the simulations can be found in table format in Appendix H. In total, 142 simulations have been carried out (30 extra simulations respect to the experiment plan).

6.1. Analysis of high-lift devices and gear landing deployment

In Figure 6.1, the distance of F-APP deployment for the three different implementations and in each of the simulated weather scenarios is displayed. The number of simulations for each scenario is displayed in the variable “N” (see subsection 5.2.5. to know how many simulations are done in each case).

F-APP can be optimized and changed by the three implementations. However, the two implementations developed in this project (the strategic and the tactical methods) have a wider range of values meaning that they have more freedom to change the position of flaps approach. In Figure 6.1, it can be also observed that with the tactical implementation, the distance of the flaps approach deployment varies significantly. This is explained because the tactical controller can move aircraft configurations continuously while the strategic case only re-plans these changes in case the aircraft goes outside the maximum time and/or energy bounds.

The change of the gear position is another novel contribution of this project. Indeed, the reference implementation is not able to change the moment when the gear is deployed;

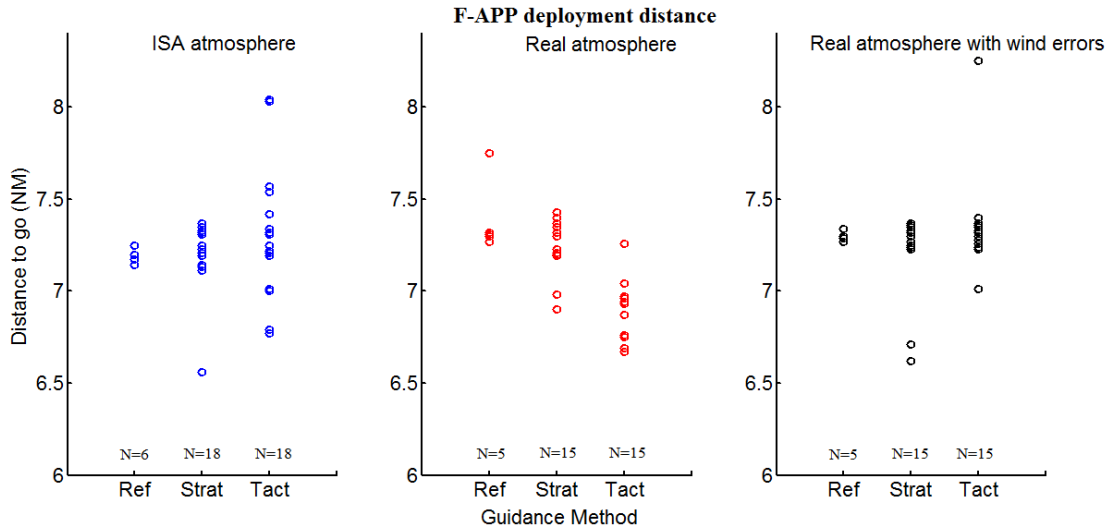

Figure 6.1: F-APP deployment distance of the simulations

being always given by the nominal trajectory at a specific altitude. In Figure 6.2, this can be perfectly seen. In the reference case, gear is always fixed at the same distance (there is a small difference between the simulations because data is recorded every 5 seconds), while in the strategic and tactical case, the aircraft can deploy gear much before if it is needed for optimal reasons.

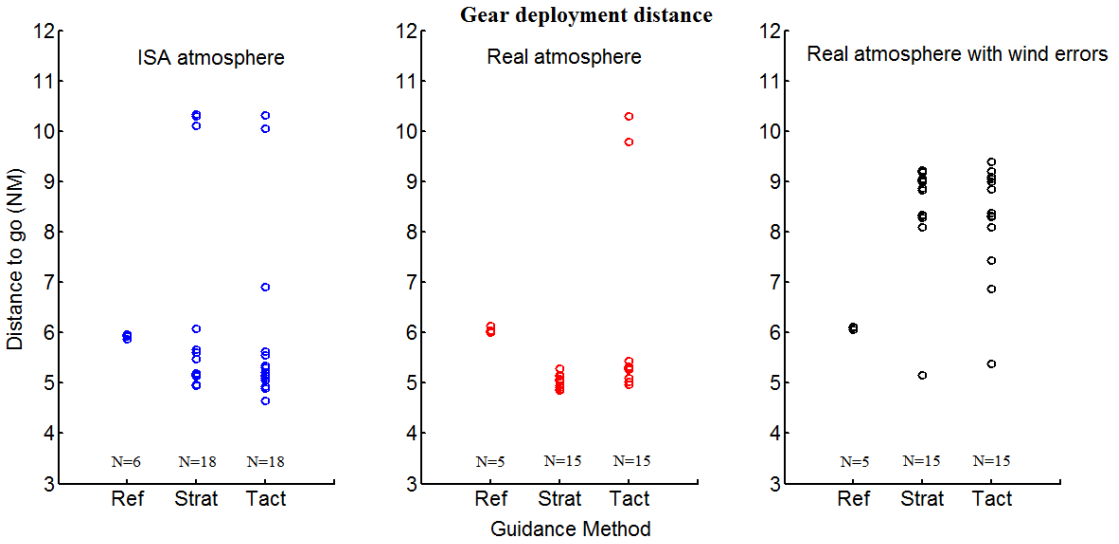

Figure 6.2: Gear deployment distance of the simulations

In this case, it is also interesting to see which RTAs produce the gear to be deployed before F-APP or earlier than usually. In Figure 6.3, it can be seen that for delayed RTAs, the distance from the RWY is increased respect to earlier RTAs. In fact, for an RTA of +60, all the scenarios of the new implementations choose to deploy gear before flaps approach since the aircraft needs to arrive later. Analogously, graphs for real and real with wind prediction errors atmosphere can be observed in section G.7..

It is worth noticing in Figure 6.2 that the gear deployment is generally earlier for the case of a real atmosphere with wind errors. In our case, the real atmosphere scenario has a strong

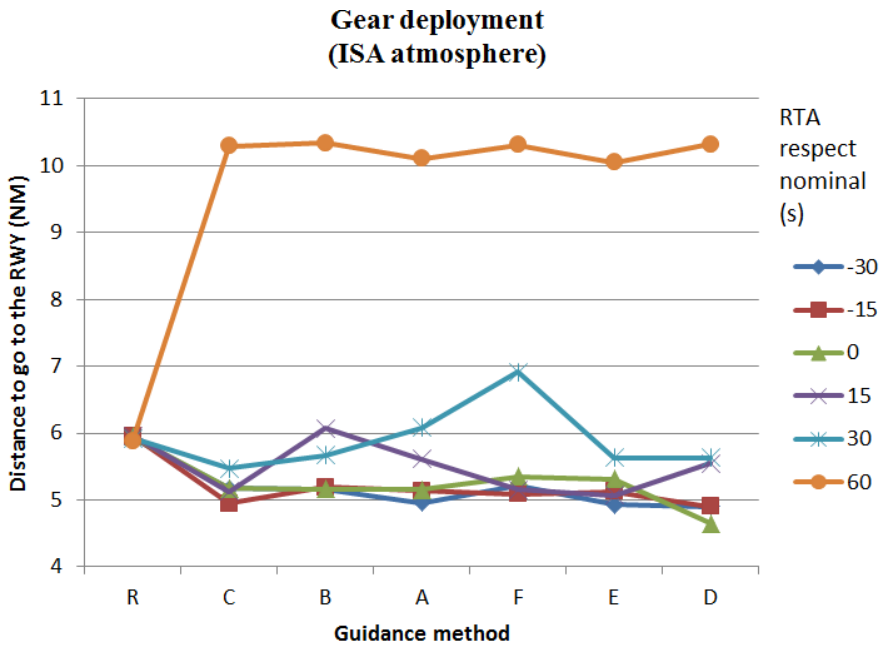

Figure 6.3: Gear deployment distance for RTAs

headwind in the last part of the flight (even more with wind prediction errors). This seems to produce to advance the gear when a re-plan is triggered due to energy deviations in the last part of the flight (not in the initial point of the trajectory). This can be explained with the combination of Figure 6.1 and Figure 6.4. When flying a real atmosphere (and especially with wind errors), there are usually more re-plans because of energy deviations. In these cases, the optimizer finds that it is more optimal to advance gear and delay the deployment of F-APP and F-LND if compared with the ISA case, as it can be seen in the aforementioned figures.

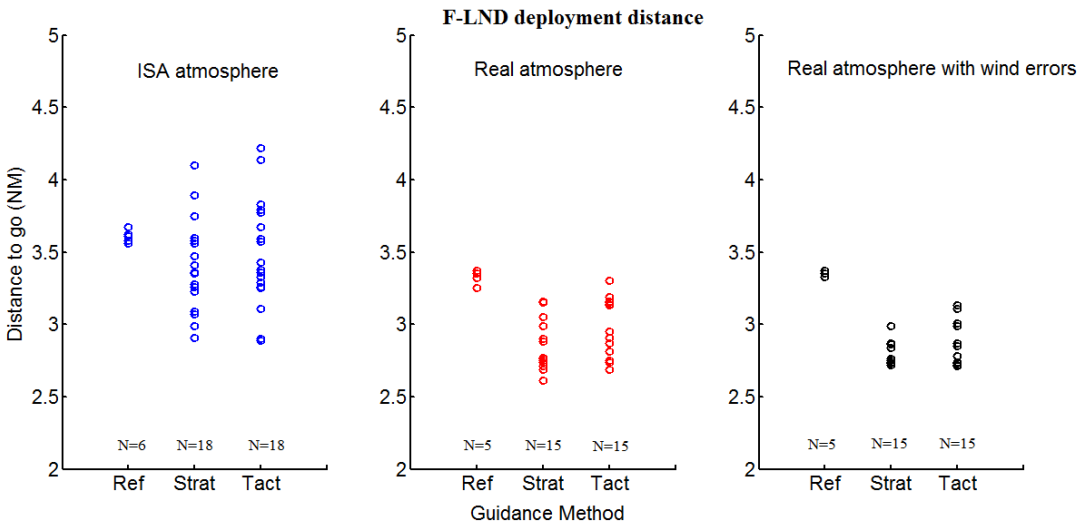

Figure 6.4: F-LND deployment distance of the simulations

In general, when increasing the ”time to next configuration”, high-lift devices cannot be deployed as earlier as when this value is near 0 (see section G.6., section G.7. and section G.8.).

It is also worth noticing that with the two new implementations, the earliest and latest RTAs that can be requested are greater than with the baseline case. In the real atmosphere scenarios, the new implementations can achieve -1 second more in the earliest trajectory and nearly +20 seconds more in the latest trajectory.

6.2. Number of re-plans and execution time of the re-planning algorithm

Another important issue before starting discussing about the hypothesis is how many re-plans have generated each implementation and their execution time (time the optimizer took to converge to a solution).

In Figure 6.5, it can be seen the execution time of the initial re-plan, which is triggered to comply with the requested RTA. Both the tactical and strategic solutions have slower execution time since more phases are optimized and more equations and variables are involved. In fact, they should have in theory the same execution time between themselves since the optimization part is the same for both tactical and strategic solution.

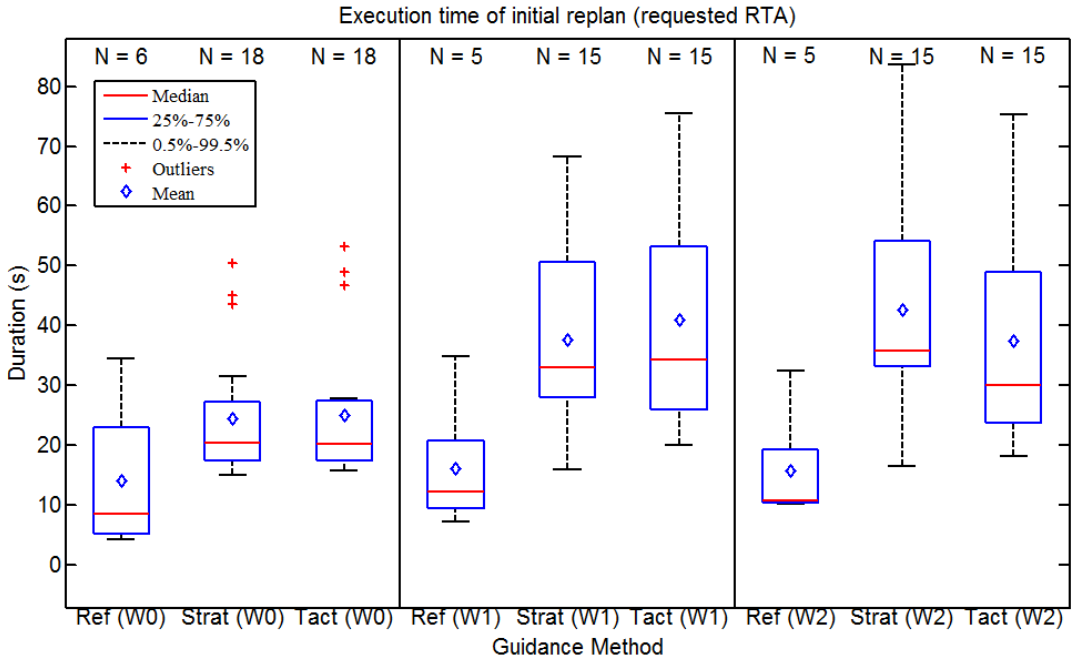

Figure 6.5: Execution time of initial re-plan

On the other hand, the number of succeeded re-plans done during the flight is displayed in Figure 6.6. As it can be seen, when having wind errors, the number of re-plans is increased since the energy goes out of the bounds faster. The reason that the reference case has less re-plans is not because the energy deviation is less (in fact energy deviations are similar in all the cases), but because it is unable to do a re-plan when requested since it is too close to the last phase of the optimization. Indeed, Table 6.1 shows that the percentage of unable re-plans further than 6 NM (which corresponds to 2000 ft of altitude) from the runway threshold is much greater in the reference case. When having wind prediction

errors, more succeeded re-plans are found since the energy goes out of the bounds earlier and then it has no problem to solve the optimal problem.

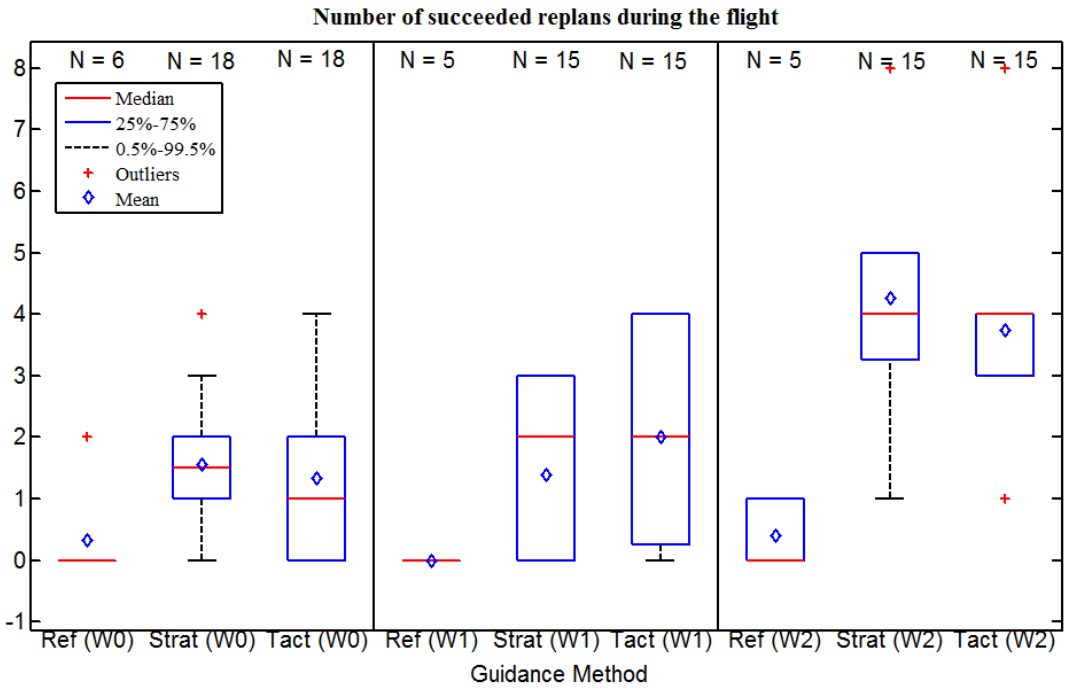

Figure 6.6: Number of succeeded re-plans during the flight

Guidance method	Percentage of simulations
Reference	81.25 %
Strategic	22.92 %
Tactical	29.17 %

Table 6.1: Percentage of simulations where an unable re-plan is found when aircraft is further than 6 NM from the RWY

Finally, in Figure 6.7 the execution time of the succeeded re-plans (not unable) can be seen. The time is roughly the same for all the implementations. It is considerably less than the initial re-plan since the guess passed to the solver is better (the current flown plan) than the one passed to the optimizer the first time, which is the nominal trajectory computed with backwards integration. Moreover, fewer phases are left when a re-plan is triggered since it usually happens at the last part of the route.

6.3. Time deviation

The first hypothesis of this project (**H1.a**) is to see if all the implementations are within 5 seconds of time deviation and if the two new implementations improve the time metering. Figure 6.8 shows a boxplot in which the results of the three implementations for ISA atmosphere (W0), real atmosphere (W1) and real atmosphere with wind errors (W2) are displayed. From this figure, it can be seen that the time deviation does not lie within the

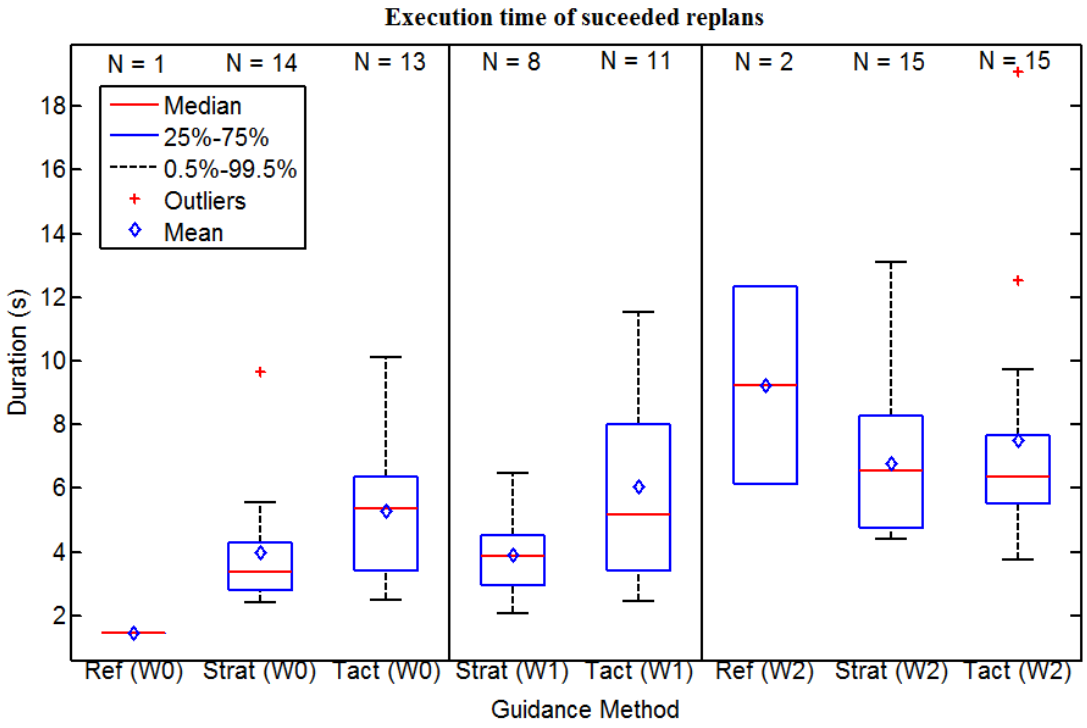

Figure 6.7: Execution time of succeeded re-plans

limits (marked by a dash-dot line) for the case of real atmosphere with wind prediction errors.

Moreover, it seems that the two new implementations produce a greater time deviation. The cause of this is that the aircraft follows path on elevator when the glideslope (G/S) is intercepted, meaning that the speed is then followed by controlling thrust. The engines are not as fast as the elevator to follow the speed plan. Hence, the actual speed of the aircraft is always greater than the planned speed producing a negative time deviation when the glideslope is intercepted. This negative time deviation is of around -5 seconds.

The difference between the strategic/tactical implementation and the reference is that the reference implementation is unable to give a correct re-plan when the aircraft is just before the G/S (only one phase is left to be optimized) while the other implementations give a re-plan that nullify the time deviation. The problem is that before G/S, the aircraft in these simulations have always had a positive time deviation. Hence, a re-plan is counterproductive for the time deviation since while the new implementations start at 0 s of time deviation after the re-plan, the reference implementation starts at +2 seconds. This can be seen in Figure 6.9 (strategic implementation) and Figure 6.10 (reference). It can be seen that the amount of time lost in the last part of the flight is roughly the same (-5 seconds), but the reference case (since it has not triggered any re-plan) starts at +2 seconds producing less time deviation at the runway.

In order to confirm this theory, the time deviation at the G/S interception has also been recorded, with the result shown in Figure 6.11.

As it can be seen, in the G/S interception, which is the last point of the trajectory where the calibrated airspeed is followed by the elevator, the time deviation is always better with

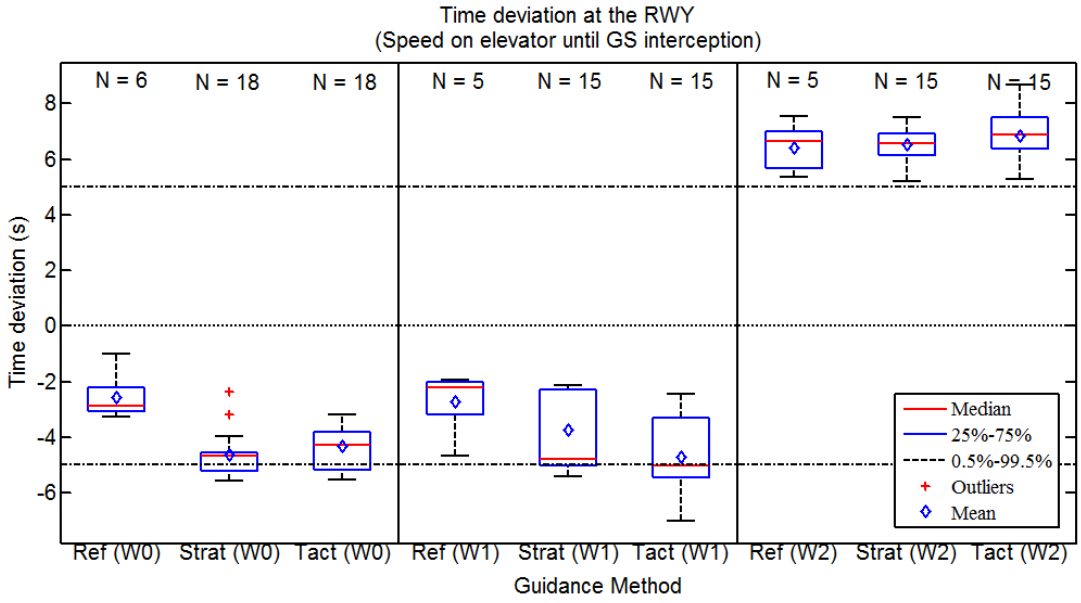

Figure 6.8: Time deviation at the RWY (speed on elevator until G/S interception)

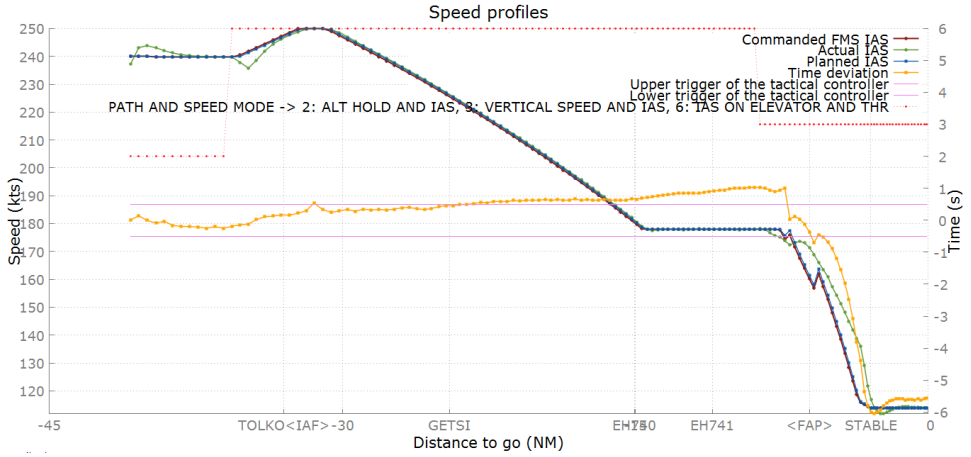

Figure 6.9: Time deviation during the flight (dynamic aircraft configuration scheduling)

the implementations of the current project, with the tactical configuration showing even a better time metering performance. It is also interesting to highlight that usually the time deviation is less if less ”time to next configuration” is used (see section G.2.), since the optimizer has more freedom to optimize.

In order to better understand the speed on thrust issue, some simulations have been done following speed on elevator until the runway. The results in Figure 6.12 (scenarios with wind prediction errors have not been simulated) support what has been said so far: if speed on elevator is followed until the runway, there is not anymore a negative time deviation and the results lie within the required 5 seconds of deviation, showing a better performance with the dynamic scheduling implementations.

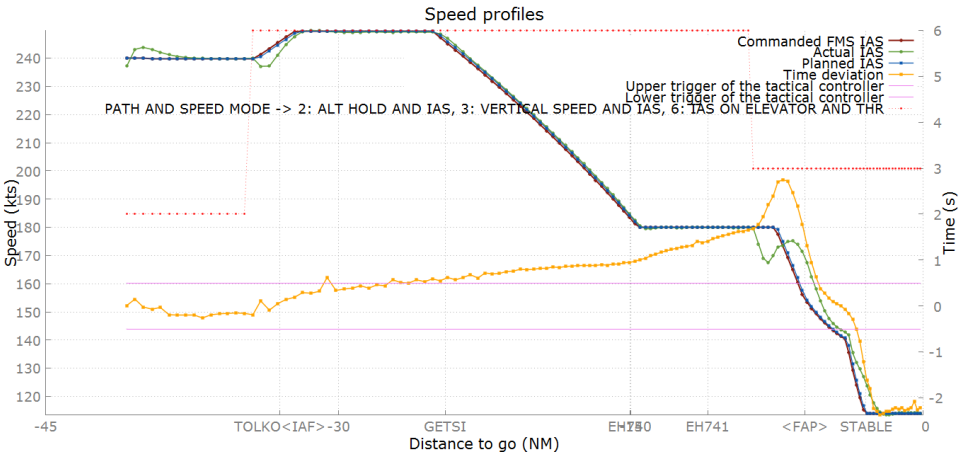

Figure 6.10: Time deviation during the flight (static aircraft configuration)

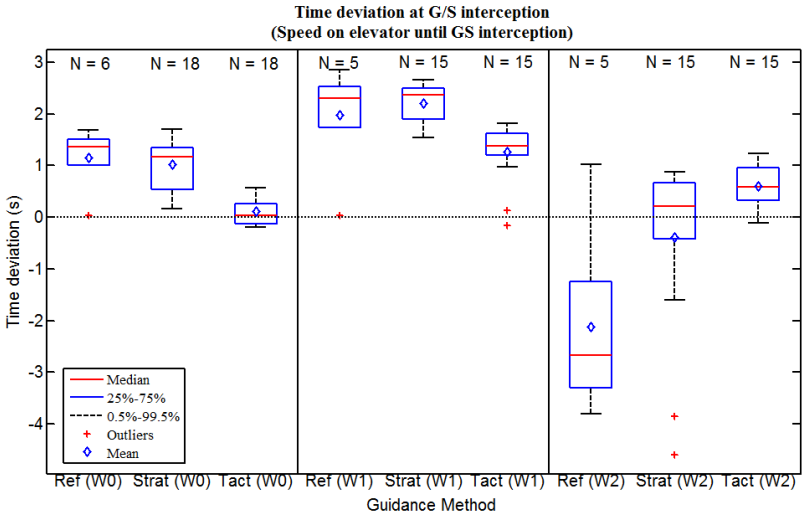

Figure 6.11: Time deviation at the glideslope interception

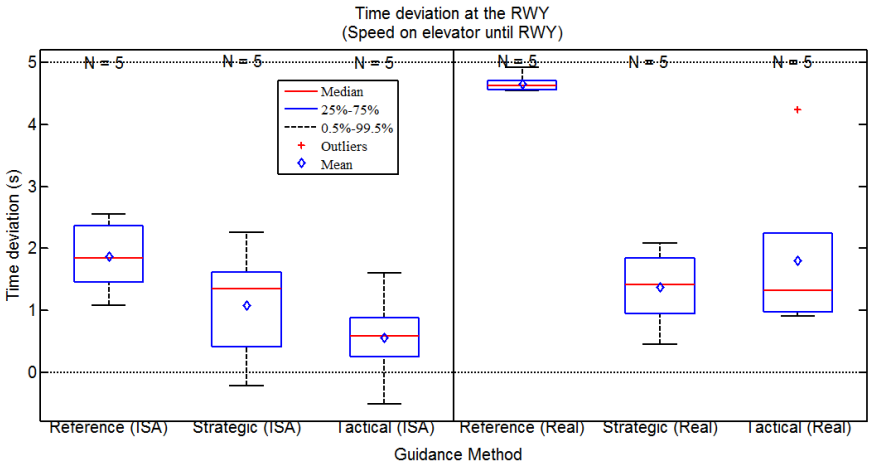

Figure 6.12: Time deviation at the RWY (speed on elevator until RWY)

Figure 6.13 shows how well the time deviation is controlled if speed on elevator is used until the RWY. It can be also seen that now the re-plan (when time deviation goes from +3 seconds to nearly 0 seconds) is beneficial for the time deviation.

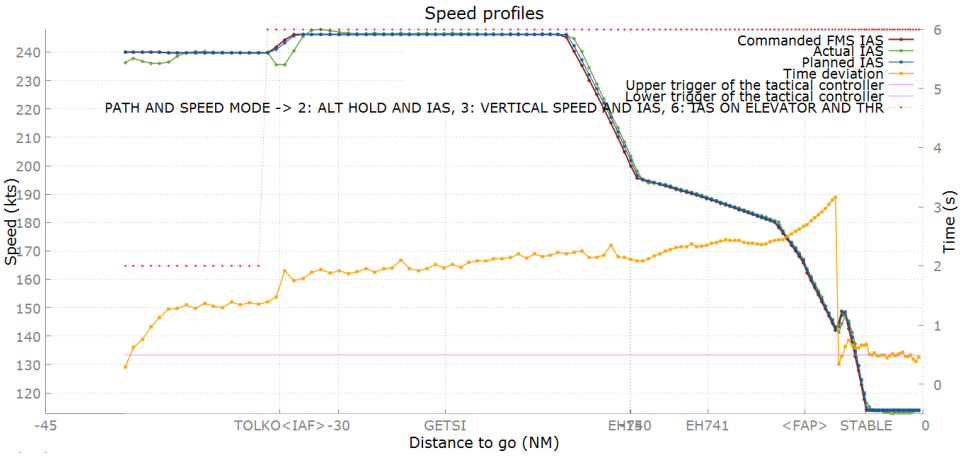

Figure 6.13: Time deviation during a flight (strategic implementation) following speed on elevator until the RWY

The drawback of using speed on elevator until the RWY is that there can be altitude deviations in the glideslope because of modeling errors. These altitude errors can be seen in Figure 6.14.

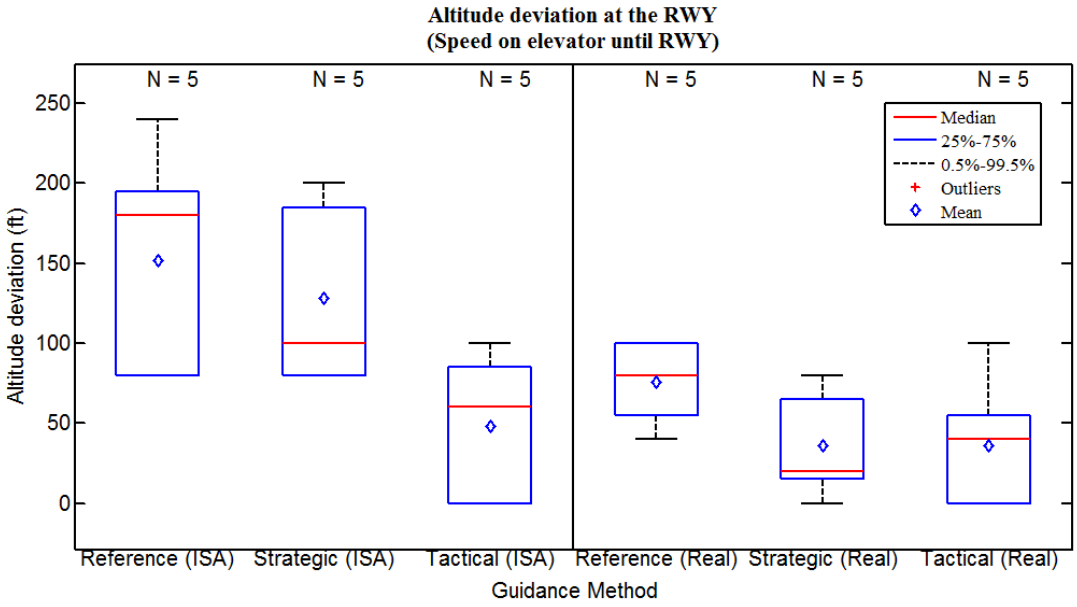

Figure 6.14: Altitude deviation at the RWY when following speed on elevator until it

In conclusion, the results shown in Figure 6.8 are somehow misleading since they depend on the particular used scenario (with wind errors, for instance, the time deviation is more or less the same). What it is clear is that the time deviation is not correctly followed because of the slow response of the engines, which cause a consistent amount of negative time deviation of around -5 seconds in all the cases. A proposed solution for this is to take into account this slow response in the optimization algorithm.

Finally, the difference between the tactical controller and the strategic solution can be seen in Figure 6.15, where we can observe that the tactical controller is able to maintain the time deviation within a small margin (0.5 seconds) during more part of the flight than using only strategic re-planning.

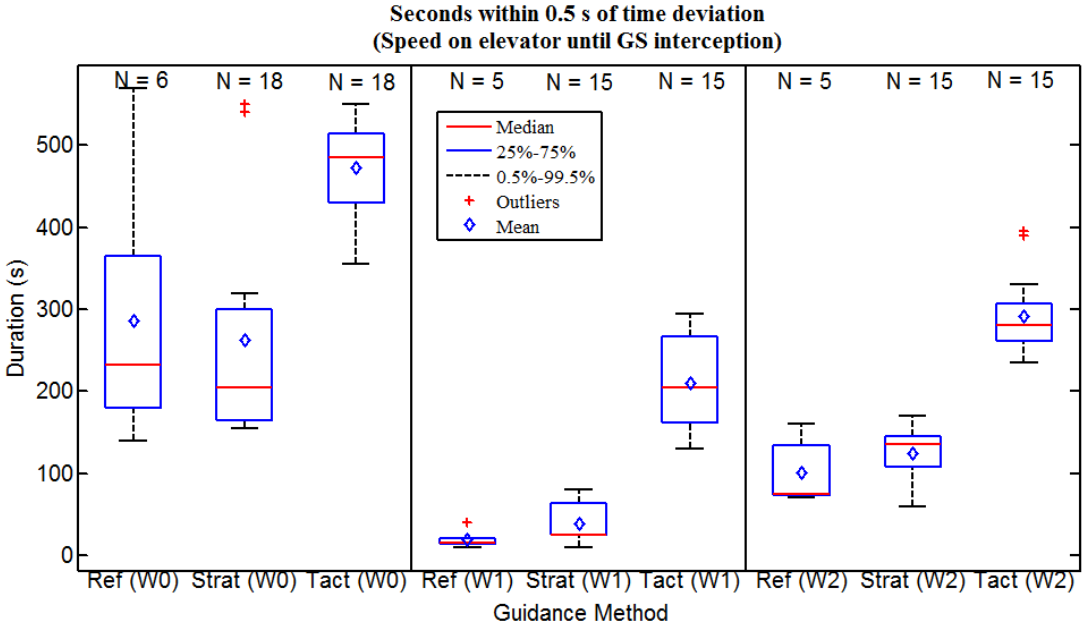

Figure 6.15: Portion of the flight when time deviation is less than 0.5 seconds

From all the mentioned results, when following speed on elevator only until the G/S interception, **H1.a** is not validated since then, in some cases, the strategic and tactical solution shows bigger errors. However, if speed on elevator is used until the runway, this hypothesis is largely verified.

On the other hand, **H1.b** is verified since the tactical controller shows better time metering than the strategic solution in most cases and it always maintain the time deviation within 0.5 seconds during more flown distance.

6.4. Stabilization altitude

H2 states that the aircraft needs to be stabilized at 1000 ft AGL. According to the criteria of the stabilization altitude defined in section 5.3., Figure 6.16 shows that the stabilization altitude is less than 1000 ft in most of the cases.

The restrictive variables are thrust and speed. They achieve their values later than expected. This can be observed in Figure 6.17 and Figure 6.18. The speed (to achieve the Final Approach Speed (FAS)) is the most critical variable for the reference scenario while the thrust is the most critical one for the dynamic high-lift devices scheduling implementation. In any case, it is shown that both the strategic and tactical solutions improve the stabilization altitude respect to the baseline case.

In this case, **H2** cannot be validated since the mean stabilization altitude for the two implementations is less than 1000 ft though being better than the baseline. It is worth noticing

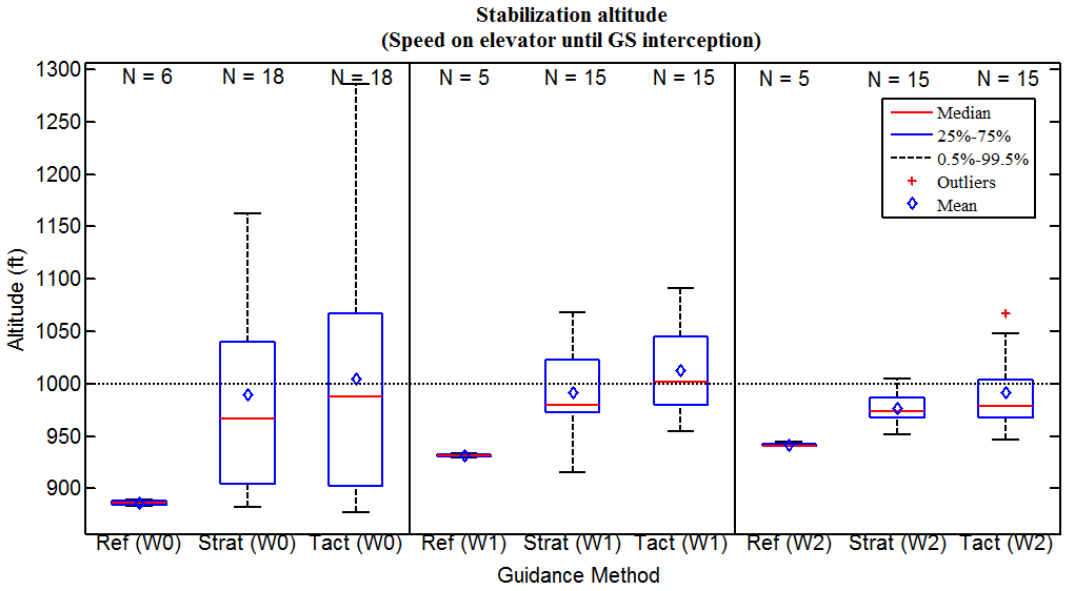

Figure 6.16: Stabilization altitude during the flight

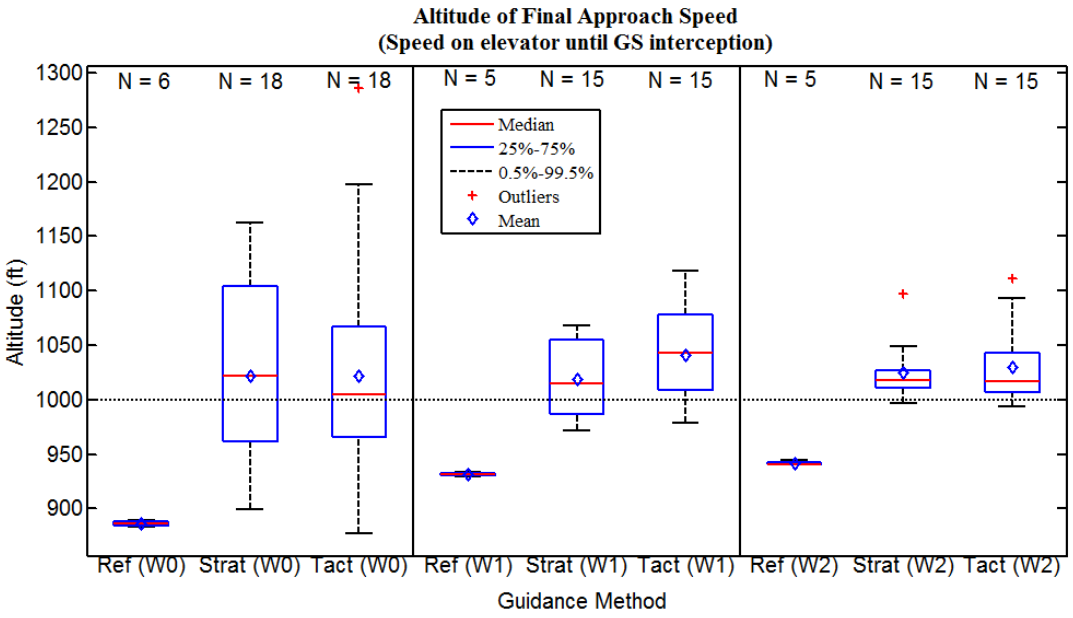

Figure 6.17: Altitude of flight where the Final Approach Speed is obtained

that if speed is followed by the elevator until the RWY, the stabilization altitude is verified in all the implementations (see Figure 6.19).

Finally, it has been observed (see section G.4.) that later RTAs usually produce higher stabilization altitudes.

6.5. Fuel and speed brakes usage

In Figure 6.20, the fuel consumption throughout the flight can be seen.

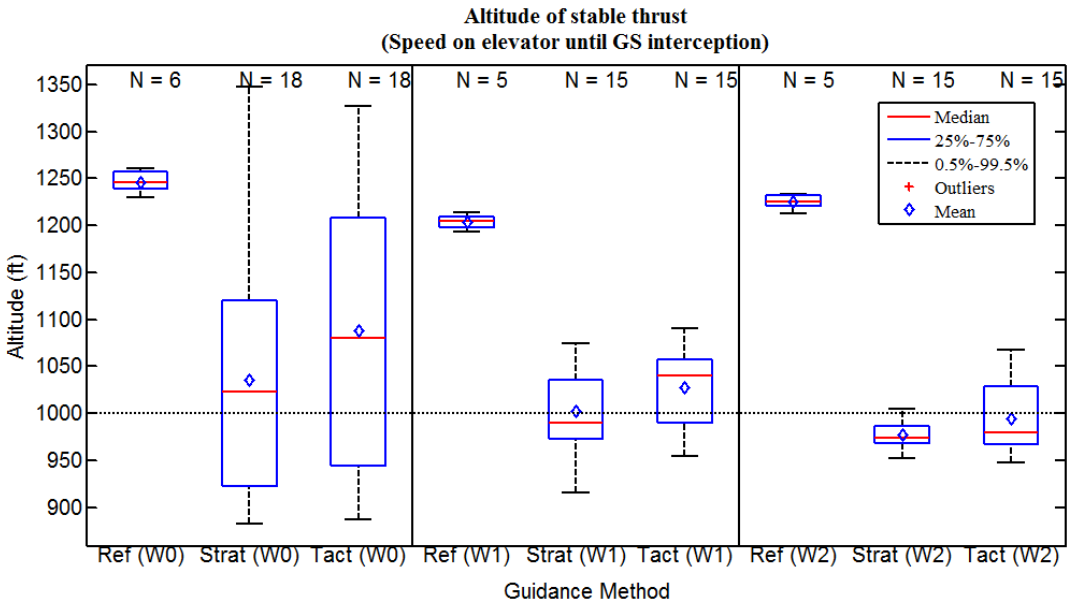

Figure 6.18: Altitude where stable thrust for Final Approach Speed is obtained

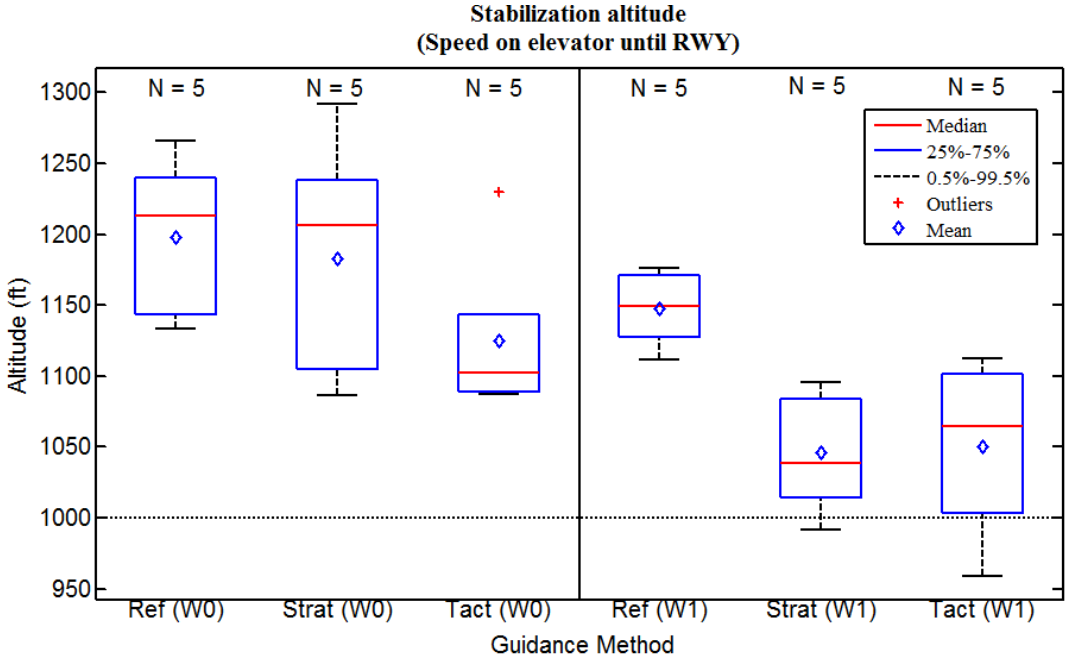

Figure 6.19: Stabilization altitude following speed on elevator until the RWY

In this case, it can be seen that **H3.b** is validated since the dynamic high-lift devices scheduling always helps decreasing the fuel consumption (around 0.5%-1.5%). The exact percentage of reduction respect to the baseline case can be found in Table 6.2. Fuel consumption is usually greater for later RTAs (see section G.5.).

On the other hand, **H3.d** is also validated since tactical controller usually has a greater mean of fuel consumption than the strategic solution. This is because the tactical controller does not optimize the small changes it applies on the flaps/gear, while the strategic case is looking to minimize the fuel consumption.

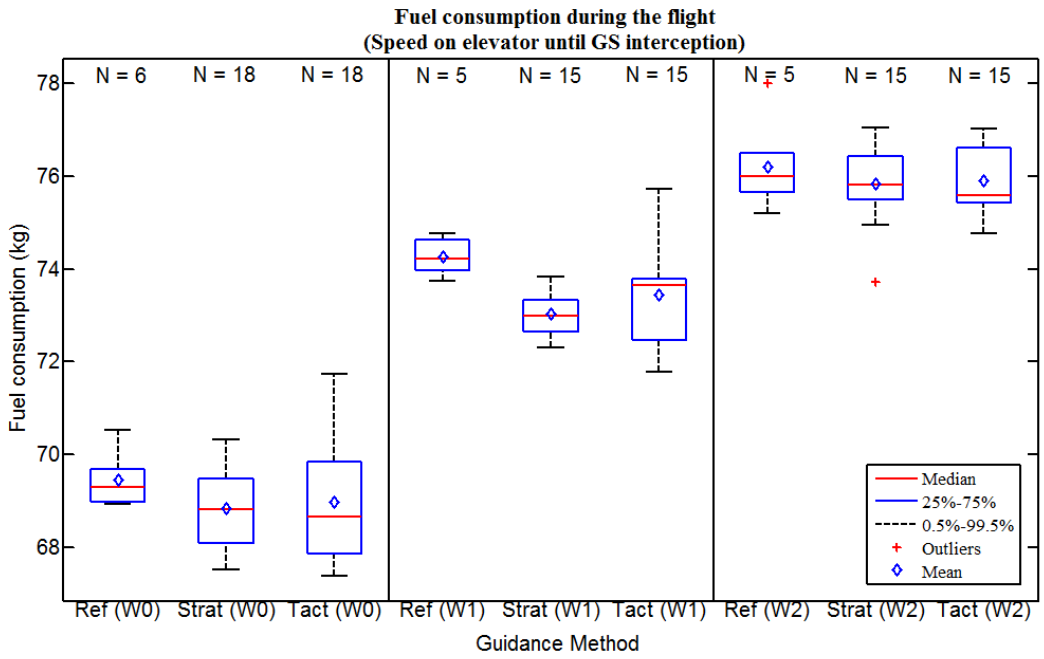

Figure 6.20: Fuel consumption throughout the flight

	Strategic guidance	**Tactical guidance**
ISA atmosphere	-0.89 %	-0.70 %
Real atmosphere	-1.68 %	-1.11 %
Real atmosphere + wind prediction errors	-0.47 %	-0.37 %

Table 6.2: Reduction (%) in average fuel burned respect to the baseline case

Figure 6.21 shows the fuel consumption if speed on elevator is followed until the RWY (thus, the planned trajectory is correctly followed). The decrease of fuel consumption is even greater: around 2.5 % of decrease (see Table 6.3) respect to the 1% if speed on elevator is only followed until the G/S interception. This shows again the importance of correctly following the speed and correctly modelling the aircraft performance.

	Strategic guidance	**Tactical guidance**
ISA atmosphere	-2.24 %	-1.32 %
Real atmosphere	-1.80 %	-2.80 %

Table 6.3: Reduction (%) in average fuel burned following speed on elevator until the RWY

Finally, **H3.a** is also validated since the dynamic aircraft configuration scheduling never uses speed brakes while the baseline implementation (fixed aircraft configuration) use speed brakes on the cases left in Table 6.4.

This table shows that speed brakes are used in two kinds of cases. The first one is to arrive later (+30s or +15 s). The other case is when an earlier RTA is requested and thrust is set on maximum power during a greater part of the flight, then it is necessary to descent from a higher altitude and speed brakes are used to aid achieving this steep descent. Moreover,

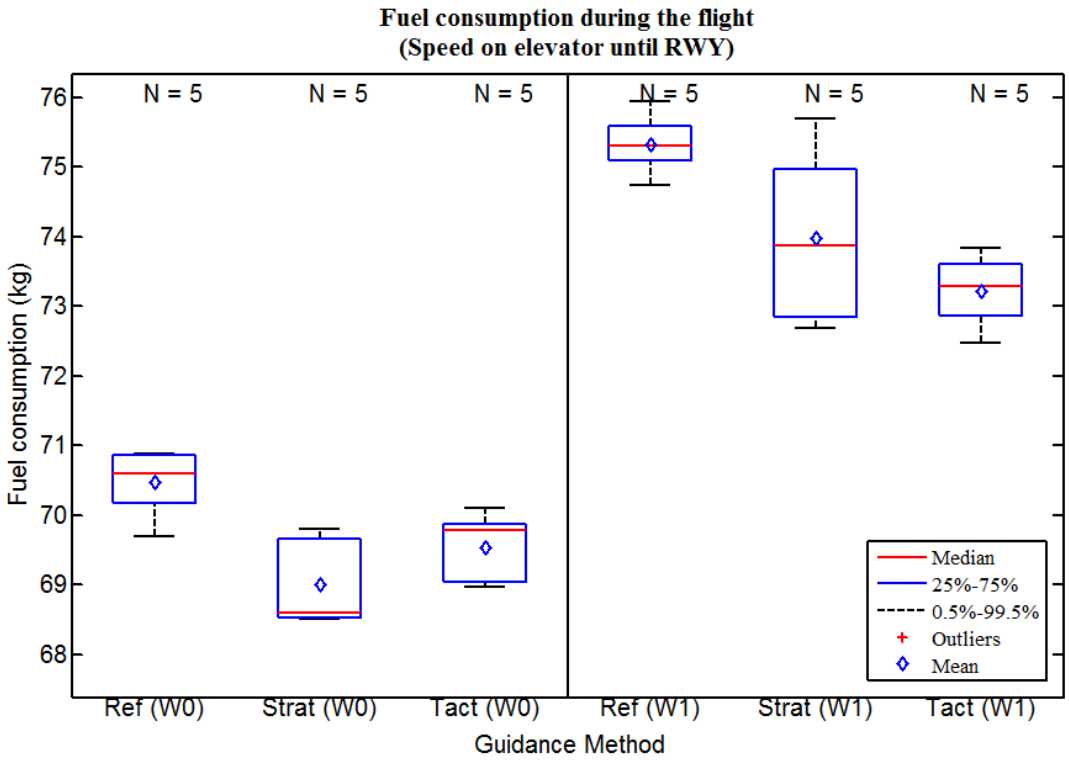

Figure 6.21: Fuel consumption following speed on elevator until the RWY

Scenario	RTA (respect to nominal ETA) (s)	Weather scenario	Duration of speed brakes usage (s)	Occurances of speed brakes usage
Reference	-30	W0 (ISA)	65.43	2
Reference	-30	W1 (Real)	55.31	2
Reference	+30	W1 (Real)	20.25	1
Reference	-30	W2 (Offsets)	55.26	2
Reference	+15	W2 (Offsets)	55.55	1
Reference	+30	W2 (Offsets)	20.10	1

Table 6.4: Cases where speed brakes are used

speed brakes are used more in real atmosphere with wind errors.

H3.d is also validated since neither strategic nor tactical solution use speed brakes.

CONCLUSIONS

This project shows that it is feasible to dynamically schedule aircraft high-lift devices and gear deployment in order to produce more efficient aircraft trajectory while meeting a specific Required Time of Arrival (RTA). It is also shown that it is possible to assign gear deployment at any point of the descent independently of the other flaps/slats configurations. The tactical implementation has demonstrated that it is possible to continuously control the planned aircraft configuration changes during the descent in order to maintain the time deviation within a required bound.

Results demonstrate that by correctly scheduling flaps and gear, the fuel burned during the flight is reduced in all the studied weather scenarios. Moreover, speed brakes are not used at all when the aircraft has the possibility to change the moment of flaps/slats and gear deployment. Another advantage of the dynamic scheduling of flaps/slats and gear is that the aircraft can obtain more likely a feasible re-plan closer to the runway and a wider margin of possible RTAs compared to the baseline case (without using high-lift devices scheduling).

Moreover, the required time deviation at the runway threshold is not met in some scenarios. It has been observed that the main cause of this deviation is the change from speed on elevator to speed on thrust when intercepting the glideslope. Aircraft engines are not able to correctly follow the calibrated airspeed (CAS) since their response is too slow compared to the elevator. This means that with speed on elevator, the rotational dynamics of the aircraft can be neglected since they are much faster than the translational dynamics (thus, a model with 3 degrees of freedom can be used, not being necessary a 6 degrees model with forces and moments), but it seems that the engines' dynamics cannot be neglected since they are slower. The proposed solution to this problem would be to take into account the thrust dynamics (namely the thrust derivative) in order to correctly model the slow response of the engines so that no time deviations are produced in the last part of the flight. This solution would also probably improve the stabilization altitude since it is seen that due to the high speeds (compared to the plan), the stabilization altitude lies below 1000 ft.

In the near future, the strategic solution will be tested in a set of human-in-the-loop experiments including real flight tests. In these tests, the operational acceptance of the dynamic aircraft high-lift devices will be assessed and it is foreseen that the aircraft performance is improved to correctly fit the reality.

BIBLIOGRAPHY

[1] R. Verhoeven, R. Dalmau, X. Prats, and N. de Gelder. Real-time aircraft continuous descent trajectory optimization with atc time constraints using direct collocation methods. In *Proceedings of the 29th Congress of the International Council of the Aeronautical Sciences*, St. Petersburg (Russia), September 2014. ICAS (International Council of the Aeronautical Sciences). xiii, 3

[2] IVAO division procedures (spain). https://ivao.aero/flightops/divprocedures.php?id=ES, March 2015. IVAO. xv, 80

[3] B. Gunston. *The Cambridge Aerospace Dictionary*. Cambridge University Press, Cambridge, UK, 2004. i

[4] NextGen Office. FAA's NextGen Implementation Plan 2012. Technical report, FAA, Washington DC, USA, March 2012. 1

[5] SESAR. European ATM Master Plan. Technical Report TR DLM-0602-001-03-00, EUROCONTROL, July 2006. 1

[6] Clean Sky Joint Undertaking. Annual Implementation Plan 2014. Technical Report CS-GB-2013-13-12 doc8a, EUROCONTROL, December 2013. 1, 2, 4

[7] ICAO, Montreal, Canada. *Continuous Descent Operations (CDO) Manual - Doc 9931 AN/476*, 2010. 1

[8] X. Prats, M. Pérez-Batlle, C. Barrado, S. Vilardaga, I. Bas, F. Birling, R. Verhoeven, and A. Marsman. Enhancement of a time and energy management algorithm for continuous descent operations. In *Proceedings of the 14th AIAA Aviation Technology, Integration, and Operations Conference, AIAA Aviation and Aeronautics Forum and Exposition*, Atlanta, Georgia (USA), June 2014. AIAA (American Institude of Aeronautics and Astronautics). (AIAA paper 2014-3151). 1, 4, 18

[9] P.M.A de Jong, F.J.L Bussink, N. de Gelder, R.P.M. Verhoeven, and M. Mulder. Time and Energy Management during Descent and Approach for Aircraft. In *Proceedings of the 5th International Conference on Research in Air Transportation - ICRAT 2012, Berkeley, California, May 22 - 25*, pages 1–6. FAA and EUROCONTROL, May 2012. 1

[10] L.D'Alto D.Garrido-López and R.Gómez Ledesma. A Novel Four-Dimensional Guidance for Continuous Descent Approaches. In *Proceedings of the 28th Digital Avionics Systems Conference*, pages 23–29, Orlando, Florida (USA), October 2009. 3

[11] M. A. Gómez Tierno et al. *Mecánica de vuelo*. Garceta Grupo, Madrid, Spain, 2nd edition, 2012. 5

[12] R. Dalmau. TEMO versus FMS performance comparison. Final degree project, Castelldefels School of Telecommunication and Aerospace Engineering (EETAC), Barcelona – Castelldefels, Catalonia (Spain), July 2014. 5

[13] X. Prats and R. Dalmau. FASTOP: D2.2 Mathematical Model. Technical report, Clean Sky, November 2013. FASTOP project. 7, 9, 13, 20, 30, 47

[14] J.T. Betts and E.J. Cramer. Application of Direct Transcription to Commercial Aircraft Trajectory Optimization. *Journal of Guidance, Control and Dynamics*, 18(1):151–159, January - February 1995. 9

[15] J.T. Betts. *Practical Methods for Optimal Control Using Nonlinear Programming*. Society for Industrial and Applied Mathematics, Seattle (WA), USA, 2nd edition, 2010. 9, 13, 18

[16] Model Types Description. http://www.gams.com/modtype/modeltyp.htm, March 2015. GAMS Development Corporation. 12

[17] Model Types. http://www.gams.com/modtype/, March 2015. GAMS Development Corporation. 12, 20

[18] B.W. Fitzpatrick B. Collins-Sussman and C.M. Pilato. *Version Control with Subversion: For Subversion 1.7*. Standford (CA), USA, 2011. (Manual). 15

[19] Unix tutorial. http://www.tutorialspoint.com/unix/, March 2015. tutorialspoint.com. 15

[20] T. Williams and C. Kelley. *Gnuplot 4.6: An Interactive Plotting Program*, 4.6 edition, 2014. (Manual). 15, 20

[21] J. Groeneweg. Ethernet I/F Management and Programming Utilities II. Technical Report NLR-TR-2007-090, Nationaal Lucht- en Ruimtevaartlaboratorium, Amsterdam, The Netherlands, October 2007. (Unclassified). 15

[22] M.J.D Valens. Manual of the NLR Research Flight Management System. Technical Report NLR-TR-2007-869, Nationaal Lucht- en Ruimtevaartlaboratorium, Amsterdam, The Netherlands, December 2007. (Unclassified). 15

[23] Honeywell. *A320 Flight Management System Pilot's Guide*. USA, January 1993. (Manual). 15

[24] M.J. Merchant. *FORTRAN 77. Language and Sytle*. Wadsworth Publishing Company, Belmont (CA), USA, 1981. 16

[25] J. Ellen Perry and H.D. Levin. *An Introduction to Object-Oriented Design in C++*. Addison-Wesley Publishing Company, North Carolina, USA, January 1996. 16

[26] F.J. Ceballos Sierra. *Enciclopedia del lenguaje C++*. Ra-Ma Editorial, Madrid, Spain, 2nd edition edition, 2009. 16

[27] X. Prats, I. Bas, and S. Vilardaga. FASTOP: D1.1 Problem Definition. Technical report, Clean Sky, May 2013. FASTOP project. 18, 20

[28] Mathematical Modeling Tools. http://www.aimms.com/operations-research/mathematical-modeling-tools/, June 2015. AIMMS. 20

[29] Conopt Home Page. http://www.conopt.com, March 2015. ARKI Consulting & Development A/S. 20

[30] GAMS Development Corporation. *GAMS - The Solver Manuals*. GAMS Development Corporation, Washington, DC, USA, March 2015. 20, 85

[31] GAMS Development Corporation. *GAMS - A User's Guide*. GAMS Development Corporation, Washington, DC, USA, December 2014. 20

[32] S. Vilardaga, I. Bas, and R. Isanta. FASTOP: D3.3 Software Design. Technical report, Clean Sky, May 2014. FASTOP project. 20

[33] J. L. De Prins et al. Enhanced Self-Spacing Algorithm for Three-Degree Decelerating Approaches. *Journal of guidance, control and dynamics*, 30(2):576–590, March-April 2007. 30

[34] NLR. Operations Manual Research Aircraft. Technical Report OMB_PHLAB_42, Nationaal Lucht- en Ruimtevaartlaboratorium, Amsterdam, The Netherlands, August 2013. (Confidential). 47

[35] AIS netherlands. http://www.ais-netherlands.nl/, June 2015. Air Traffic Control of the Netherlands. 48

[36] Airspeed definition. https://www.ivao.aero/training/documentation/books/PP_ADC_airspeed.pdf, April 2015. IVAO. 79

[37] Altimeter setting procedures. http://www.ais-netherlands.nl/aim/2015-05-14-AIRAC/eAIP/pdf/EH-ENR-1.7.pdf, June 2015. AIP Netherlands. 80

[38] Use of barometric altitude and geometric altitude information in ADS-B message for ATC applications. Technical Report SEA/BOB ADS-B WG/8 – WP/6, ICAO, Yangon, Myanmar, December 2012. 80

[39] G.W. Bluman and S. Kumei. *Dimensional analysis, modelling and invariance. In Symmetries and Differential Equations*. Springer-Verlag, 2nd edition, 1989. 82

[40] M. Cohen. Standard intrinsic module ISO_C_BINDING. http://www.nag.com/nagware/np/r52_doc/iso_c_binding.html, June 2015. Nihon Numerical Algorithms Group KK. 87

[41] Weinan E and Tiejun Li. Lecture 10 Polynomial interpolation. http://dsec.pku.edu.cn/~tieli/notes/num_meth/lect10.pdf, May 2015. 89

APPENDICES

APPENDIX A. SPEED AND ALTITUDE DEFINITION

Since speed and altitude are the key magnitudes to compute the energy of an aircraft, it is interesting to correctly define them, at least, for non-familiarized readers. Henceforth, when talking of speed and altitude, the type of variable used will be explicitly specified.

A.1. Speed

In the aeronautic field, there are basically four recurrent types of speed: CAS, TAS, GS and IAS.

IAS, as said in reference [36], stands for the speed of an aircraft as shown on its pitot tube airspeed indicator. If this IAS is corrected for instrument and position errors, CAS is obtained. During clean flight, CAS is really similar to IAS. However, when flaps are deployed (field of the current study), the angle of incidence of the pitot tube changes and indicated airspeed is a few knots lower than calibrated airspeed. CAS is the speed that is displayed in the cockpit and that can be seen by the pilot.

Then, TAS is the speed of the aircraft relative to the air-mass in which it is flying. At sea level, TAS=CAS, but when increasing the altitude or changing the air temperature, TAS is considerably higher than CAS. For this reason, TAS cannot be measured directly. True airspeed can be easily computed from the Mach number and the temperature of the atmosphere:

$$TAS = a_0 \cdot M \sqrt{\frac{\tau}{\tau_0}} \tag{A.1}$$

where $a_0 = 661.48$ kt is the speed of the sound at sea level and $\tau_0 = 288.15$ K.

TAS can also be computed from the indicated airspeed assuming an error of 2% when below 12000 ft:

$$TAS = IAS \cdot \left(1 + 0.02 \cdot \frac{h_G}{1000}\right) \tag{A.2}$$

Where h_G is the geometric altitude expressed in feets.

Finally, GS is the speed of the aircraft relative to the ground. It can be easily computed by adding the wind to the TAS:

$$GS = TAS + V_w \tag{A.3}$$

A.2. Altitude

When referring to altitude, both **barometric altitude** (h_p) and **geometric altitude** (h_G) can be used.

The first altitude is used for on-board aircraft instruments in order to give the altitude of the aircraft. In order to pass from pressure to altitude, a standard rate drop is assumed. If being below the Transition Altitude (TA), the pressure is referenced to the local sea level pressure supplied by ATC (QNH). If the aircraft is above the Transition Level (TL), the pressure is referenced to ISA[1]. Note that since the TA and the TL are not the same (because TL must be a standard flight level and depends on the local pressure while TA is a fixed altitude), there is a layer where descending and ascending aircraft are flying with a different pressure reference. See Figure A.1 for a graphical representation of this situation.

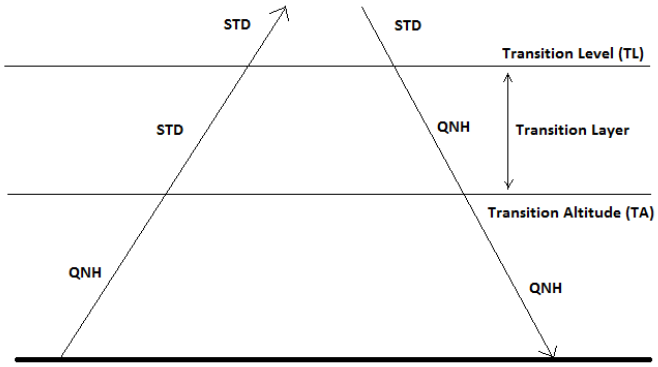

Figure A.1: Transition altitude and level

In the Netherlands, as said in [37], TA is 3000 for IFR flights and 3500 for VFR flights. The TL is at or above 4000 ft and it is determined hourly.

The transition altitude and level depends on each country. Thus, for instance, in Spain, TA is 6000 ft (except Madrid and Granada), while TL follows Table A.1.

QNH (hPa)	942.2-959.4	959.5-977.1	977.2-995.0	995.1-1013.2	1013.3-1031.6	1031.7-1050.3
TL	090	085	080	075	070	065

Table A.1: Transition levels depending on the local QNH (Source: [2])

Obviously, barometric altitude has some drawbacks, as said in [38]. Basically, there is the problem of having a different temperature than the expected one with ISA. This makes the rate to be non-uniform with the corresponding errors in the computation of the altitude. Though this big drawback, barometric altitude is the altitude shown in the cockpit of an aircraft.

The geometric altitude is the difference between the aircraft and the mean sea level given by a Global Positioning System (GPS). Hence, the only error in this kind of altitude is due to the GPS constellation error.

[1] ISA atmosphere assumes 15 Celsius degrees and 1013.25 hPa at standard sea level.

APPENDIX B. DRAG AND THRUST MODEL FOR C550

B.1. Drag modeling

The drag coefficient is modeled in our case as follows:

$$C_D = C_{D_{base}}(M, C_L, f) + \Delta C_{D_{sb}}(\beta) + \Delta C_{D_{gear}}(\beta_{gear}, f) \tag{B.1}$$

The drag coefficient is basically formed by a basic term, the contribution of speed brakes and the contribution of gear. Where f means that this contribution depends on the flaps configuration: clean, flaps approach and flaps land.

For our model, the base term is obtained from a polynomial of 4th degree in the case of clean configuration and 3rd degree for the case of F-APP or F-LND configuration. A 4th degree polynomial consists of 15 coefficients while a 3rd degree polynomial consists of 10 coefficients. These coefficients are specific for the C550 model and achieve a better modeling than other models, such as the Eurocontrol BADA model. By knowing in which aircraft configuration the aircraft is (clean, flaps approach or flaps land), the polynomial value only depends on the Mach and CL. So, for instance, for the case of clean configuration, the base term of C_D is obtained as:

$$C_{D_{base}}(M, C_L, f) = \sum_{i=0}^{4} \sum_{j=0}^{4-i} c_{i+j}(f) M^j C_L^i \tag{B.2}$$

where:

$$M = \frac{v}{\sqrt{\gamma_a \cdot R \cdot \tau}} \tag{B.3}$$

R is the gas constant (287.05287 $m^2/(s^2K)$), γ_a is the aerodynamic flight path angle and τ is the temperature.

On the other hand, the contribution of speed brakes is modelled as:

$$\Delta C_{D_{sb}}(\beta) = c_{sb1} \cdot \beta + c_{sb2} \cdot \beta^2 \tag{B.4}$$

where β can be 0, when speed brakes are not used, or 1, when speed brakes are being used.

Finally, the contribution of the gear also depends on the flaps configuration. However, for a given aircraft configuration, there is only one constant coefficient to obtain the contribution of gear:

$$\Delta C_{D_{gear}}(\beta_{gear}, f) = \beta_{gear} \cdot c_{gear}(f) \tag{B.5}$$

$\beta_{gear} = 0, 1$ is similar to the β representing the speed brakes, but applying for the gear.

C_L is obtained for all the aforementioned equations by applying the following formula:

$$C_L = \frac{2\left(\cos\gamma - \frac{\dot{w}_v \cdot \tan\gamma}{g}\right)}{mg\cos\phi \cdot S\rho v^2} \tag{B.6}$$

B.2. Thrust modeling

Thrust depends on several variables according to the Buckingham Π technique of dimensional analysis (see [39]). These variables are present in the following equation:

$$T = \#engines \cdot \delta \cdot f(N1c, M) \tag{B.7}$$

Where:

$$\begin{aligned} \delta &= \frac{p}{p_{SSL}} \\ N1c &= \frac{N1}{\sqrt{\theta}} \\ \theta &= \frac{\tau}{\tau_{SSL}} \end{aligned} \tag{B.8}$$

τ and p are respectively the temperature and pressure. $N1$ is the percentage of rotational speed of the low-pressure spool. The polynomial to obtain the thrust is just a 5th polynomial like the following one:

$$f(N1c, M) = \sum_{i=0}^{5} \sum_{j=0}^{5-i} p_{i+j} N1c^j M^i \tag{B.9}$$

The fuel flow can be also obtained by applying the following formula:

$$FF = \#engines \cdot \frac{\delta}{g} \cdot (1+0.2M^2)^{3.5} \cdot \sqrt{\theta \cdot (1+0.2M^2)} \cdot f\left(\frac{N2}{\sqrt{\theta \cdot (1+0.2M^2)}}, M\right) \tag{B.10}$$

Where the function f, in this case, is a 3rd degree polynomial instead of being a 5th degree one.

$N2$, the rotational speed of the high-pressure spool, can be obtained from $N1$ variable with the following 3rd degree polynomial:

$$N2 = \sum_{i=0}^{3} \sum_{j=0}^{3-i} p_{ij}^{N2} N1^j M^i \tag{B.11}$$

On the other hand, $N1_{idle}$, $N1$ when the spool is spinning at idle thrust, is obtained by applying a 5th degree polynomial (21 coefficients). Thus:

$$N1_{idle} = f(M,h) = \sum_{i=0}^{5} \sum_{j=0}^{5-i} c_{ij}^{idle} M^j h^i \tag{B.12}$$

Finally, the throttle, which goes from 0 to 1, can be obtained by applying the following formula:

$$\pi = \frac{N1 - N1_{idle}}{N1_{max} - N1_{idle}} \tag{B.13}$$

where, in the case of C550, $N1_{max}$=104.0.

APPENDIX C. WORKAROUND TO IMPLEMENT A TIME CONSTRAINT BETWEEN AIRCRAFT CONFIGURATIONS AVOIDING NON DIFFERENTIABLE FUNCTIONS

In order to get a correct optimized trajectory when gear is flexible, it is needed to leave a time constraint between gear and F-APP/F-LND. The issue is how to model this time difference in GAMS. At first glance, it may seem easy to do it by defining the following equation for the time when F-APP or F-LND are deployed for the first time:

$$\left| \frac{x_{sw} - x(t)}{v(t)} \right| \geq 15 \tag{C.1}$$

where x_{sw} is the distance where gear is deployed and $x(t)$ and $v(t)$ are respectively the distance and speed of the aircraft at a specific time/node. This equation should be defined two times: one for the F-APP node and another for F-LND node. However, the previous equation contains an absolute function. So to include the aforementioned constraint into our model, the model should change from an NLP to a DNLP. However, as said in subsection 1.5.3., DNLP models are not smooth and there is no guarantee that our optimizer solves this model in a correct way. The best alternative is to use another function instead of the absolute one. A good approximation (for small values of δ) is:

$$\sqrt{\left(\frac{x_{sw} - x(t)}{v(t)} \right)^2 + \delta} \geq 15 \tag{C.2}$$

A good interval for the values of δ is between 0.001 and 0.0001 as said in the manual of the CONOPT solver [30]. This ensures to have acceptable execution and convergence times for the solver and not to have big errors from the absolute function. The approximation error is maximum when the term inside the absolute function is 0; then the error is equal delta. The problem with the aforementioned equation is that it usually falls in local minima with the result that speed brakes are used when not needed at all.

The best solution is to use the following two equations:

$$f_{plus} + f_{minus} \geq 15 \tag{C.3}$$

$$f_{plus} - f_{minus} = \frac{x_{sw} - x(t)}{v(t)} \tag{C.4}$$

where f_{plus} and f_{minus} are free positive variables. This does not fall into any local minima, but, to be the exact solution, either f_{plus} or f_{minus} must be 0, since if both equations are combined, one of the following two solutions are found, where it can be observed that one of the aforementioned variables has to be 0 to verify the original equation:

$$2f_{minus} + \frac{x_{sw} - x(t)}{v(t)} \geq 15 \tag{C.5}$$

$$2f_{plus} - \frac{x_{sw} - x(t)}{v(t)} \geq 15 \tag{C.6}$$

In order to fix one of the variables to 0, the following two equations can be defined in GAMS:

$$f_{minus} \leq \delta \cdot M \tag{C.7}$$

$$f_{plus} \leq (1 - \delta) \cdot M \tag{C.8}$$

Where M is a big value, such as the time of the entire flight, and δ is a value from 0 to 1. Ideally, δ should be either 0 or 1. If the exact solution is desired, then a MINLP model has to be used. A knob has been implemented so that the user can choose this option. The other option is to use the variable $\beta_{gear}(t)$ as δ. Remember that $\beta_{gear}(t)$ takes values from 0 to 1 (0.5 is where gear is deployed). This last option can be done with the NLP model. Hence, it is faster since when using MINLP, first the NLP model has to be solved and then the integer variables are found. However, using NLP is less exact since it can happen that it does not verify the constraint (e.g. when the optimizer tells that gear is deployed really close to F-APP, then the equations for F-APP, not for F-LND, will have a δ value near 0.5 when it should be 0 or 1).

As it can be seen, it is not easy to implement all the desired constraints. In any case, as it is said, in the current implementation there is the option to solve the model fast but approximating this constraint of time or slow (more or less investing double the time) but being sure that the constraints of time are maintained.

APPENDIX D. INTERACTION BETWEEN RFMS AND TACTICAL CONTROLLER THREAD

The tactical controller of this project is written in C++ language. However, as previously said in this report, the RFMS, which is responsible to call the tactical controller each time that the time deviation between the plan and the real trajectory is greater than 0.5 seconds, is written in Fortran 90. Hence, in order to be able to call the controller, "ISO_C_BINDING" mechanism is used. This is a standardized mechanism provided by Fortran in order to interoperate with C. Basically, it enables to reference procedures defined in C and the interoperability of types between both languages (see [40]).

Note that Fortran can only interact with C and not C++. Hence, in order to completely make the program interoperable the command "extern 'C' " is used, which makes a function written in C++ to have a C linkage so that the C client can link to this specified function.

Once the interaction between languages has been explained, it is interesting to briefly explain the functions that are called by the RFMS (see section 4.1. for the diagram of functions of the tactical controller that the RFMS calls):

- **killThread**: Every time that a new strategic re-plan is called due to a new RTA or a deviation of energy, the active thread of the tactical controller is killed if it is working at that precise moment since the working plan will change.
- **setTactVariables**: Some variables of the tactical controller are set after obtaining a correct plan. These variables are necessary to know if the controller is busy making computations and to know the value of the exit code of the controller.
- **destroyThread**: Close the handle of the thread if the tactical controller thread has already finished. This is tried in every loop of the RFMS if the tactical control has been activated.
- **updateTactVariables**: To obtain information about the exit code of the controller, whether it is busy or not and the number of the cycle[1]. These variables are used, then, to know if the RFMS has to call or not the tactical controller. And for instance, if the tactical controller has finished a specific cycle with an exit code of 0, then the RFMS has to redraw the trajectory on the ND with the new location of the different aircraft configuration.
- **mainControllerThread**: This function is the responsible to start the execution of the tactical controller. It is called every time that all the following conditions are met:
  - The tactical control is active.
  - The tactical controller is not busy.
  - The previous exit code has been 0, 1 and now there is a negative deviation or -1 and now there is a delay in the time deviation.
  - The aircraft is not too close to an aircraft configuration.
  - The time deviation is greater than half a second.

[1] Cycle is each time the tactical controller is called (when the deviation in time is greater than 0.5 seconds).

All the aforementioned functions are only called externally from the tactical controller and, thus, have to be defined correctly with an ”ISO_C_BINDING” structure.

APPENDIX E. EQUATIONS INVOLVED IN THE TRAJECTORY UPDATE OF THE TACTICAL CONTROLLER

In this appendix, the equations involved in the trajectory update made by the tactical controller are explained. This trajectory update consists of the changes made in the variables of the affected phases (before and after the aircraft configuration) of the trajectory.

Note that when a variable is highlighted with $var^{(0)}$, it means the original plan, or the plan of the previous cycle of the tactical controller, which has not been modified during the computations of the current tactical cycle. Moreover, *i-1* node is closer to the RWY than *i* node.

So, the new time at each node is obtained applying Euler collocation:

$$t_i = t_{i-1} - dt \tag{E.1}$$

Then, as said in section 4.4., it is assumed that the calibrated airspeed is maintained at each node, which is a reasonable hypothesis since the same aircraft configuration is used at each node. This is because only the location of nodes is changed, but each node has the same associated aircraft configuration and speed brakes:

$$\begin{aligned} CAS_i &= CAS_i^{(0)} \\ \dot{CAS}_i &= \frac{CAS_{i-1} - CAS_i}{dt} \\ \beta_i &= \beta_i^{(0)} \\ \beta_{gear_i} &= \beta_{gear_i}^{(0)} \\ config_i &= config_i^{(0)} \end{aligned} \tag{E.2}$$

To obtain pressure and temperature, the tactical controller interpolates. In order to obtain the most precise possible value of the related variables, the Lagrange interpolation is used. In our case, a 3rd degree polynomial is used (thus, using 4 points) instead of a linear interpolation. The Lagrange polynomial follows this equation:

$$f(x) = \sum_{i=0}^{n} \left(\prod_{\substack{m=0 \\ m \neq i}}^{n} \frac{x - x_m}{x_i - x_m} \right) f(x_i) \tag{E.3}$$

Where *n* is the order of the polynomial. As said in reference [41], the error produced by this interpolation is:

$$\varepsilon = \frac{\prod_{i=0}^{n}(x - x_i)}{(n+1)!} \cdot \left(max_{x \in [x_0, x_n]} |y(x)| \right) \tag{E.4}$$

where the last term is the greatest value of the original data inside the interval of the chosen points. Here it can be seen that the error decreases if the points around the x value, in

whose y value remains the interest, are tighter and if a higher order polynomial is used. However, it is important to bear in mind that when increasing the degree of the polynomial it is more probable that the Runge's phenomenon occurs, especially if not the correct nodes are taken. This phenomenon is a problem of oscillation at the edge of an interval and it is quite similar to the Gibbs phenomenon in the Fourier series. This instability of high order polynomials added to the higher complexity of the polynomial are the main reasons why not a higher degree polynomial has been chosen for the interpolations.

Temperature and pressure are interpolated according to altitude assuming same $\dot{h}$ as the original plan:

$$\begin{aligned} \tau_i &= interp(h_{i-1} - \dot{h}_{i-1}^{(0)} \cdot dt, \vec{h}^{(0)}, \vec{\tau}^{(0)}) \\ p_i &= interp(h_{i-1} - \dot{h}_{i-1}^{(0)} \cdot dt, \vec{h}^{(0)}, \vec{p}^{(0)}) \\ \rho_i &= \frac{p_i}{R\tau_i} \end{aligned} \tag{E.5}$$

Once these three important magnitudes are obtained, the modified TAS and Mach can be computed:

$$\begin{aligned} \mu &= \frac{\gamma_a - 1}{\gamma_a} \\ A &= \left(\frac{\mu \cdot CAS_i^2 \cdot \rho_{SSL}}{2 \cdot p_{SSL}} + 1 \right)^{\frac{1}{\mu}} - 1 \\ TAS_i &= \sqrt{\frac{2}{\mu} \cdot \frac{p_i}{\rho_i} \cdot \left(\left(\frac{p_{SSL}}{A \cdot p_i + 1} \right)^{\mu} - 1 \right)} \\ \dot{v}_i &= \frac{TAS_{i-1} - TAS_i}{dt} \\ M_i &= \frac{TAS_i}{\sqrt{\gamma_a R \tau_i}} \end{aligned} \tag{E.6}$$

In a similar way to the pressure and temperature, the winds can also be interpolated and their derivatives obtained:

$$\begin{aligned} w_{s_i} &= interp(h_{i-1} - \dot{h}_{i-1}^{(0)} \cdot dt, \vec{h}^{(0)}, \vec{w_s}^{(0)}) \\ w_{x_i} &= interp(h_{i-1} - \dot{h}_{i-1}^{(0)} \cdot dt, \vec{h}^{(0)}, \vec{w_x}^{(0)}) \\ w_{n_i} &= interp(h_{i-1} - \dot{h}_{i-1}^{(0)} \cdot dt, \vec{h}^{(0)}, \vec{w_n}^{(0)}) \\ w_{e_i} &= interp(h_{i-1} - \dot{h}_{i-1}^{(0)} \cdot dt, \vec{h}^{(0)}, \vec{w_e}^{(0)}) \end{aligned} \tag{E.7}$$

$$\begin{aligned} \dot{w}_{n_i} &= \frac{w_{n_{i-1}} - w_{n_i}}{dt} \\ \dot{w}_{e_i} &= \frac{w_{e_{i-1}} - w_{e_i}}{dt} \\ \bar{w}_{x_i} &= \frac{w_{x_{i-1}}}{TAS_i} \end{aligned}$$

Another assumption made in section 4.4. is that the following variables are maintained at each node:

$$\begin{aligned} \chi_i &= \chi_i^{(0)} \\ \phi_i &= \phi_i^{(0)} \\ m_i &= m_i^{(0)} \end{aligned} \tag{E.8}$$

Then, depending on the type of phase the aircraft is, variables are computed differently:

- **GS phases**: γ is maintained in each node, which is a good assumption since the glideslope has to be followed. Thrust is changed according to the new drag (see Appendix B). N_{1_i} and π_i are then computed according to this thrust.

- **FPA phase**: This is just the phase before the glideslope where a fixed flight path angle is maintained during the entire phase. γ is computed as follows:

$$\begin{aligned} \bar{w}_{s_i} &= \frac{w_{s_i}}{TAS_i} \\ \gamma_i &= \arcsin\left(\sin\gamma_g \cdot \left(\sqrt{1-\bar{w}_{x_i}^2-(\bar{w}_{s_i}\cdot\sin\gamma_g)^2}+\bar{w}_{s_i}\cdot\cos\gamma_g\right)\right) \end{aligned} \tag{E.9}$$

  Where γ_g is just the flight path angle respect to the ground necessary the necessary one to have the change of the aircraft configuration at an altitude corresponding to the descent of the original plan.

- **Other phases**: Thrust is maintained at each node (it will be idle so that the TEMO philosophy is verified) and gamma will change (following an iterative process; not using the complex equations of computation of flight path angle) to maintain this thrust using the following formula of computation of thrust depending on gamma:

$$T_i = m_i \cdot \left(\dot{w}_{v_i} + (g+F)\cdot\sin\gamma_i + \frac{CAS_i}{TAS_i}\cdot G\cdot \dot{CAS}_i\right) + D_i \tag{E.10}$$

  where:

$$\begin{aligned} F &= R\cdot\left(\frac{p_{SSL}\cdot A\cdot\tau_i\cdot g\cdot\rho_i\cdot(A\frac{p_{SSL}}{p}+1)^{\mu-1}}{p_i^2-\frac{\lambda}{\mu}\cdot\left(\left(A\frac{p_{SSL}}{p}+1\right)^{\mu}-1\right)}\right) \\ G &= \theta_i\cdot\frac{p_{SSL}}{p_i}\cdot\left(A\frac{p_{SSL}}{p}+1\right)^{\mu-1}\cdot\left(\frac{\mu\cdot CAS_i^2\cdot\rho_{SSL}}{2\cdot p_{SSL}}+1\right)^{\left(\frac{1}{\mu}-1\right)} \end{aligned} \tag{E.11}$$

In any case, regardless of the type of phase, the modified drag is computed as follows:

$$
\begin{aligned}
\dot{w}_{v_i} &= \dot{w}_{n_i} \cdot \left(\sqrt{\cos^2\gamma_i - \bar{w}_{x_i}^2} \cdot \cos\chi_i + \bar{w}_{x_i} \cdot \sin\chi_i \right) + \dot{w}_{e_i} \cdot \left(\sqrt{\cos^2\gamma_i - \bar{w}_{x_i}^2} \cdot \sin\chi_i + \bar{w}_{x_i} \cdot \cos\chi_i \right) \\
n_z &= \frac{\cos\gamma_i - \frac{\dot{w}_{v_i} \cdot \tan\gamma_i}{g}}{\cos\phi_i} \\
C_{L_i} &= \frac{2 m_i g \cdot n_z}{S \rho_i TAS_i^2} \\
C_{D_i} &= f(M_i, C_{L_i}, \beta_i, \beta_{gear_i}, config) \\
D &= \frac{1}{2} \cdot \rho_i \cdot S \cdot TAS_i^2 \cdot C_{D_i}
\end{aligned}
\tag{E.12}
$$

where the function to get the drag coefficient is explained in subsection 1.4.1..

With all this information, most of the derivatives can be obtained, which are important for computations of next nodes. The derivative of distance, also called ground speed, is the variable that is being summed node after node to compare the final value in that phase with the theoretical value computed with Equation 4.4:

$$
\begin{aligned}
\dot{x}_i &= \sqrt{TAS_i^2 \cdot \cos^2\gamma_i - w_{x_i}^2} + w_{s_i} \\
x_i &= x_{i-1} - \dot{x}_i \cdot dt \\
\\
\dot{h}_i &= TAS_i \cdot \sin\gamma_i \\
h_i &= h_{i-1} - \dot{h}_i \cdot dt \\
\\
\dot{\gamma}_i &= \frac{\gamma_{i-1} - \gamma_i}{dt}
\end{aligned}
\tag{E.13}
$$

Finally, to compute the barometric altitude, pressure and temperature are re-computed again, now that the correct value of altitude is known:

$$
\begin{aligned}
\tau_i &= interp(h_i, \vec{h}^{(0)}, \vec{\tau}^{(0)}) \\
p_i &= interp(h_i, \vec{h}^{(0)}, \vec{p}^{(0)}) \\
h_{p_i} &= \frac{\tau_{SSL}}{\lambda} \cdot \left(1 - \frac{p}{QNH}^{\frac{R \cdot \lambda}{g_{SSL}}} \right)
\end{aligned}
\tag{E.14}
$$

APPENDIX F. AIP CHARTS

F.1. EHGG aerodrome chart (ADC)

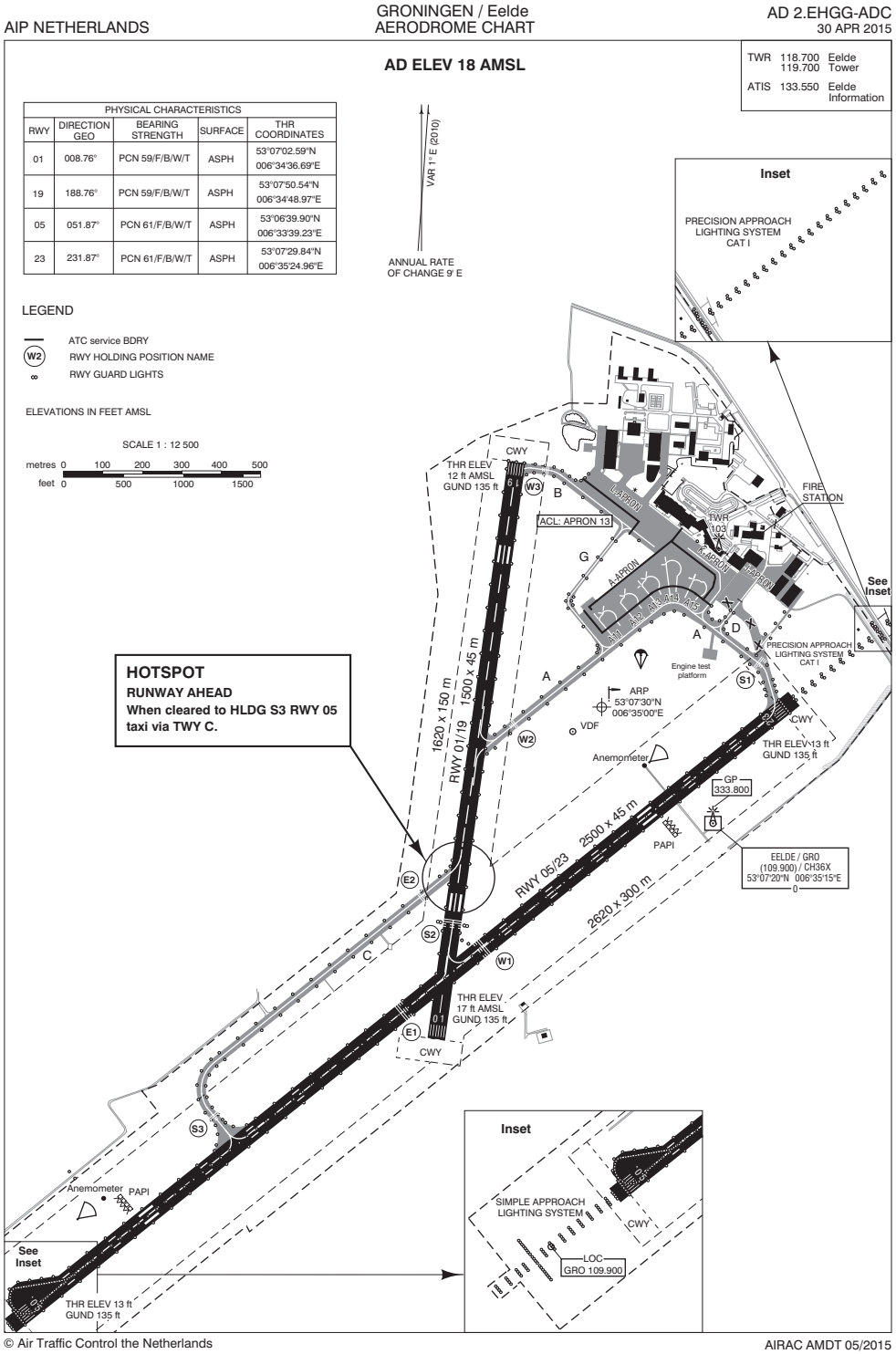

F.2. EHGG standard arrival chart (STAR)

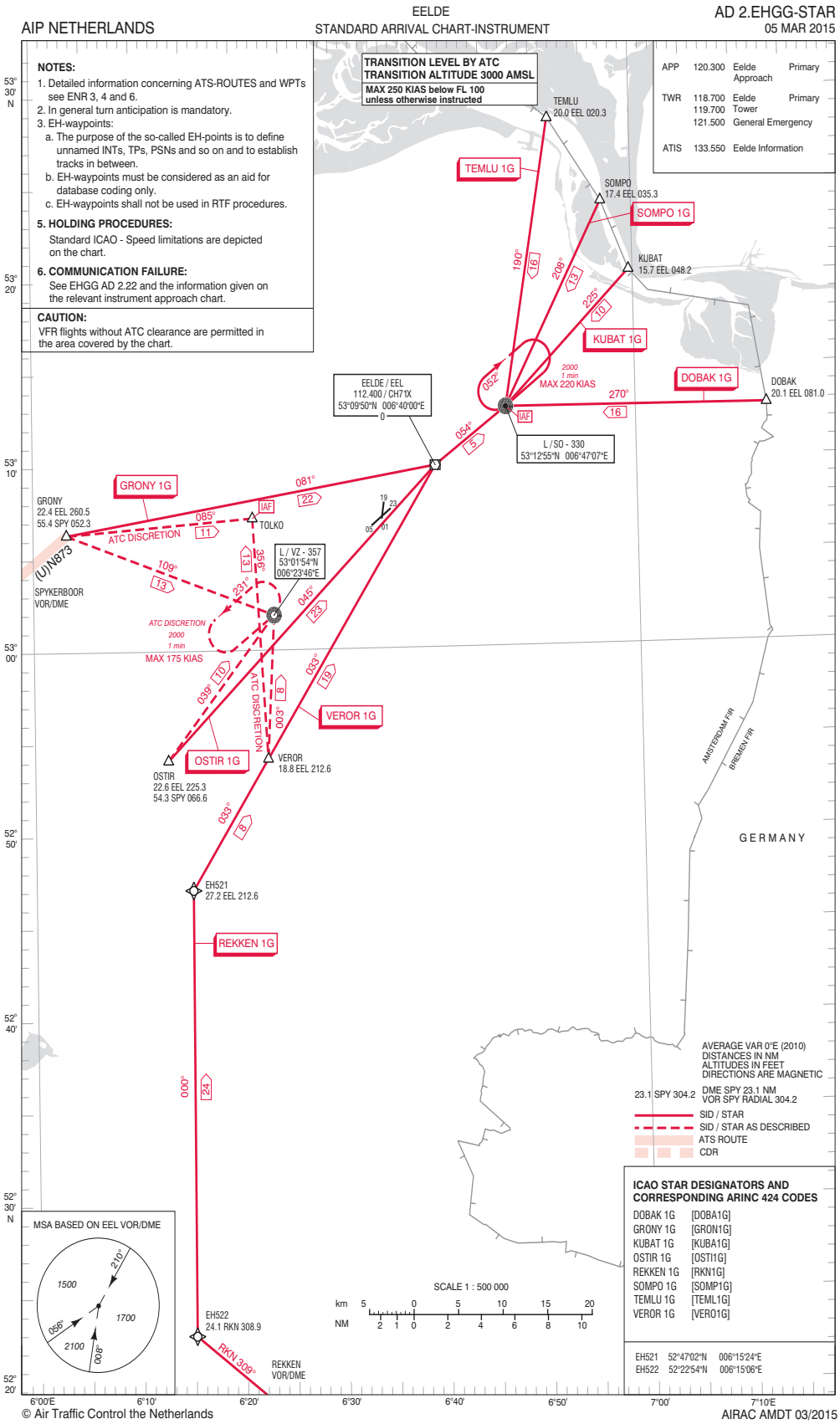

F.3. EHGG RNAV instrument approach chart RWY 23 TOLKO (IAC)

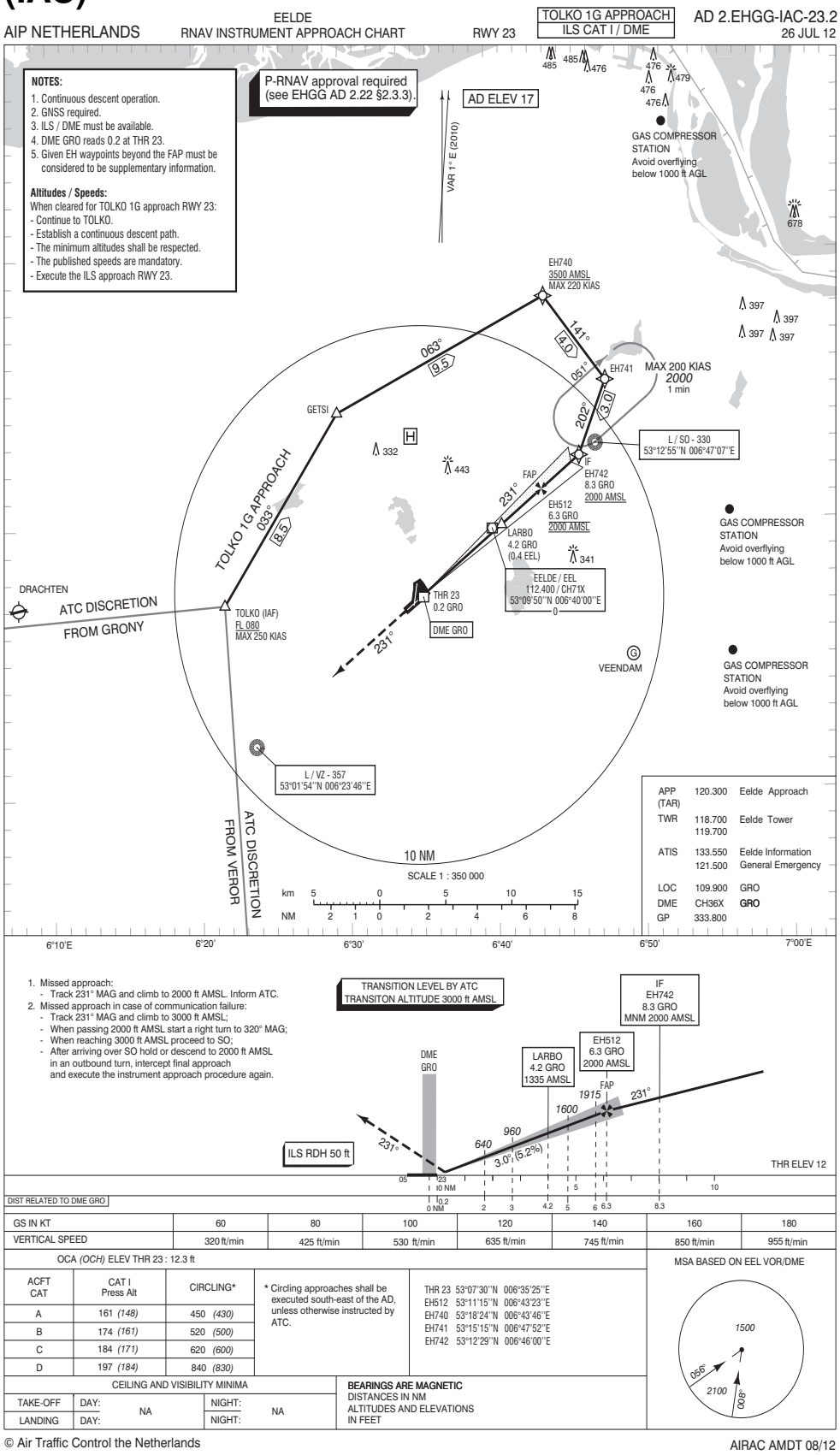

APPENDIX G. GRAPHS OF THE RESULTS FOR EACH SCENARIO VARIANT

In this appendix, we can find the plots of each weather atmosphere with all the scenarios of the experiment matrix (see Table 5.4). In chapter 6, these plots have been combined in order to get 1 plot of each section of the appendix.

All the simulations left herein have been done with speed on elevator only until the glideslope.

G.1. Time deviation at the RWY

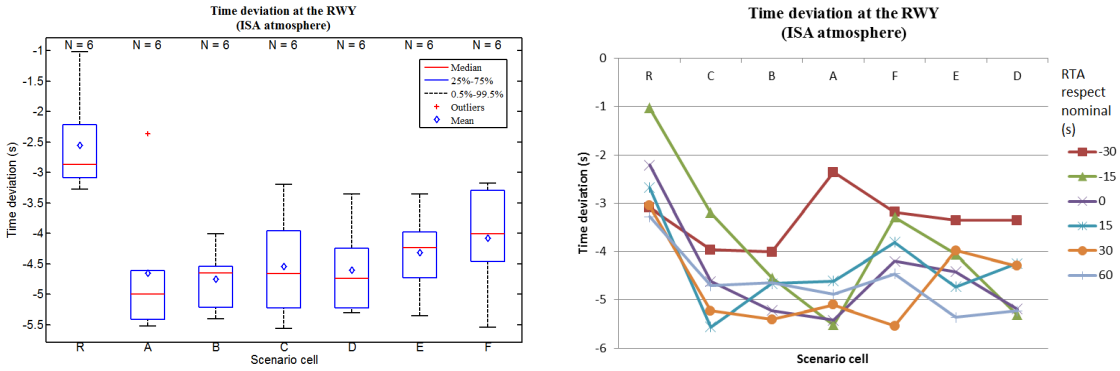

(a) Boxplot

(b) Influence of RTAs

Figure G.1: Time deviation at the RWY (ISA atmosphere)

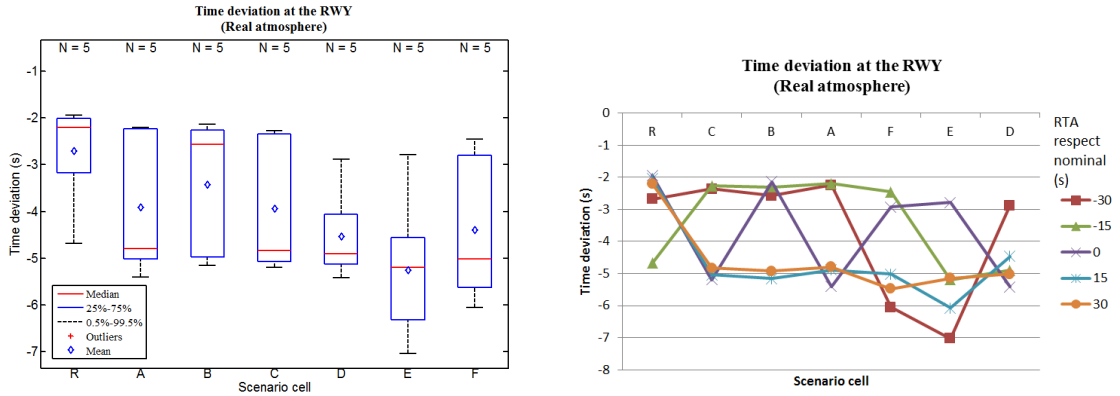

(a) Boxplot

(b) Influence of RTAs

Figure G.2: Time deviation at the RWY (Real atmosphere)

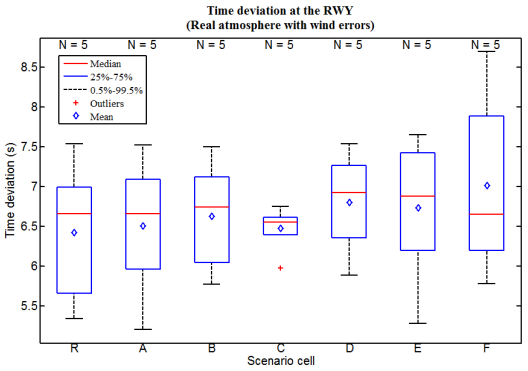

(a) Boxplot

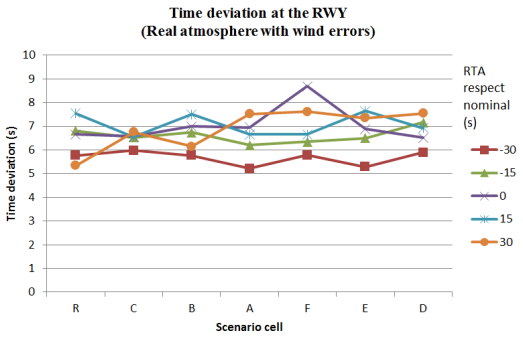

(b) Influence of RTAs

Figure G.3: Time deviation at the RWY (Real atmosphere with wind prediction errors)

G.2. Time deviation at G/S

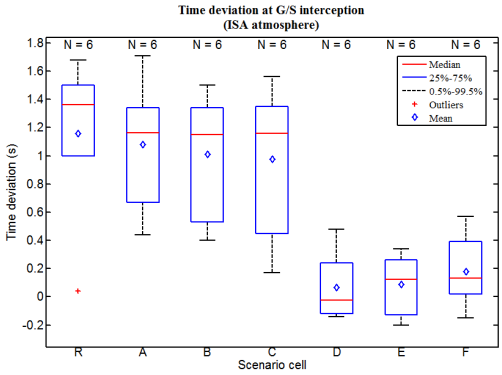

(a) Boxplot

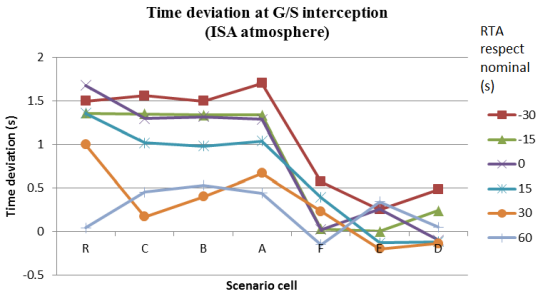

(b) Influence of RTAs

Figure G.4: Time deviation at the G/S interception (ISA atmosphere)

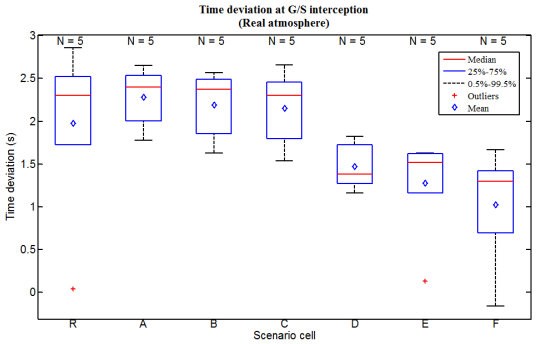

(a) Boxplot

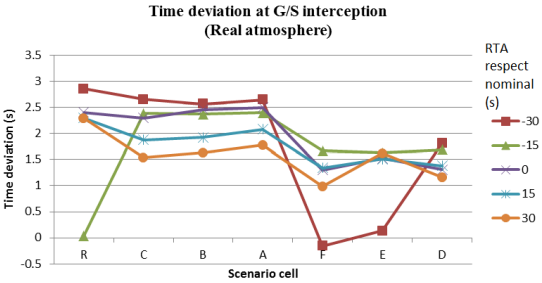

(b) Influence of RTAs

Figure G.5: Time deviation at the G/S interception (Real atmosphere)

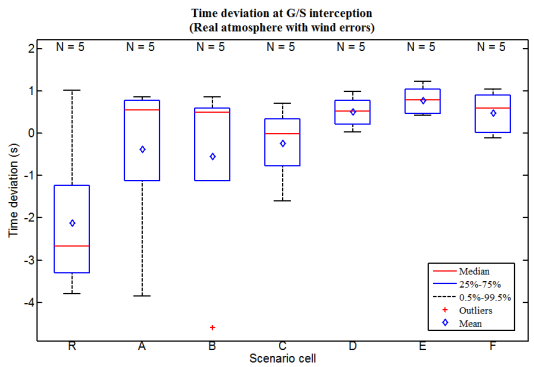

(a) Boxplot

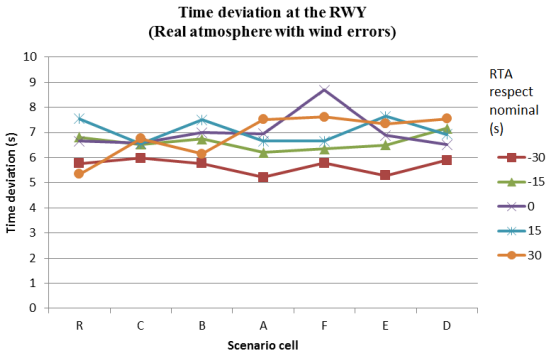

(b) Influence of RTAs

Figure G.6: Time deviation at the G/S interception (Real atmosphere with wind prediction errors)

G.3. Portion of the time when time deviation is less than 0.5 seconds

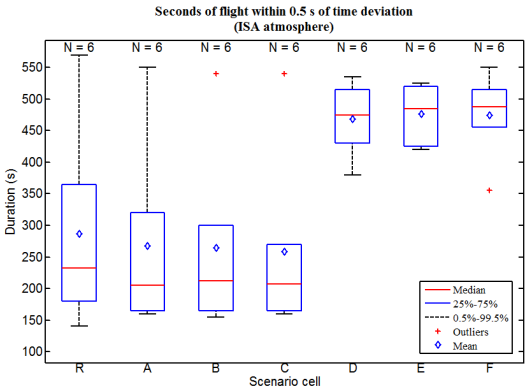

(a) Boxplot

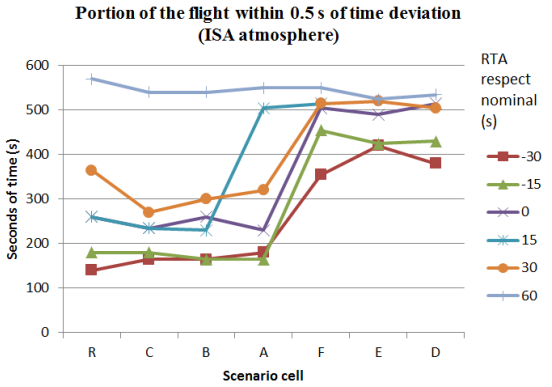

(b) Influence of RTAs

Figure G.7: Portion of the flight when time deviation is less than 0.5 s (ISA atmosphere)

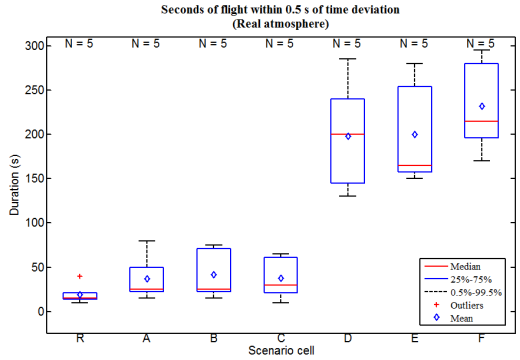

(a) Boxplot

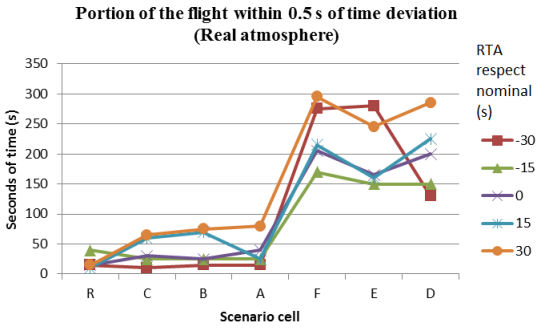

(b) Influence of RTAs

Figure G.8: Portion of the flight when time deviation is less than 0.5 s (Real atmosphere)

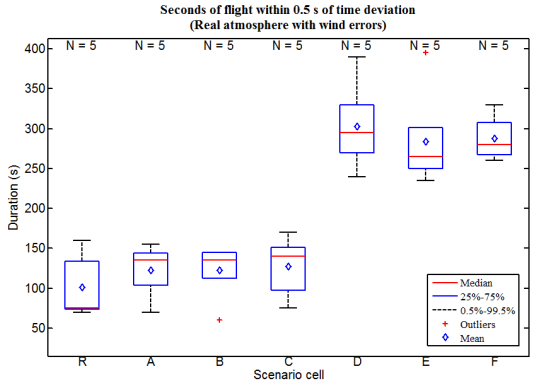

(a) Boxplot

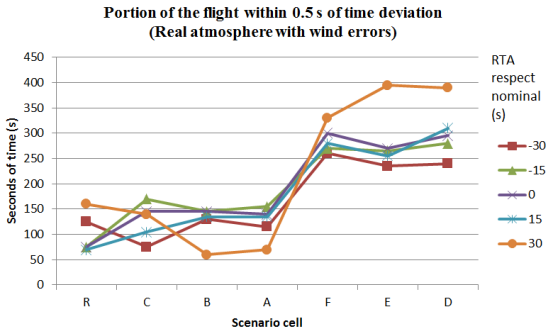

(b) Influence of RTAs

Figure G.9: Portion of the flight when time deviation is less than 0.5 s (Real atmosphere with wind prediction errors)

G.4. Stabilization altitude

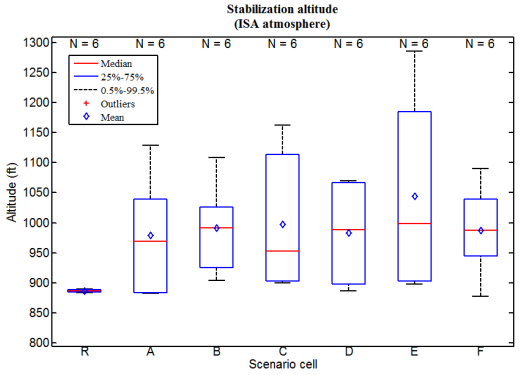

(a) Boxplot

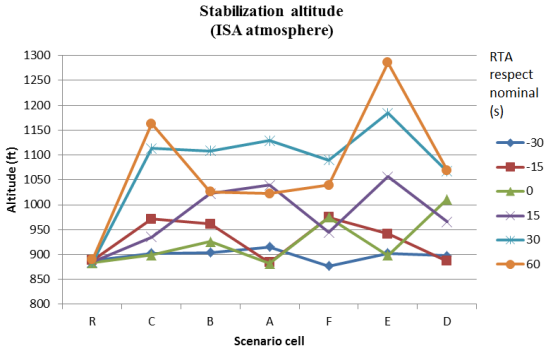

(b) Influence of RTAs

Figure G.10: Stabilization altitude (ISA atmosphere)

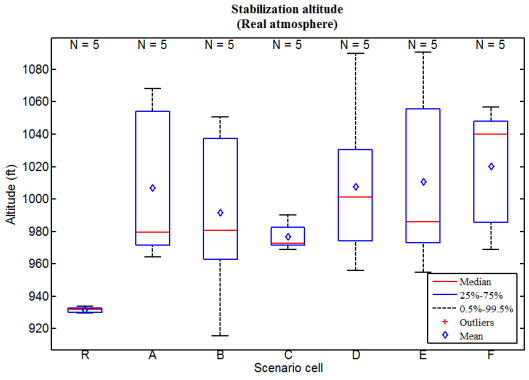

(a) Boxplot

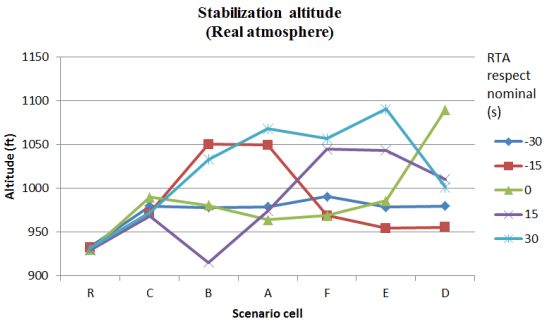

(b) Influence of RTAs

Figure G.11: Stabilization altitude (Real atmosphere)

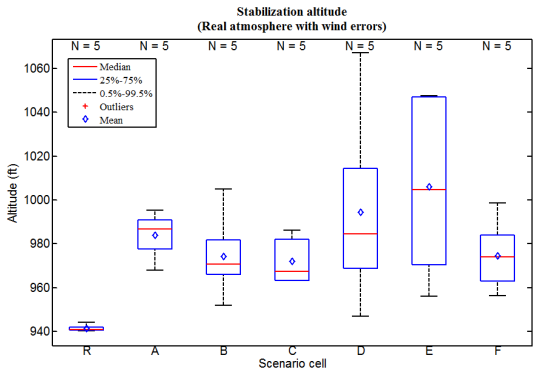

(a) Boxplot

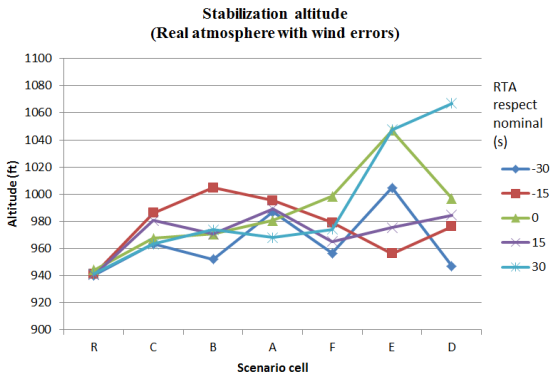

(b) Influence of RTAs

Figure G.12: Stabilization altitude (Real atmosphere with wind prediction errors)

G.5. Fuel consumption

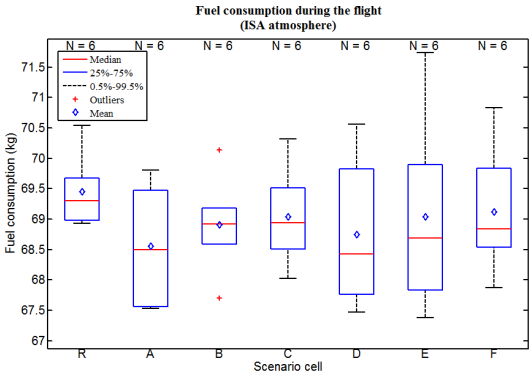

(a) Boxplot

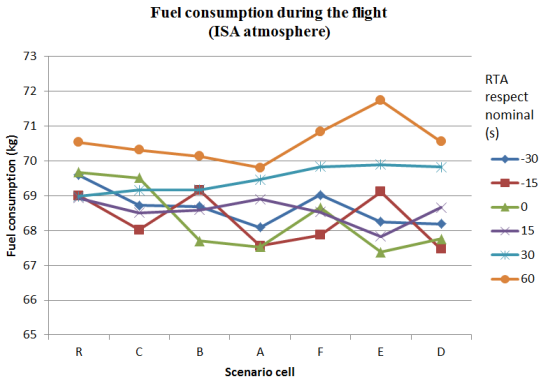

(b) Influence of RTAs

Figure G.13: Fuel consumption during the flight (ISA atmosphere)

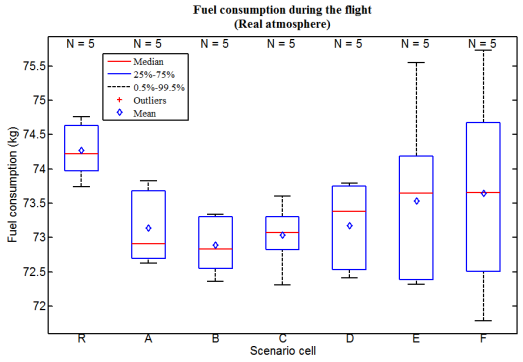

(a) Boxplot

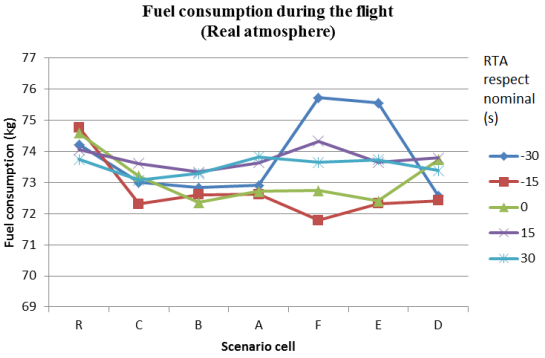

(b) Influence of RTAs

Figure G.14: Fuel consumption during the flight (Real atmosphere)

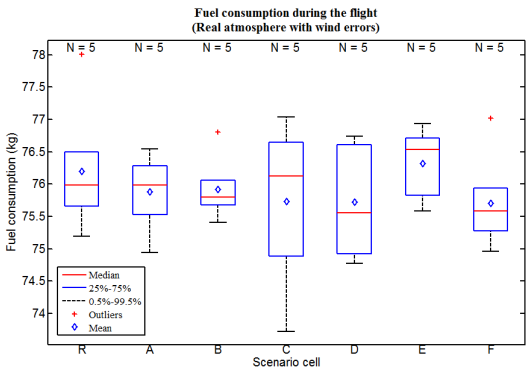

(a) Boxplot

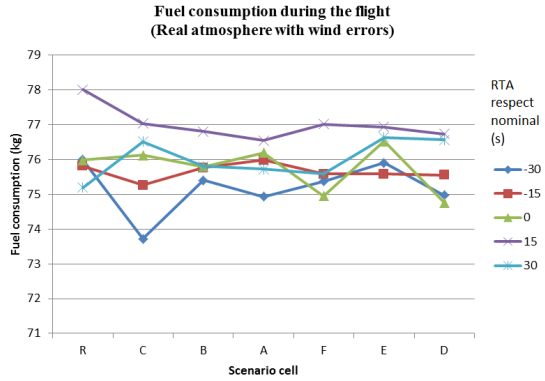

(b) Influence of RTAs

Figure G.15: Fuel consumption during the flight (Real atmosphere with wind prediction errors)

G.6. F-APP deployment

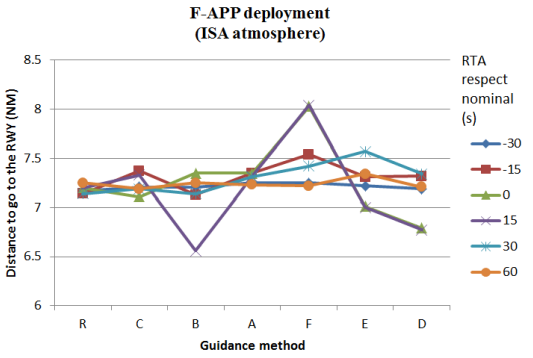

(a) ISA atmosphere

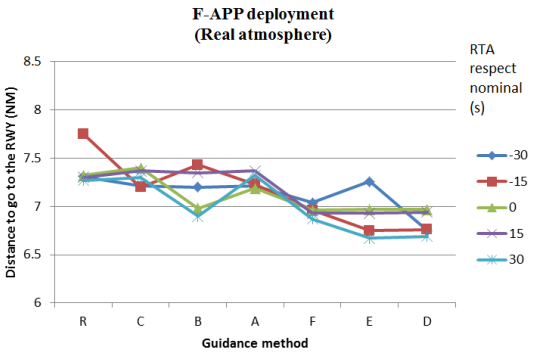

(b) Real atmosphere

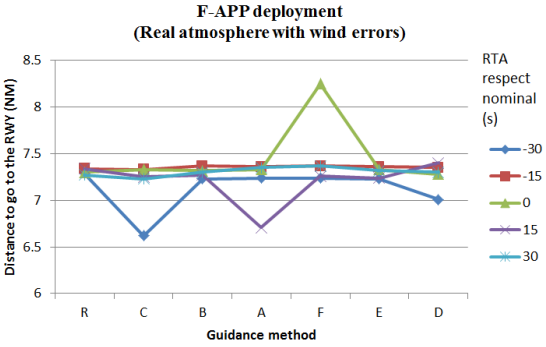

(c) Real atmosphere with wind prediction errors

Figure G.16: F-APP deployment distance vs RTA

G.7. Gear deployment

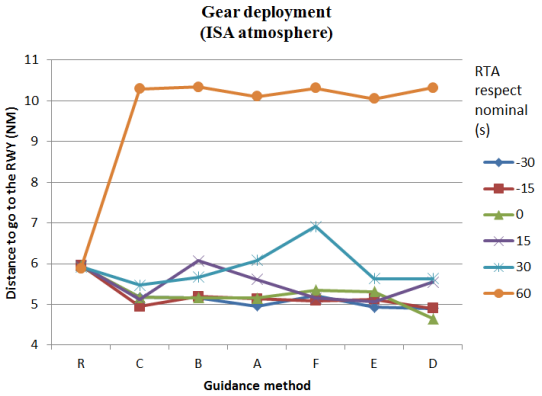

(a) ISA atmosphere

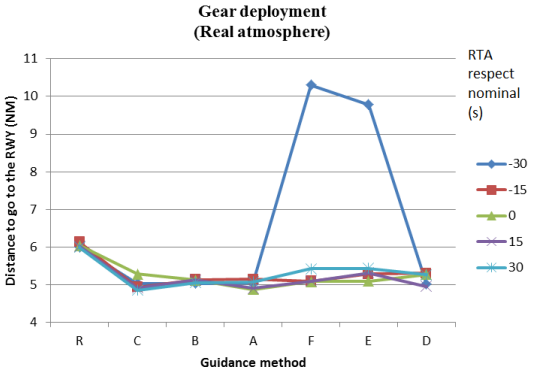

(b) Real atmosphere

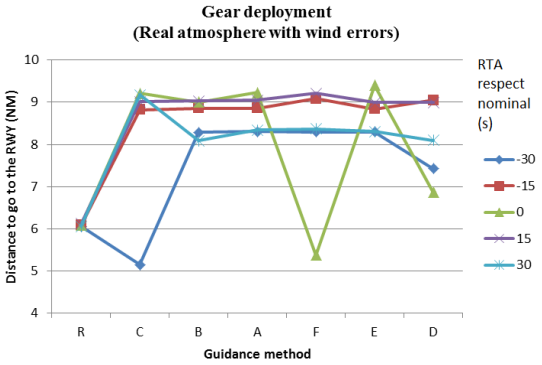

(c) Real atmosphere with wind prediction errors

Figure G.17: Gear deployment distance vs RTA

G.8. F-LND deployment

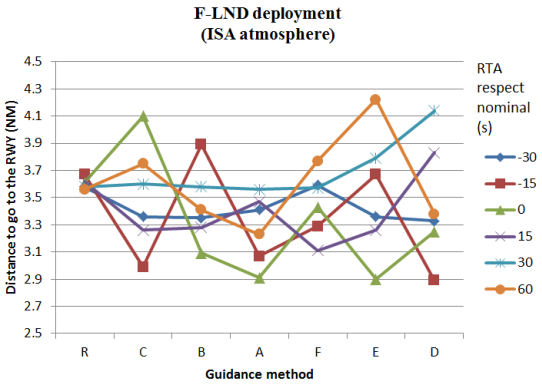

(a) ISA atmosphere

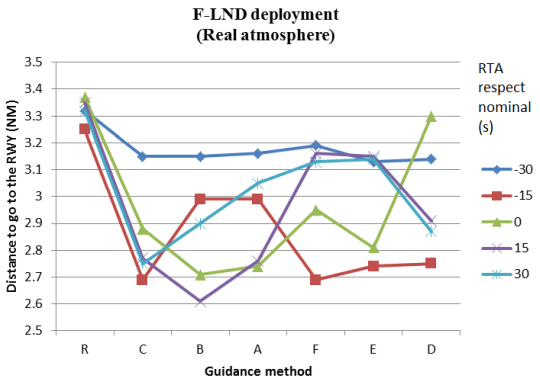

(b) Real atmosphere

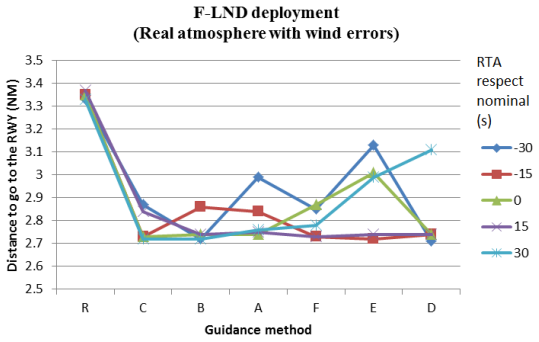

(c) Real atmosphere with wind prediction errors

Figure G.18: F-LND deployment distance vs RTA

G.9. Number of re-plans due to energy deviation

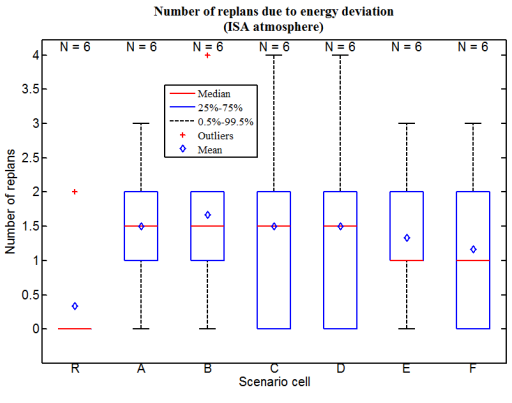

(a) Boxplot

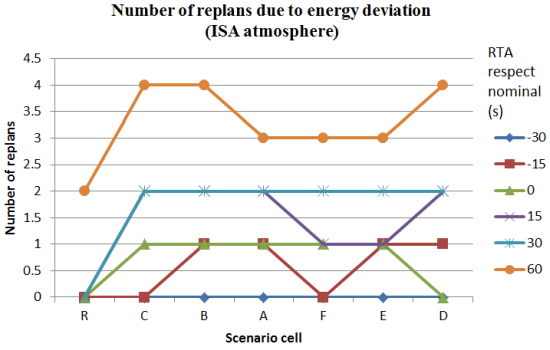

(b) Influence of RTAs

Figure G.19: Number of re-plans (ISA atmosphere)

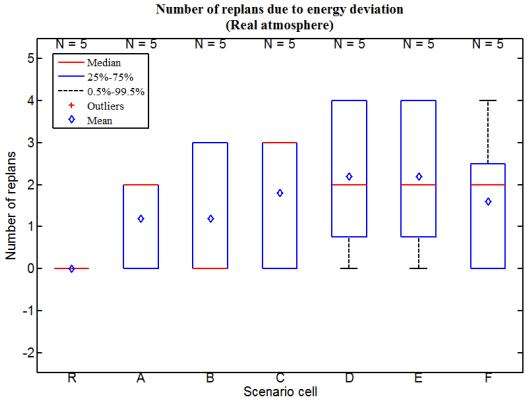

(a) Boxplot

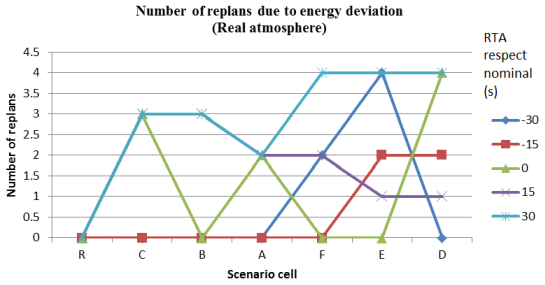

(b) Influence of RTAs

Figure G.20: Number of re-plans (Real atmosphere)

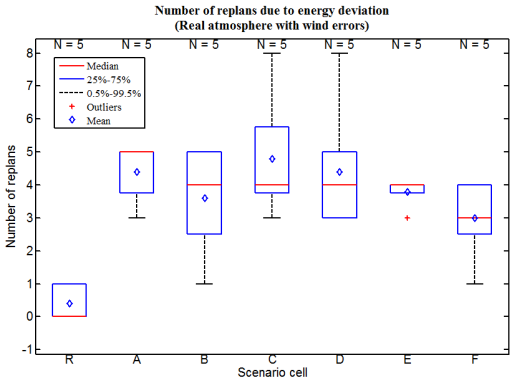

(a) Boxplot

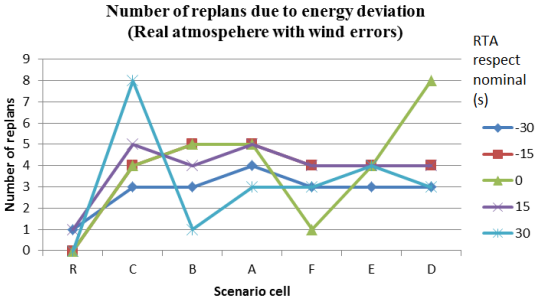

(b) Influence of RTAs

Figure G.21: Number of re-plans (Real atmosphere with wind prediction errors)

APPENDIX H. TABLES OF RESULTS

In this appendix, all the resulting data from the simulations can be found in table format. These tables have been used in order to obtain the plots and results of this report.

H.1. ISA atmosphere

Inputs			Time deviation					
Guidance Method	Time to next conf. (s	RTA (s)	RWY (s)	Mean (s)	Median (s)	within 0.5 (s	1000 (s)	GS (s) -> last TEMO point
Reference	-	-30	-3.09	0.138	0.65	140	-2.6	1.5
Reference	-	-15	-1.02	0.57939	0.87	180	-0.33	1.36
Reference	-	0	-2.21	0.3445	0.57	205	-1.62	1.68
Reference	-	15	-2.68	0.0954	0.39	260	-2.09	1.36
Reference	-	30	-3.05	-0.14638	0.22	365	-2.59	1
Reference	-	60	-3.28	-0.41367	0.09	570	-2.87	0.04
Strategic	0	-30	-3.96	0.0398	0.68	165	-3.65	1.56
Strategic	0	-15	-3.2	-0.0933	0.505	180	-3.55	1.35
Strategic	0	0	-4.62	-0.3528	0.58	160	-4.24	1.3
Strategic	0	15	-5.56	-0.6593	0.345	235	-6.01	1.02
Strategic	0	30	-5.23	-0.7585	0.275	270	-5.34	0.17
Strategic	0	60	-4.71	-0.8997	0	540	-4.66	0.45
Strategic	30	-15	-4.54	-0.337	0.495	165	-4.25	1.34
Strategic	30	0	-5.22	-0.5449	0.505	155	-5.43	1.32
Strategic	30	60	-4.65	-0.7258	0.16	540	-5.09	0.53
Strategic	30	15	-4.66	-0.5614	0.31	260	-4.77	0.98
Strategic	30	-30	-4.01	0.0028	0.66	165	-3.74	1.5
Strategic	30	30	-5.41	-0.8289	0.255	300	-5.54	0.4
Strategic	60	-15	-5.52	-0.6205	0.43	165	-5.82	1.34
Strategic	60	0	-5.42	-0.5778	0.5	160	-5.75	1.29
Strategic	60	60	-4.89	-0.9015	0.07	550	-5.34	0.44
Strategic	60	15	-4.61	-0.4921	0.375	230	-4.59	1.04
Strategic	60	-30	-2.36	0.3877	0.68	180	-2.2	1.71
Strategic	60	30	-5.1	-0.7831	0.27	320	-5.26	0.67
Tactical	0	-30	-3.18	-0.2025	0.16	355	-2.63	0.57
Tactical	0	-15	-3.29	-0.5989	-0.05	455	-3.2	0.03
Tactical	0	0	-4.2	-0.7341	-0.02	470	-4.12	0.02
Tactical	0	15	-3.81	-0.6648	-0.01	505	-4.2	0.39
Tactical	0	30	-5.54	-1.0513	-0.045	515	-5.66	0.23
Tactical	0	60	-4.46	-0.8074	-0.015	550	-4.25	-0.15
Tactical	30	-15	-4.05	-0.8156	-0.04	425	-3.78	0
Tactical	30	0	-4.42	-0.8533	-0.04	480	-5.03	0.26
Tactical	30	60	-5.36	-1.0946	-0.02	525	-5.36	0.34
Tactical	30	15	-4.73	-0.9708	-0.09	490	-4.87	-0.13
Tactical	30	-30	-3.35	-0.3722	0.1	420	-3.18	0.25
Tactical	30	30	-3.98	-0.8704	-0.06	520	-4.07	-0.2
Tactical	60	-15	-5.31	-1.0031	0.01	430	-5.64	0.24
Tactical	60	0	-5.19	-1.0516	0	445	-5.18	-0.1
Tactical	60	60	-5.23	-1.0203	-0.02	535	-5.38	0.05
Tactical	60	15	-4.25	-0.7738	-0.08	515	-3.8	-0.12
Tactical	60	-30	-3.35	-0.2629	0.065	380	-2.75	0.48
Tactical	60	30	-4.3	-0.8296	-0.02	505	-4.1	-0.14

Table H.1: Time deviation results for ISA atmosphere

Inputs			Outputs					
Guidance Method	Time to next conf. (s	RTA (s)	FLND (ft)	G (ft)	GS (ft)	T (ft)	V (ft)	STABLE (ft)
Reference	-	-30	1225.77	1953.97	2750.3	1241.111	887.7783	887.7783
Reference	-	-15	1247.74	1874.43	1874.43	1238.683	888.4253	888.4253
Reference	-	0	1235.74	1964.54	2650.67	1260.235	883.2341	883.2341
Reference	-	15	1236.95	1967.03	2718.17	1256.828	885.1642	885.1642
Reference	-	30	1224.63	1954.66	2752.78	1249.834	884.1572	884.1572
Reference	-	60	1216.63	1947.18	2820.42	1229.666	889.6958	889.6958
Strategic	0	-30	1145.42	1728.09	2003.98	922.9101	902.4453	902.4453
Strategic	0	-15	1026.53	1639.68	2750.44	971.1878	1024.99	971.1878
Strategic	0	0	1378.22	1709.42	2794.08	1347.633	899.3587	899.3587
Strategic	0	15	1110.52	1699.61	2836.26	935.3767	1018.608	935.3767
Strategic	0	30	1218.03	1806.54	2742.21	1119.599	1113.613	1113.613
Strategic	0	60	1268.16	3831.77	2960.17	1188.358	1162.906	1162.906
Strategic	30	-15	1315.76	1715.66	2750.5	1259.164	961.4136	961.4136
Strategic	30	0	1057.83	1706.87	2790.51	925.685	995.1014	925.685
Strategic	30	60	1157.14	3807.5	2937.12	1026.11	1104.503	1026.11
Strategic	30	15	1119.18	2023.75	2829.16	1022.494	1038.784	1022.494
Strategic	30	-30	1142.14	1724.05	2007.56	918.5231	903.9935	903.9935
Strategic	30	30	1212.12	1870.97	2730.92	1108.336	1126.377	1108.336
Strategic	60	-15	1044.64	1703.24	2737.14	884.0166	968.5115	884.0166
Strategic	60	0	999.78	1705.08	2793.66	882.211	969.1362	882.211
Strategic	60	60	1102.3	3733.98	2969.03	1022.79	1084.796	1022.79
Strategic	60	15	1179.15	1854.55	2827.33	1063.926	1039.574	1039.574
Strategic	60	-30	1156.85	1645.43	2733.68	915.6317	925.9421	915.6317
Strategic	60	30	1208.27	2008.6	2730.22	1128.646	1157.309	1128.646
Tactical	0	-30	1219.74	1726.54	2683.61	1152.634	877.0677	877.0677
Tactical	0	-15	1123.52	1684.74	2806	1093.419	975.1596	975.1596
Tactical	0	0	1166.59	1771.86	2867.53	1049.894	999.3261	999.3261
Tactical	0	15	1064.06	1707.64	2812.34	944.3688	1011.269	944.3688
Tactical	0	30	1206.7	2304.26	2743.5	1090.06	1093.332	1090.06
Tactical	0	60	1274.45	3806.79	2918.05	1235.987	1039.684	1039.684
Tactical	30	-15	1242.65	1698.78	2796.19	1208.623	941.4253	941.4253
Tactical	30	0	995.79	1756.03	2817.91	898.0703	994.2692	898.0703
Tactical	30	60	1417.93	3736.69	2795.9	1325.643	1286.101	1286.101
Tactical	30	15	1111.27	1676.3	2938.31	1056.528	1062.709	1056.528
Tactical	30	-30	1144.8	1637.86	2748.27	902.565	909.8748	902.565
Tactical	30	30	1277.64	1859.48	2746.93	1184.541	1197.186	1184.541
Tactical	60	-15	993.96	1624.76	2737.98	886.9284	973.6643	886.9284
Tactical	60	0	1107.73	1544.26	2773.76	1018.84	1010.824	1010.824
Tactical	60	60	1149.76	3753.56	2847.97	1069.497	1094.042	1069.497
Tactical	60	15	1292.34	1842.68	2799.4	1235.287	965.8502	965.8502
Tactical	60	-30	1134.11	1623.95	2654.32	898.4297	897.6729	897.6729
Tactical	60	30	1392.13	1860.1	2720.03	1327.41	1066.92	1066.92

Table H.2: Stabilization results for ISA atmosphere

Inputs			Outputs						
Guidance Method	Time to next conf. (s)	RTA (s)	Fuel (kg)	SPD BRK time (s)	SPD BRK occ	Initial replan (s)	Energy replans	Mean time replans (s)	Median time replans (s)
Reference	-	-30	69.5974	65.43	2	11.107	0	0	0
Reference	-	-15	68.9996	0	0	5.959	0	0	0
Reference	-	0	69.6779	0	0	22.964	0	0	0
Reference	-	15	68.9297	0	0	34.492	0	0	0
Reference	-	30	68.9779	0	0	5.179	0	0	0
Reference	-	60	70.5368	0	0	4.134	2	1.474	1.474
Strategic	0	-30	68.7198	0	0	31.497	0	0	0
Strategic	0	-15	68.0187	0	0	43.478	0	0	0
Strategic	0	0	69.5161	0	0	18.423	1	3.307	3.307
Strategic	0	15	68.5079	0	0	15.272	2	3.463	3.463
Strategic	0	30	69.1631	0	0	14.929	2	5.5615	5.5615
Strategic	0	60	70.3138	0	0	20.966	4	4.09875	2.262
Strategic	30	-15	69.1505	0	0	50.514	1	3.244	3.244
Strategic	30	0	67.7039	0	0	17.878	1	2.418	2.418
Strategic	30	60	70.1366	0	0	21.747	4	4.025	1.5135
Strategic	30	15	68.5897	0	0	17.769	2	3.276	3.276
Strategic	30	-30	68.6957	0	0	27.284	0	0	0
Strategic	30	30	69.1771	0	0	17.316	2	4.274	4.274
Strategic	60	-15	67.5561	0	0	45.116	1	2.793	2.793
Strategic	60	0	67.5275	0	0	19.766	1	2.403	2.403
Strategic	60	60	69.8038	0	0	22.371	3	4.633	2.839
Strategic	60	15	68.9027	0	0	16.786	2	2.5665	2.5665
Strategic	60	-30	68.0906	0	0	24.742	0	0	0
Strategic	60	30	69.4684	0	0	15.647	2	9.6645	9.6645
Tactical	0	-30	69.0205	0	0	27.488	0	0	0
Tactical	0	-15	67.8727	0	0	53.134	0	0	0
Tactical	0	0	68.6574	0	0	17.644	1	2.542	2.542
Tactical	0	15	68.5338	0	0	18.751	1	3.354	3.354
Tactical	0	30	69.8347	0	0	15.709	2	10.124	10.124
Tactical	0	60	70.8329	0	0	21.606	3	4.592	3.276
Tactical	30	-15	69.1154	0	0	48.984	1	3.448	3.448
Tactical	30	0	67.3794	0	0	19.282	1	4.586	4.586
Tactical	30	60	71.7332	0	0	22.184	3	6.458333333	4.571
Tactical	30	15	67.8306	0	0	15.85	1	7.55	7.55
Tactical	30	-30	68.2539	0	0	25.241	0	0	0
Tactical	30	30	69.8979	0	0	17.316	2	5.351	5.351
Tactical	60	-15	67.4707	0	0	46.675	1	2.496	2.496
Tactical	60	0	67.7605	0	0	16.068	0	0	0
Tactical	60	60	70.5588	0	0	19.281	4	6.22425	6.435
Tactical	60	15	68.662	0	0	20.982	2	5.499	5.499
Tactical	60	-30	68.1894	0	0	27.861	0	0	0
Tactical	60	30	69.8259	0	0	17.082	2	6.318	6.318

Table H.3: Fuel, speed brakes and re-plans results for ISA atmosphere

Inputs			Outputs					
Guidance Method	Time to next conf. (s	RTA (s)	hFA (ft)	xFA (NM)	hG (ft)	xG (NM)	hFL (ft)	xFL (NM)
Reference	-	-30	2383.26	7.17	2038.76	5.92	1225.77	3.58
Reference	-	-15	2065.27	7.14	1905.17	5.96	1247.74	3.67
Reference	-	0	2403.15	7.2	2050.1	5.95	1235.74	3.61
Reference	-	15	2401.08	7.2	2052.2	5.96	1236.95	3.62
Reference	-	30	2374.24	7.14	2038	5.92	1224.63	3.58
Reference	-	60	2398.95	7.25	2022.68	5.88	1216.63	3.56
Strategic	0	-30	2130.58	7.21	1809.59	5.17	1145.45	3.36
Strategic	0	-15	2429.89	7.37	1710.74	4.95	1026.53	2.99
Strategic	0	0	2362.73	7.11	1783	5.17	1378.22	4.1
Strategic	0	15	2413.24	7.33	1773.82	5.13	1110.52	3.26
Strategic	0	30	2393.27	7.19	1884.79	5.47	1218.03	3.6
Strategic	0	60	2376.19	7.19	3927.41	10.29	1268.16	3.75
Strategic	30	-15	2372.89	7.13	1789.07	5.19	1315.76	3.89
Strategic	30	0	2423.43	7.35	1781.79	5.16	1057.83	3.09
Strategic	30	60	2391.87	7.25	3903.96	10.34	1157.14	3.41
Strategic	30	15	2179.77	6.56	2106.3	6.07	1119.18	3.28
Strategic	30	-30	2133.66	7.21	1806.96	5.16	1142.14	3.35
Strategic	30	30	2379.39	7.14	1950.34	5.67	1212.12	3.58
Strategic	60	-15	2425.85	7.35	1776.55	5.14	1044.64	3.07
Strategic	60	0	2423.54	7.35	1779.95	5.15	999.78	2.91
Strategic	60	60	2383.1	7.23	3827.35	10.1	1102.3	3.23
Strategic	60	15	2411.75	7.32	1932.19	5.61	1179.15	3.47
Strategic	60	-30	2408.43	7.25	1726.32	4.96	1156.85	3.41
Strategic	60	30	2419.04	7.31	2093.96	6.08	1208.27	3.56
Tactical	0	-30	2418.13	7.25	1808.47	5.21	1219.74	3.59
Tactical	0	-15	2482	7.54	1756.4	5.09	1123.52	3.29
Tactical	0	0	2630.11	8.03	1845.07	5.35	1166.59	3.43
Tactical	0	15	2629.87	8.04	1779.37	5.15	1064.06	3.11
Tactical	0	30	2446.88	7.42	2385.07	6.91	1206.7	3.57
Tactical	0	60	2382.07	7.22	3901.62	10.31	1274.45	3.77
Tactical	30	-15	2420.95	7.31	1772.16	5.13	1242.65	3.67
Tactical	30	0	2326.64	7.01	1833.21	5.31	995.79	2.9
Tactical	30	60	2413.85	7.34	3832.48	10.05	1417.93	4.22
Tactical	30	15	2317.02	7	1748.79	5.07	1111.27	3.26
Tactical	30	-30	2396.14	7.22	1717.91	4.93	1144.8	3.36
Tactical	30	30	2493.83	7.57	1935.04	5.63	1277.64	3.79
Tactical	60	-15	2420.99	7.32	1697.43	4.9	993.96	2.89
Tactical	60	0	2261.72	6.79	1614.65	4.65	1107.73	3.25
Tactical	60	60	2386	7.21	3851.15	10.32	1149.76	3.38
Tactical	60	15	2245.41	6.77	1925.81	5.55	1292.34	3.83
Tactical	60	-30	2396	7.19	1704.33	4.9	1134.11	3.33
Tactical	60	30	2430.08	7.34	1939.46	5.63	1392.13	4.14

Table H.4: Flaps and gear deployment results for ISA atmosphere

H.2. Real atmosphere

Inputs			Time deviation					
Guidance Method	Time to next conf. (s	RTA (s)	RWY (s)	Mean (s)	Median (s)	within 0.5 (s	1000 (s)	GS (s) -> last TEMO point
Reference	-	-30	-2.68	1.58	2.24	15	-1.26	2.86
Reference	-	-15	-4.68	0.807	1.925	40	-3.33	0.04
Reference	-	0	-1.94	1.6283	1.94	15	-0.33	2.41
Reference	-	15	-2.04	1.5344	1.8	10	-0.52	2.3
Reference	-	30	-2.2	1.4604	1.74	15	-0.68	2.29
Strategic	0	-30	-2.36	1.6095	2.18	10	-1.45	2.66
Strategic	0	-15	-2.27	1.2571	1.95	25	-2.18	2.39
Strategic	0	0	-5.19	0.5596	1.95	30	-5.08	2.3
Strategic	0	15	-5.04	0.3185	1.81	60	-5.01	1.88
Strategic	0	30	-4.83	0.2399	1.6	65	-4.7	1.54
Strategic	30	-15	-2.3	1.2738	1.96	25	-1.71	2.37
Strategic	30	0	-2.14	1.3314	2.01	25	-2.07	2.46
Strategic	30	15	-5.16	0.3285	1.795	70	-5.21	1.93
Strategic	30	-30	-2.57	1.5395	2.16	15	-1.51	2.57
Strategic	30	30	-4.92	0.2569	1.68	75	-4.44	1.63
Strategic	60	-15	-2.2	1.3095	1.95	25	-1.64	2.4
Strategic	60	0	-5.4	0.3787	1.96	40	-5.6	2.5
Strategic	60	15	-4.89	0.4487	1.845	25	-5.05	2.08
Strategic	60	-30	-2.25	1.6555	2.21	15	-1.25	2.65
Strategic	60	30	-4.79	0.3274	1.72	80	-4.06	1.78
Tactical	0	-30	-6.05	-0.4499	0.05	275	-4.98	-0.16
Tactical	0	-15	-2.46	0.43875	0.61	170	-2.44	1.67
Tactical	0	0	-2.92	0.2476	0.32	205	-2.41	1.3
Tactical	0	15	-5.02	-0.246	0.15	215	-4.59	1.34
Tactical	0	30	-5.48	-0.5108	0.06	295	-5.16	0.98
Tactical	30	-15	-5.19	-0.1804	0.58	150	-5.56	1.63
Tactical	30	0	-2.79	0.3148	0.51	165	-2.6	1.52
Tactical	30	15	-6.07	-0.3429	0.49	160	-5.41	1.51
Tactical	30	-30	-7.03	-0.6972	0.105	280	-6.07	0.13
Tactical	30	30	-5.15	-0.321	0.07	245	-4.6	1.62
Tactical	60	-15	-4.9	-0.1046	0.595	150	-5.33	1.69
Tactical	60	0	-5.42	-0.3369	0.23	200	-4.83	1.31
Tactical	60	15	-4.46	0.00289	0.38	225	-4.06	1.38
Tactical	60	-30	-2.88	0.7404	1.29	130	-1.91	1.82
Tactical	60	30	-5.02	-0.371	0.12	285	-5.14	1.16

Table H.5: Time deviation results for Real atmosphere

Inputs			Outputs					
Guidance Method	Time to next conf. (s)	RTA (s)	FLND (ft)	G (ft)	GS (ft)	T (ft)	V (ft)	STABLE (ft)
Reference	-	-30	1199.96	2071.53	2867.89	1192.891	933.6959	933.6959
Reference	-	-15	1180.73	2111.53	2742.07	1198.641	932.4667	932.4667
Reference	-	0	1213.64	2087.79	2759.67	1205.153	930.1218	930.1218
Reference	-	15	1208.17	2081.88	2772.57	1213.719	929.7612	929.7612
Reference	-	30	1201.29	2070.97	2770.66	1207.609	931.852	931.852
Strategic	0	-30	1135.51	1756.6	2714.84	1021.254	980.0316	980.0316
Strategic	0	-15	986.22	1720.52	2758.28	972.4873	1009.529	972.4873
Strategic	0	0	1045.51	1835.59	2899.07	990.1385	1042.854	990.1385
Strategic	0	15	1003.99	1717.15	2902.7	968.7008	1005.775	968.7008
Strategic	0	30	1003.72	1701.39	2923.9	972.3197	1015.364	972.3197
Strategic	30	-15	1082.79	1784.81	2774.78	1050.576	1059.295	1050.576
Strategic	30	0	991.88	1780.77	2812.85	980.7873	1014.96	980.7873
Strategic	30	15	955.88	1783.31	2875.4	915.6832	971.957	915.6832
Strategic	30	-30	1137.74	1754.38	2805.1	1032.287	978.3192	978.3192
Strategic	30	30	1056.75	1763.49	2923.14	1033.161	1058.552	1033.161
Strategic	60	-15	1084.91	1791.32	2766.69	1049.526	1058.711	1049.526
Strategic	60	0	994.55	1701.9	2896.3	964.048	1014.482	964.048
Strategic	60	15	997.98	1714.95	2861.86	974.1642	1024.996	974.1642
Strategic	60	-30	1143.15	1757.82	2720.29	1035.854	979.3363	979.3363
Strategic	60	30	1102.96	1764.19	2910.24	1074.056	1068.04	1068.04
Tactical	0	-30	1147.58	4303.53	2996.98	1057.872	991.0374	991.0374
Tactical	0	-15	984.94	1766.94	2811.99	968.9369	1007.333	968.9369
Tactical	0	0	1071.35	1767.94	2888.81	1039.887	1058.56	1039.887
Tactical	0	15	1136.75	1775.56	2863.62	1045.04	1084.228	1045.04
Tactical	0	30	1122.62	1889.27	2932.93	1056.916	1101.902	1056.916
Tactical	30	-15	996.11	1831.96	2809.54	954.5841	1012.515	954.5841
Tactical	30	0	1019.39	1777.68	2812.49	985.9683	1021.256	985.9683
Tactical	30	15	1133.41	1847.86	2863.4	1046.928	1043.823	1043.823
Tactical	30	-30	1132.25	3758.55	2957.46	1083.426	978.8986	978.8986
Tactical	30	30	1132.95	1891.95	2921.33	1090.829	1118.023	1090.829
Tactical	60	-15	998.04	1840.38	2737.04	955.8594	1013.231	955.8594
Tactical	60	0	1182.41	1830.99	2904.18	1089.881	1108.745	1089.881
Tactical	60	15	1057.78	1725.62	2865.78	1010.622	1043.168	1010.622
Tactical	60	-30	1133.92	1751.19	2768.98	1023.876	979.9925	979.9925
Tactical	60	30	1040.8	1835.03	2916.02	1001.25	1055.671	1001.25

Table H.6: Stabilization results for Real atmosphere

Inputs			Outputs						
Guidance Method	Time to next conf. (s)	RTA (s)	Fuel (kg)	SPD BRK time (s)	SPD BRK occ	Initial replan (s)	Energy replans	Mean time replans (s)	Median time replans (s)
Reference	-	-30	74.2198	55.31	2	34.867	0	0	0
Reference	-	-15	74.7631	0	0	7.113	0	0	0
Reference	-	0	74.5938	0	0	12.199	0	0	0
Reference	-	15	74.0517	0	0	10.077	0	0	0
Reference	-	30	73.7447	20.25	1	15.927	0	0	0
Strategic	0	-30	72.9984	0	0	36.067	0	0	0
Strategic	0	-15	72.3063	0	0	19.718	0	0	0
Strategic	0	0	73.2087	0	0	68.297	3	6.484333333	7.067
Strategic	0	15	73.6067	0	0	31.45	3	4.487333333	5.475
Strategic	0	30	73.07	0	0	51.777	3	3.411	2.589
Strategic	30	-15	72.6134	0	0	21.528	0	0	0
Strategic	30	0	72.3648	0	0	51.48	0	0	0
Strategic	30	15	73.3377	0	0	28.002	3	4.560666667	4.384
Strategic	30	-30	72.8355	0	0	28.065	0	0	0
Strategic	30	30	73.2944	0	0	44.258	3	2.995	2.714
Strategic	60	-15	72.6272	0	0	15.975	0	0	0
Strategic	60	0	72.7196	0	0	56.363	2	2.9095	2.9095
Strategic	60	15	73.6346	0	0	30.701	2	2.075	2.075
Strategic	60	-30	72.9124	0	0	32.9	0	0	0
Strategic	60	30	73.8249	0	0	47.674	2	4.3445	4.3445
Tactical	0	-30	75.7257	0	0	30.638	2	10.9745	10.9745
Tactical	0	-15	71.7909	0	0	25.054	0	0	0
Tactical	0	0	72.7444	0	0	75.551	0	0	0
Tactical	0	15	74.3239	0	0	28.392	2	7.2695	7.2695
Tactical	0	30	73.6518	0	0	53.508	4	3.12	2.4725
Tactical	30	-15	72.3175	0	0	20.031	2	4.493	4.493
Tactical	30	0	72.4127	0	0	57.284	0	0	0
Tactical	30	15	73.6438	0	0	21.731	1	6.319	6.319
Tactical	30	-30	75.5532	0	0	34.321	4	11.517	11.4665
Tactical	30	30	73.7336	0	0	52.448	4	4.2935	4.118
Tactical	60	-15	72.4141	0	0	20.81	2	2.441	2.441
Tactical	60	0	73.7338	0	0	75.567	4	5.17125	4.6485
Tactical	60	15	73.7889	0	0	38.922	1	8.268	8.268
Tactical	60	-30	72.5693	0	0	31.123	0	0	0
Tactical	60	30	73.3811	0	0	48.953	4	2.67175	2.145

Table H.7: Fuel, speed brakes and re-plans results for Real atmosphere

Inputs			Outputs					
Guidance Method	Time to next conf. (s	RTA (s)	hFA (ft)	xFA (NM)	hG (ft)	xG (NM)	hFL (ft)	xFL (NM)
Reference	-	-30	2515.42	7.31	2145.37	6	1199.96	3.32
Reference	-	-15	2643.39	7.75	2191.8	6.14	1180.73	3.25
Reference	-	0	2530.04	7.32	2163.3	6.05	1213.64	3.37
Reference	-	15	2512.74	7.3	2154.89	6.03	1208.17	3.35
Reference	-	30	2515.27	7.27	2143.2	6	1201.29	3.32
Strategic	0	-30	2503.93	7.21	1824.57	5.04	1135.51	3.15
Strategic	0	-15	2498.83	7.2	1782.79	4.94	986.22	2.69
Strategic	0	0	2532.73	7.4	1898.52	5.29	1045.51	2.88
Strategic	0	15	2523.02	7.37	1783.51	4.92	1003.99	2.77
Strategic	0	30	2506.69	7.3	1762.4	4.86	1003.72	2.75
Strategic	30	-15	2547.86	7.43	1846.81	5.14	1082.79	2.99
Strategic	30	0	2418.64	6.98	1848.6	5.13	991.88	2.71
Strategic	30	15	2522.34	7.35	1848.18	5.13	955.98	2.61
Strategic	30	-30	2496.52	7.2	1824.7	5.04	1137.74	3.15
Strategic	30	30	2388.43	6.9	1829.34	5.06	1056.75	2.9
Strategic	60	-15	2505.98	7.23	1851.84	5.15	1084.91	2.99
Strategic	60	0	2488.24	7.19	1767.61	4.88	994.55	2.74
Strategic	60	15	2529.26	7.37	1784.8	4.91	997.98	2.76
Strategic	60	-30	2502.33	7.21	1826.23	5.05	1143.15	3.16
Strategic	60	30	2513.11	7.32	1833.18	5.08	1102.96	3.05
Tactical	0	-30	2412.74	7.04	4434.84	10.3	1147.58	3.19
Tactical	0	-15	2401.56	6.96	1830.52	5.1	984.94	2.69
Tactical	0	0	2402.61	6.96	1829.05	5.09	1071.35	2.95
Tactical	0	15	2395.03	6.93	1843.18	5.1	1136.75	3.16
Tactical	0	30	2362.17	6.87	1958.71	5.43	1122.62	3.13
Tactical	30	-15	2342.85	6.75	1897.29	5.29	996.11	2.74
Tactical	30	0	2407.37	6.97	1833.88	5.1	1019.39	2.81
Tactical	30	15	2394.16	6.93	1911.92	5.32	1133.41	3.15
Tactical	30	-30	2495.95	7.26	3879.68	9.78	1132.25	3.13
Tactical	30	30	2312.65	6.67	1961.8	5.44	1132.95	3.14
Tactical	60	-15	2350.81	6.76	1902.58	5.31	998.04	2.75
Tactical	60	0	2400.97	6.97	1895.56	5.28	1182.41	3.3
Tactical	60	15	2393.63	6.94	1789.55	4.96	1057.78	2.91
Tactical	60	-30	2347.16	6.75	1817.86	5.02	1133.92	3.14
Tactical	60	30	2301.65	6.69	1908.69	5.27	1040.8	2.87

Table H.8: Flaps and gear deployment results for Real atmosphere

H.3. Real atmosphere with wind prediction errors

Inputs			Time deviation					
Guidance Method	Time to next conf. (s	RTA (s)	RWY (s)	Mean (s)	Median (s)	within 0.5 (s	1000 (s)	GS (s) -> last TEMO point
Reference	-	-30	5.77	0.174963	0.55	125	0.24	-3.13
Reference	-	-15	6.81	0.62413	1.06	75	1.29	-1.99
Reference	-	0	6.66	0.2418	0.81	75	1.1	-2.67
Reference	-	15	7.54	0.8392	0.955	70	2.12	1.02
Reference	-	30	5.34	-0.64408	-0.15	160	-0.24	-3.8
Strategic	0	-30	5.98	0.615185	0.91	75	-0.94	-1.6
Strategic	0	-15	6.53	0.72478	0.605	170	-0.57	0.22
Strategic	0	0	6.57	0.77085	0.74	145	-0.78	0.71
Strategic	0	15	6.55	0.559722	0.625	105	-0.63	-0.5
Strategic	0	30	6.75	0.10136	0.42	140	-0.84	-0.01
Strategic	30	-15	6.74	0.86652	0.715	145	-0.44	0.86
Strategic	30	0	6.99	0.86305	0.66	145	-0.65	0.51
Strategic	30	15	7.5	0.908125	0.785	135	-0.02	0.5
Strategic	30	-30	5.77	0.787037	0.88	130	-1.32	0.03
Strategic	30	30	6.14	-0.8349	-0.93	60	-0.88	-4.59
Strategic	60	-15	6.21	0.88384	0.76	155	-1.01	0.75
Strategic	60	0	6.95	0.860071	0.75	140	-0.64	0.55
Strategic	60	15	6.66	0.6775	0.57	135	-0.45	-0.21
Strategic	60	-30	5.21	0.70963	0.885	115	-1.2	0.87
Strategic	60	30	7.52	-0.08027	0.62	70	0.69	-3.85
Tactical	0	-30	5.78	1.01163	0.86	260	-1.18	0.59
Tactical	0	-15	6.34	0.984275	0.73	270	-0.83	0.86
Tactical	0	0	8.69	1.334539	0.7	300	1.29	0.07
Tactical	0	15	6.65	1.024722	0.59	280	-0.65	1.04
Tactical	0	30	7.62	1.090748	0.62	330	0.77	-0.11
Tactical	30	-15	6.5	1.029855	0.725	265	-0.95	0.43
Tactical	30	0	6.88	1.12234	0.79	270	0.29	0.8
Tactical	30	15	7.65	1.22722	1.01	255	0.2	1.23
Tactical	30	-30	5.28	0.971185	0.89	235	-0.94	0.99
Tactical	30	30	7.35	0.94102	0.38	395	0.43	0.48
Tactical	60	-15	7.17	1.0167	0.665	280	-0.11	0.99
Tactical	60	0	6.51	0.8612	0.46	295	-0.75	0.52
Tactical	60	15	6.92	0.90056	0.39	310	-0.32	0.28
Tactical	60	-30	5.89	1.067926	1.05	240	-1.28	0.7
Tactical	60	30	7.54	0.88653	0.1	390	0.59	0.04

Table H.9: Time deviation results for Real atmosphere with wind prediction errors

Inputs			Outputs					
Guidance Method	Time to next conf. (s	RTA (s)	FLND (ft)	G (ft)	GS (ft)	T (ft)	V (ft)	STABLE (ft)
Reference	-	-30	1205.41	2090.41	2894.41	1225.487	940.2592	940.2592
Reference	-	-15	1212.12	2101.96	2954.41	1230.881	940.9791	940.9791
Reference	-	0	1208.37	2100.57	2909.71	1212.342	944.2383	944.2383
Reference	-	15	1216.33	2076.23	2088	1233.614	940.636	940.636
Reference	-	30	1203.68	2093.81	2928.91	1223.227	941.3635	941.3635
Strategic	0	-30	1036.8	1797.64	2903.34	963.4104	1007.972	963.4104
Strategic	0	-15	997.09	3216.83	2927.79	986.1023	1016.941	986.1023
Strategic	0	0	992.04	3452.45	3009.76	967.4258	1011.805	967.4258
Strategic	0	15	1028.37	3360.35	2964.21	980.6443	1025.829	980.6443
Strategic	0	30	988.92	3515.61	2850.2	963.264	1012.934	963.264
Strategic	30	-15	1035.93	3240.52	3085.58	1004.923	1049.262	1004.923
Strategic	30	0	994.94	3356.43	3065.4	970.5978	1020.451	970.5978
Strategic	30	15	995.4	3329.89	3064.08	970.7742	1018.219	970.7742
Strategic	30	-30	989.77	2800.22	2887.28	951.9799	996.8093	951.9799
Strategic	30	30	992.33	2853.28	2974.49	973.8898	1010.969	973.8898
Strategic	60	-15	1031.02	3248.28	2925.55	995.4325	1042.777	995.4325
Strategic	60	0	996.56	3464.46	3037.9	980.6795	1027.849	980.6795
Strategic	60	15	999.83	3360.53	2971.41	989.373	1022.159	989.373
Strategic	60	-30	1075.07	2797.94	2879.33	986.8508	1097.598	986.8508
Strategic	60	30	1001.14	3005.16	2868.82	968.0232	1009.48	968.0232
Tactical	0	-30	1028.28	2795.15	2882.38	956.3866	1001.72	956.3866
Tactical	0	-15	992.89	3374.58	2925.33	979.0733	1015.332	979.0733
Tactical	0	0	1036.3	1865.77	3079.95	998.6231	1043.785	998.6231
Tactical	0	15	992.07	3404.08	3020.98	965.1646	1008.434	965.1646
Tactical	0	30	1005.8	3024.69	2909.69	974.1178	1012.423	974.1178
Tactical	30	-15	992.25	3202.74	3047.91	956.1747	1006.736	956.1747
Tactical	30	0	1087.69	3538.26	2951.81	1046.964	1056.069	1046.964
Tactical	30	15	992.93	3290.23	3028.02	975.3453	1021.189	975.3453
Tactical	30	-30	1122.82	2807.55	2899.24	1037.895	1004.8	1004.8
Tactical	30	30	1079.89	2975.44	2975.44	1047.612	1093.093	1047.612
Tactical	60	-15	996.05	3345.15	3066.89	976.2242	1017.191	976.2242
Tactical	60	0	997	2363.15	2918.2	1001.492	1039.877	997
Tactical	60	15	994.69	3294.25	3038.51	984.67	1024.638	984.67
Tactical	60	-30	987.62	2535.76	2856.52	946.9852	993.4407	946.9852
Tactical	60	30	1111.18	2861.02	2861.02	1067.035	1110.833	1067.035

Table H.10: Stabilization results for Real atmosphere with wind prediction errors

Guidance Method	Time to next conf. (s)	RTA (s)	Fuel (kg)	SPD BRK time (s)	SPD BRK occ	Initial replan (s)	Energy replans	Mean time replans (s)	Median time replans (s)
Reference	-	-30	75.9964	55.26	2	32.448	1	12.34	12.34
Reference	-	-15	75.8114	0	0	10.14	0	0	0
Reference	-	0	75.9859	0	0	10.624	0	0	0
Reference	-	15	78.0035	55.55	1	10.53	1	6.115	6.115
Reference	-	30	75.1905	20.1	1	14.851	0	0	0
Strategic	0	-30	73.7223	0	0	35.849	3	5.142666667	4.633
Strategic	0	-15	75.2654	0	0	22.261	4	7.21125	6.31
Strategic	0	0	76.1278	0	0	61.636	4	6.5365	6.4505
Strategic	0	15	77.0358	0	0	32.885	5	4.7674	2.746
Strategic	0	30	76.5169	0	0	54.46	8	4.42275	2.5505
Strategic	30	-15	75.7693	0	0	21.965	5	7.4444	6.63
Strategic	30	0	75.7961	0	0	83.679	5	8.1186	6.209
Strategic	30	15	76.8094	0	0	34.679	4	4.4345	1.7865
Strategic	30	-30	75.4018	0	0	34.196	3	4.830666667	1.653
Strategic	30	30	75.8084	0	0	48.656	1	13.119	13.119
Strategic	60	-15	75.9846	0	0	16.536	5	9.2974	4.914
Strategic	60	0	76.1916	0	0	67.892	5	8.3464	8.034
Strategic	60	15	76.5471	0	0	34.976	5	4.5114	2.231
Strategic	60	-30	74.9368	0	0	38.236	4	8.662	5.031
Strategic	60	30	75.728	0	0	52.931	3	4.727333333	1.888
Tactical	0	-30	75.3765	0	0	36.411	3	6.422	2.402
Tactical	0	-15	75.5787	0	0	18.096	4	6.55575	7.5975
Tactical	0	0	74.9554	0	0	75.302	1	4.493	4.493
Tactical	0	15	77.0167	0	0	27.207	4	6.79375	5.842
Tactical	0	30	75.5836	0	0	55.817	3	5.335666667	2.106
Tactical	30	-15	75.5819	0	0	22.527	4	19.06725	23.603
Tactical	30	0	76.5305	0	0	66.253	4	9.742	9.2505
Tactical	30	15	76.9331	0	0	27.019	4	6.357	6.6535
Tactical	30	-30	75.9076	0	0	37.877	3	12.54766667	3.9
Tactical	30	30	76.638	0	0	43.805	4	6.0275	8.751
Tactical	60	-15	75.5563	0	0	22.324	4	6.267	5.304
Tactical	60	0	74.7672	0	0	20	8	3.754	2.3015
Tactical	60	15	76.7389	0	0	28.158	4	7.956	2.6365
Tactical	60	-30	74.9748	0	0	29.968	3	6.219	4.758
Tactical	60	30	76.5637	0	0	50.669	3	5.039	5.039

Table H.11: Fuel, speed brakes and re-plans results for Real atmosphere with wind prediction errors

Inputs			Outputs					
Guidance Method	Time to next conf. (s	RTA (s)	hFA (ft)	xFA (NM)	hG (ft)	xG (NM)	hFL (ft)	xFL (NM)
Reference	-	-30	2508.18	7.29	2161.57	6.06	1205.41	3.33
Reference	-	-15	2514.34	7.34	2172.53	6.09	1212.12	3.35
Reference	-	0	2511.66	7.3	2171.78	6.09	1208.37	3.35
Reference	-	15	2179.84	7.34	2088	6.12	1216.33	3.37
Reference	-	30	2502.33	7.27	2162.04	6.06	1203.68	3.33
Strategic	0	-30	2299.62	6.62	1872.37	5.15	1036.8	2.87
Strategic	0	-15	2501.15	7.33	3327.96	8.82	997.09	2.73
Strategic	0	0	2511.97	7.33	3560.4	9.21	992.04	2.73
Strategic	0	15	2478.04	7.25	3447.37	9.01	1028.37	2.84
Strategic	0	30	2479.71	7.23	3612.08	9.18	988.92	2.72
Strategic	30	-15	2517.28	7.37	3357.62	8.86	1035.93	2.86
Strategic	30	0	2498.01	7.32	3467.53	9	994.94	2.74
Strategic	30	15	2496.39	7.27	3423.27	9.03	995.4	2.74
Strategic	30	-30	2489.44	7.23	2887.28	8.29	989.77	2.72
Strategic	30	30	2491.68	7.3	2974.49	8.09	992.33	2.72
Strategic	60	-15	2513.08	7.36	3371.41	8.86	1031.02	2.84
Strategic	60	0	2509.39	7.33	3576.18	9.23	996.56	2.74
Strategic	60	15	2323.69	6.71	3460.7	9.05	999.83	2.75
Strategic	60	-30	2497.82	7.24	2879.33	8.31	1075.07	2.99
Strategic	60	30	2505.15	7.35	3101.6	8.34	1001.14	2.76
Tactical	0	-30	2493.53	7.24	2882.38	8.3	1028.28	2.85
Tactical	0	-15	2514.29	7.37	3482.98	9.09	992.89	2.73
Tactical	0	0	2830.24	8.25	1930.56	5.38	1036.3	2.87
Tactical	0	15	2494.5	7.26	3497.44	9.21	992.07	2.73
Tactical	0	30	2511.8	7.37	3123.49	8.37	1005.8	2.78
Tactical	30	-15	2517.15	7.36	3320.79	8.84	992.25	2.72
Tactical	30	0	2513.5	7.33	3645.48	9.4	1087.69	3.01
Tactical	30	15	2491.9	7.24	3390.34	8.99	992.93	2.74
Tactical	30	-30	2494.09	7.23	2899.24	8.3	1122.82	3.13
Tactical	30	30	2498.5	7.32	3083.81	8.31	1079.89	2.99
Tactical	60	-15	2511.11	7.35	3456.37	9.05	996.05	2.74
Tactical	60	0	2492.09	7.28	2428.88	6.87	997	2.74
Tactical	60	15	2523.94	7.4	3386.62	8.99	994.69	2.74
Tactical	60	-30	2412.51	7.01	2598.55	7.43	987.62	2.71
Tactical	60	30	2494.78	7.3	2981.88	8.1	1111.18	3.11

Table H.12: Flaps and gear deployment results for Real atmosphere with wind prediction errors

H.4. Speed on elevator until RWY

Inputs			Time deviation	Altitude dev.			
Guidance Method	Time to next conf. (s	RTA (s)	RWY (s)	within 0.5 (s	(ft)		
Reference	-	-15	4.62	5	40	R	Real
Reference	-	-30	4.92	5	60	R	Real
Reference	-	0	4.54	5	100	R	Real
Reference	-	15	4.64	5	80	R	Real
Reference	-	30	4.56	5	100	R	Real
Strategic	0	-30	1.77	220	60	C	Real
Strategic	0	-15	0.46	90	0	C	Real
Strategic	0	0	1.12	20	20	C	Real
Strategic	0	15	2.08	55	80	C	Real
Strategic	0	30	1.42	90	20	C	Real
Tactical	0	-30	1.32	315	40	F	Real
Tactical	0	-15	4.24	160	100	F	Real
Tactical	0	0	0.99	140	0	F	Real
Tactical	0	15	0.91	215	0	F	Real
Tactical	0	30	1.58	235	40	F	Real
Reference	-	-15	2.55	165	80	R	ISA
Reference	-	-30	1.85	115	180	R	ISA
Reference	-	0	2.3	170	80	R	ISA
Reference	-	15	1.58	230	180	R	ISA
Reference	-	30	1.08	280	240	R	ISA
Strategic	0	-30	2.26	150	80	C	ISA
Strategic	0	-15	1.41	165	180	C	ISA
Strategic	0	0	1.35	155	200	C	ISA
Strategic	0	15	-0.21	275	100	C	ISA
Strategic	0	30	0.63	590	80	C	ISA
Tactical	0	-30	1.61	350	60	F	ISA
Tactical	0	-15	0.64	590	0	F	ISA
Tactical	0	0	0.59	630	0	F	ISA
Tactical	0	15	-0.51	490	80	F	ISA
Tactical	0	30	0.51	650	100	F	ISA

Table H.13: Time deviation results following speed on elevator until the RWY

Inputs			Outputs							
Guidance Method	Time to next conf. (s	RTA (s)	FLND (ft)	G (ft)	T (ft)	V (ft)	STABLE (ft)			
Reference	-	-15	1204.8	1868.23	1158.496	1111.789	1111.789	R	Real	
Reference	-	-30	1246.37	1915.52	1149.8	1149.082	1149.082	R	Real	
Reference	-	0	1223.82	1893.87	1178.696	1133.126	1133.126	R	Real	
Reference	-	15	1261.66	1930.74	1212.949	1169.654	1169.654	R	Real	
Reference	-	30	1268.06	1937.14	1220.427	1176.292	1176.292	R	Real	
Strategic	0	-30	1096.02	3552.58	1107.637	1159.717	1096.02	C	Real	
Strategic	0	-15	1146.15	1820.96	1028.803	1022.454	1022.454	C	Real	
Strategic	0	0	991.36	1725.55	1004.121	1067.903	991.36	C	Real	
Strategic	0	15	1080.33	1755.71	1092.606	1145.308	1080.33	C	Real	
Strategic	0	30	1038.99	1682.66	1051.605	1127.108	1038.99	C	Real	
Tactical	0	-30	1097.52	1770.42	1118.155	1119.403	1097.52	F	Real	
Tactical	0	-15	1112.81	1838.4	1124.549	1178.584	1112.81	F	Real	
Tactical	0	0	1018.71	1858.27	1029.194	1034.512	1018.71	F	Real	
Tactical	0	15	958.83	1715.22	982.6389	1047.172	958.83	F	Real	
Tactical	0	30	1064.7	1820.24	1085.402	1143.414	1064.7	F	Real	
Reference	-	-15	1309.09	1861.27	1150.588	1133.406	1133.406	R	ISA	
Reference	-	-30	1404.38	1958.77	1248.048	1231.081	1231.081	R	ISA	
Reference	-	0	1322.8	1876.67	1167.375	1146.968	1146.968	R	ISA	
Reference	-	15	1387.06	1978.18	1225.432	1213.387	1213.387	R	ISA	
Reference	-	30	1435.46	2025.05	1277.632	1266.17	1266.17	R	ISA	
Strategic	0	-30	1225.34	1618.32	1086.128	1136.408	1086.128	C	ISA	
Strategic	0	-15	1206.31	1775.14	1218.155	1221.406	1206.31	C	ISA	
Strategic	0	0	1219.99	1855.07	1254.627	1234.556	1219.99	C	ISA	
Strategic	0	15	1111.36	1756.46	1127.309	1138.262	1111.36	C	ISA	
Strategic	0	30	1292.12	1755.34	1312.647	1294.995	1292.12	C	ISA	
Tactical	0	-30	1256.86	1687.88	1102.16	1103.383	1102.16	F	ISA	
Tactical	0	-15	1450.99	1668.68	1087.292	1110.876	1087.292	F	ISA	
Tactical	0	0	1450.82	1760.66	1091.822	1089.61	1089.61	F	ISA	
Tactical	0	15	1131.88	1796.6	1114.707	1145.063	1114.707	F	ISA	
Tactical	0	30	1230.13	1817.31	1264.585	1242.36	1230.13	F	ISA	

Table H.14: Stabilization results following speed on elevator until the RWY

Inputs			Outputs								
Guidance Method	Time to next conf. (s)	RTA (s)	Fuel (kg)	SPD BRK time (s)	SPD BRK occ	Initial replan (s)	Energy replans	Mean time replans (s)	Median time replans (s)		
Reference	-	-15	75.3072	0	0	8.752	0	0	0	R	Real
Reference	-	-30	75.2137	55.22	2	29.531	0	0	0	R	Real
Reference	-	0	75.4649	0	0	11.263	0	0	0	R	Real
Reference	-	15	75.9334	0	0	17.1549	0	0	0	R	Real
Reference	-	30	74.7373	20.16	1	14.617	0	0	0	R	Real
Strategic	0	-30	75.691	0	0	28.502	4	5.7175	4.727	C	Real
Strategic	0	-15	72.6908	0	0	26.442	1	5.632	5.632	C	Real
Strategic	0	0	72.9085	0	0	77.735	1	7.113	7.113	C	Real
Strategic	0	15	74.731	0	0	32.963	1	5.46	5.46	C	Real
Strategic	0	30	73.8685	0	0	45.006	3	3.915333333	1.95	C	Real
Tactical	0	-30	73.8361	0	0	32.058	2	4.969	4.969	F	Real
Tactical	0	-15	73.5307	0	0	18.065	0	0	0	F	Real
Tactical	0	0	72.9901	0	0	72.4	1	8.299	8.299	F	Real
Tactical	0	15	72.4756	0	0	30.233	2	2.3325	2.3325	F	Real
Tactical	0	30	73.2849	0	0	51.2	2	2.9875	2.9875	F	Real
Reference	-	-15	70.6065	0	0	5.273	0	0	0	R	ISA
Reference	-	-30	70.858	65.42	2	10.062	0	0	0	R	ISA
Reference	-	0	70.8893	0	0	24.882	0	0	0	R	ISA
Reference	-	15	70.3349	0	0	28.205	0	0	0	R	ISA
Reference	-	30	69.695	0	0	4.633	0	0	0	R	ISA
Strategic	0	-30	69.6141	0	0	26.271	0	0	0	C	ISA
Strategic	0	-15	68.5251	0	0	48.313	0	0	0	C	ISA
Strategic	0	0	68.593	0	0	16.739	0	0	0	C	ISA
Strategic	0	15	68.5084	0	0	17.784	2	3.198	3.198	C	ISA
Strategic	0	30	69.7945	0	0	17.176	1	8.159	8.159	C	ISA
Tactical	0	-30	69.0543	0	0	24.383	0	0	0	F	ISA
Tactical	0	-15	70.1058	0	0	38.564	1	5.414	5.414	F	ISA
Tactical	0	0	69.7834	0	0	19.094	1	4.259	4.259	F	ISA
Tactical	0	15	68.9744	0	0	15.397	2	2.8155	2.8155	F	ISA
Tactical	0	30	69.8025	0	0	17.035	1	8.549	8.549	F	ISA

Table H.15: Fuel, speed brakes and re-plans results following speed on elevator until the RWY

Inputs			Outputs											
Guidance Method	Time to next conf. (s	RTA (s)	hFA (ft)	xFA (NM)	hG (ft)	xG (NM)	hFL (ft)	xFL (NM)	N1mean	N1max	hN1max (ft)	hmean (ft)		
Reference	-	-15	2156.06	7.28	1913.82	6	1204.8	3.26	0.508511	0.9664	17025.6	6725.372961	R	Real
Reference	-	-30	2196.13	7.32	1964.61	6.02	1246.37	3.28	0.523962	0.9789	17024.98	6966.583715	R	Real
Reference	-	0	2188.26	7.26	1949.33	6	1223.82	3.27	0.496047	0.9648	17025.94	6524.816122	R	Real
Reference	-	15	2222.41	7.27	1984.23	6.01	1261.66	3.27	0.47883	0.9666	17025.06	6393.501726	R	Real
Reference	-	30	2231.71	7.26	1989.62	6	1268.06	3.27	0.46026	0.9375	17031.59	6487.141702	R	Real
Strategic	0	-30	2179.55	7.05	3662.96	9.34	1096.02	2.76	0.526328	0.9713	17025.01	6951.88949	C	Real
Strategic	0	-15	2234.42	7.18	1860.36	5.19	1146.15	3.32	0.504126	0.9668	17026.21	6912.850498	C	Real
Strategic	0	0	2281.74	7.35	1760.94	5.11	991.36	2.75	0.4838	0.9685	17026.31	6666.35883	C	Real
Strategic	0	15	2326.91	7.32	1794.79	5.13	1080.33	2.78	0.4782	0.9694	17023.38	6443.142287	C	Real
Strategic	0	30	2245.2	6.89	1721.74	4.88	1038.99	2.78	0.457327	0.9662	17026.96	6335.3683	C	Real
Tactical	0	-30	2531.76	7.26	1812.57	5.28	1097.52	2.88	0.518745	0.9683	17026.13	6937.466729	F	Real
Tactical	0	-15	2036.73	6.86	1883.36	5.27	1112.81	2.79	0.498555	0.9683	17025.38	6824.895666	F	Real
Tactical	0	0	2090.67	6.9	1894.62	5.11	1018.71	2.87	0.484087	0.9669	17026.92	6658.830382	F	Real
Tactical	0	15	2124.9	6.67	1765.61	5.24	958.83	2.75	0.471788	0.9668	17023.89	6507.351869	F	Real
Tactical	0	30	2271.14	6.63	1867.07	5.24	1064.7	2.74	0.45593	0.9681	17023.57	6374.958032	F	Real
Reference	-	-15	2060.09	7.16	1896.61	5.97	1309.09	3.69	0.506372	0.9531	16994.95	7194.058324	R	ISA
Reference	-	-30	2154.74	7.16	1993.21	5.98	1404.38	3.69	0.526282	0.9531	16996.89	7436.691001	R	ISA
Reference	-	0	2073.93	7.16	1911.36	5.98	1322.8	3.7	0.491456	0.9531	16995.3	6978.057682	R	ISA
Reference	-	15	2140.19	7.13	2015.42	6.18	1387.06	3.67	0.472427	0.9531	16995.98	7003.341213	R	ISA
Reference	-	30	2227.01	7.37	2062.16	6.17	1435.46	3.67	0.457465	0.9531	16996.36	7028.478299	R	ISA
Strategic	0	-30	2137.93	7.24	1668.54	4.98	1225.34	3.34	0.512391	0.9531	16995.62	7407.884195	C	ISA
Strategic	0	-15	2224.11	7.33	1821.89	5.03	1206.31	2.96	0.496099	0.9531	16996.01	7357.895453	C	ISA
Strategic	0	0	2257.99	7.34	1914.27	5.25	1219.99	2.97	0.480807	0.9531	16995.81	7148.285959	C	ISA
Strategic	0	15	2216.8	6.57	1811.13	5.18	1111.36	2.9	0.45934	0.9531	16995.67	7028.330757	C	ISA
Strategic	0	30	2193.61	7.33	1805.73	5.07	1292.12	3.39	0.456775	0.9531	16995.66	6826.086921	C	ISA
Tactical	0	-30	2110.54	6.93	1757.22	5.17	1256.86	3.47	0.511936	0.9531	16996.35	7449.426409	F	ISA
Tactical	0	-15	2290.56	7.31	1732.16	4.59	1450.99	3.99	0.5051	0.9531	16994.95	7347.360051	F	ISA
Tactical	0	0	2235.87	7.12	1811.75	4.85	1450.82	4.04	0.48868	0.9531	16993.25	7134.864062	F	ISA
Tactical	0	15	2257.45	6.5	1856.1	5.33	1131.88	3.01	0.460575	0.9531	16994.61	7015.889778	F	ISA
Tactical	0	30	2152.11	7.12	1875.81	5.3	1230.13	3.22	0.456514	0.9531	16996.18	6817.636671	F	ISA

Table H.16: Flaps and gear deployment results following speed on elevator until the RWY